

Dynamics, Intermolecular Interactions, and Organization of Transmembrane β -Peptides

Dissertation

zur Erlangung des mathematisch-naturwissenschaftlichen Doktorgrades

” Doctor rerum naturalium “

der Georg-August-Universität Göttingen

im Promotionsprogramm Chemie

der Georg-August-University School of Science (GAUSS)

Submitted by

Dina Zanbot

From Tetouan (Morocco)

Göttingen 2017

Thesis Committee

Prof. Dr. Ulf Diederichsen Institute of Organic und Biomolecular Chemistry,
Georg-August University Göttingen

Prof. Dr. Claudia Steinem Institute of Organic und Biomolecular Chemistry,
Georg-August University Göttingen

Members of the Examination Commission

Reviewer

Prof. Dr. Ulf Diederichsen Institute of Organic und Biomolecular Chemistry,
Georg-August University Göttingen

Reviewer

Prof. Dr. Claudia Steinem Institute of Organic und Biomolecular Chemistry,
Georg-August University Göttingen

Further Members of the Examination Commission

Prof. Dr. Lutz Ackermann Institute of Organic und Biomolecular Chemistry,
Georg-August University Göttingen

Prof. Dr. Kai Tittmann Institute of Molecular Enzymology, Georg-August
University Göttingen

Dr. Michael John Institute of Organic und Biomolecular Chemistry,
Georg-August University Göttingen

Dr. Franziska Thomas Institute of Organic und Biomolecular Chemistry,
Georg-August University Göttingen

Day of the Oral Examination: 28 August 2017

Abstract

Cellular membranes contain a vast variety of proteins, which are practically required for every vital mechanism, such as selective transportation of ions and organic molecules, cell-cell recognition and signal transduction.^[1] Nowadays, the major concern in life science is to gather an overview about the thermodynamics and kinetics that govern the native folding and aggregational behavior of these proteins. Artificially folded polymers, or foldamers, have attracted the interest of many research groups since they showed the potential for considerable versatility in biological functions akin to natural proteins.^[2] Thus, the prudent preorganization and refinement of such molecules can shed light on the molecular forces that control the structural features of membrane proteins and thereby, explore the correlation between their conformational stability and biological activity.

In particular, β -peptides have recently been used as very promising peptide mimics with interesting conformational and functional propensities. These non-biological polymers are stable towards enzymatic degradation and they can fold into compact multihelical structures including the 14- and the 12-helix.^[3] Generally, introducing non-covalent interactions, such as hydrogen bonds and *Vander Waals* forces *via* interhelical side chains can enhance the three-dimensional stability of proteins. In this regard, β -peptides have been largely utilized as suitable folding patterns to provide information about self-assembly processes.^[4-6]

Based on this concept, the main goal of this study is to understand the dynamics and the molecular interactions of transmembrane peptides using the most common β -peptide helices, the 14- and the 12-helix, as scaffolds to introduce polar residues across turns of the helix. This preorganization is expected to strongly promote self-assembly of these helices within membranes by means of interhelical forces. Thus, the architecture of the β -peptides used in this study was based on the choice of amino acids that can preferentially induce the formation of stable 14- and 12-helices. Subsequently, one side of these helices would be functionalized with one, two and three polar β^3 -glutamine residues respectively to reinforce helix-helix interactions *via* hydrogen bonds.

As a first step, the synthetic route of β -peptides containing a large amount of hydrophobic β -residues will be developed using manual microwave-assisted Fmoc-solid phase peptide synthesis (SPPS). Then, the ability of each of these β -peptides to adopt a rigid and a specific secondary structure either in solution or within large unilamellar vesicles (LUVs) composed of POPC will be monitored by CD spectroscopy. The membrane insertion of all the peptide barrel will be confirmed by virtue of tryptophan fluorescence of the β^3 -Trp introduced near the end of the sequences.

Additionally, the self-assembly process of these transmembrane helices inside POPC LUVs will be determined using Förster Resonance Energy Transfer (FRET). For this purpose, a donor-acceptor pair will be covalently attached to all the helices in order to generate their corresponding fluorescent analogues.

The backbone of the 14- and the 12-helix vary widely in terms of their conformational properties. Based on this notion, it is expected that the self-assembly of these two helices might vary as well according to their propensities to adopt discrete types of assemblies. Therefrom, the dissimilarity (or similarity) of these helices to arrange into different three-dimensional structures will be examined.

As a last step, to investigate the possibility of higher aggregation, the conformational features of the peptide barrel will be used by introducing polar residues across two sides of the helix. Then, the aggregational behavior will be determined using FRET.

Contents

1	Biological Membranes	1
1.1	Membrane Lipids	1
1.2	Membrane Proteins	5
1.2.1	Protein-Lipid Interactions	5
1.2.2	Protein-Protein Interactions	9
2	Artificially Folded Molecular Structures	12
2.1	Foldamers	12
2.2	β -Peptides	14
2.2.1	14-Helical Secondary Structure:	16
2.2.2	12-Helical Secondary Structure:	22
2.2.3	Other Conformations of β -Peptides:	23
2.3	Biological Functions of β -Peptides	25
3	Design and Synthesis of β -Peptides	28
3.1	Design of β -Peptides	28
3.1.1	Structural Design of the 14-Helix	29
3.1.2	Structural Design of the 12-Helix	34
3.2	Synthesis of β -Peptides	36
3.2.1	Synthesis of D- β^3 -Amino Acids	36
3.2.2	Synthesis of β -Peptides	37
4	Structural Characterization	43
4.1	CD Spectroscopy	43
4.1.1	Theoretical Basis	43
4.1.2	Secondary Structure of β -Peptides in Solution and within the Membrane	44
4.2	Fluorescence Spectroscopy	50
4.2.1	Insertion of β -Peptides within the Membrane	50
4.2.2	Topological Insertion of β -Peptides into the Lipid Bilayer	53
4.3	Förster Resonance Energy Transfer Experiments	56

4.3.1	Theoretical Basis.....	56
4.3.2	Self-Assembly of Transmembrane β -Peptides.....	61
4.3.3	Higher Order Aggregates of β -Peptides.....	67
4.3.4	Helix Orientation of Transmembrane β -Sequences within the Lipid Bilayer	69
5	Conclusion.....	72
6	Experimental Part.....	75
6.1	General Synthetic Methods and Materials.....	75
6.2	Characterization.....	77
6.2.1	Analytical and Spectroscopic Methods.....	77
6.2.2	Fluorescence Spectroscopy.....	79
6.3	Synthesis of β^3 -D-Amino Acids.....	80
6.4	General Procedure for Solid Phase Peptide Synthesis (SPPS).....	81
6.5	Preparation of Peptide/Lipid Vesicles.....	84
6.5.1	Multilamellar Vesicles (MLVs).....	84
6.5.2	Large Unilamellar Vesicles (LUVs).....	84
6.6	Analytical Data.....	85
6.6.1	β^3 -D-Amino Acids.....	85
6.6.2	Synthesized β -Peptides.....	90
7	Appendix.....	108
8	Abbreviation.....	122
9	References.....	124

1 Biological Membranes

1.1 Membrane Lipids

Biological membranes are distinguished by a heterogeneous assembly, which broadly appears in aspects like the wide variety of their components, lateral organization, topology, and the conformation of proteins and lipids.^[7] In 1935, Danielli et *al.* proposed the first membrane model including proteins and they postulated that a protein layer is tightly linked to the polar head groups of the lipids, composing together cell membranes.^[8] After more than three decades, Singer et *al.* provided a more detailed conception called fluid mosaic model, in which the biological membranes are formed by an organized environment of lipids in a fluid state incorporating globular assembling of proteins and glycol-proteins.^[9] After the discovery of this phase of separation in the plane of membrane, more efforts have been made in the last decades to explore the functions and the composition of cell membranes as well as to develop new technologies for revealing the lateral heterogeneities of cells. Nowadays, biological membranes are believed to play an essential role in cellular protection and also in the control and transport of nutrients.

While lipids provide the most plentiful type of macromolecules present in membranes, proteins carry out a wide array of specific functions, including selective transport of molecules and cell-cell recognition. There are three major classes of membrane lipids: phosphoglycerides, sphingolipids and sterols. These three types of lipids are featured by a wide variety in their hydrophilic headgroups and diverse fatty acid compositions. Both, phosphoglycerides and sphingolipids, can be combined as one class called phospholipids. The latter are classical type of membrane lipids with an amphipathic character due to the presence of both, polar head groups and apolar hydrocarbon chains, forming together a stable barrier between the two aqueous compartments, which are the inside and outside of the cell membrane. Phospholipids are widely used to obtain model systems for biophysical applications to study biological and artificial molecular species in the membrane environment. In general, the lipids can be synthesized or extracted from plant- or animal-derived tissues. However, natural phospholipids are less stable than synthetic phospholipids.^[10]

Phospholipids contain a head group, a glycerol backbone and two fatty acid chains or the so-called “tails” (Figure 1.1). One oxygen group of the phosphoric acid might be esterified, giving a rise to a variety of other organic molecules including glycerol (PG), choline (PC), ethanolamine (PE), serine (PS) or inositol (PI). However, PC and PE are considered as the most used model lipids to produce liposomes since they are the most abundant phosphatides in plants and animals.^[11]

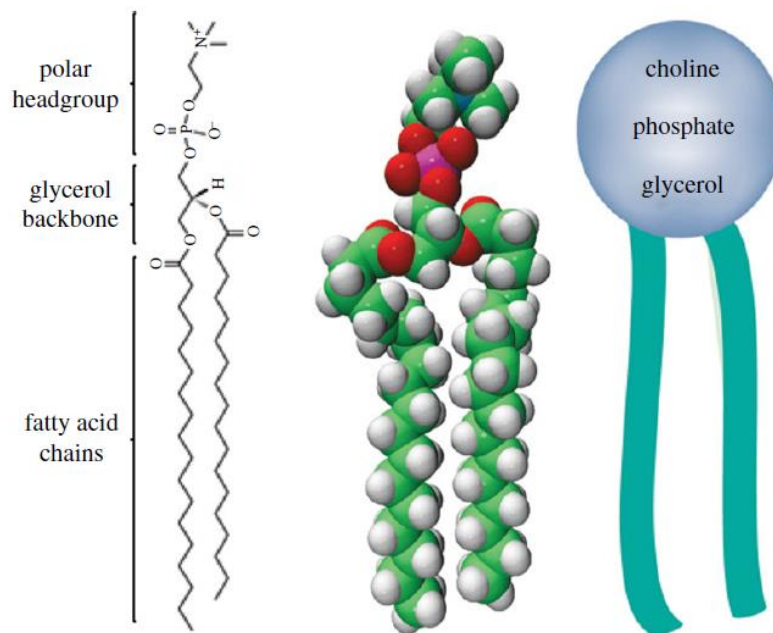


Figure 1.1: Chemical, three-dimensional and schematic illustration of L- α -phosphatidylcholine (HSPC).^[22]

The polar head groups of the outer leaflet extend outward the hydrophilic environment and can contain either charged or uncharged polar moieties. In most natural phospholipids, the fatty acid tails extend inward the cell and usually consist of about 14-24 carbon atoms with variations in length. One tail of the lipid may have one or more *cis*-double bonds that insert kinks into the hydrocarbon chains and render them difficult to pack together, leading to an alteration in membrane fluidity. The two acyl chains of the lipids are hydrophobic and solely interact with adjacent molecules *via* Van der Waals interactions. They are linked to the glycerol or sphingosine backbones *via* ester bonds.

There are two general merits of phospholipid bilayers that are critical to membrane functions.^[12] First, the interior of the phospholipid bilayer is hydrophobic and thereby,

impermeable to water-soluble substances, including ions and most biological species. This characteristic makes the structure of the phospholipids in charge of the basic function of membranes as barriers between two aqueous compartments. Second, the long acyl chains of the fatty acids move freely in the internal part of the membrane, so the inner-membrane itself is a viscous fluid and flexible. When immersed in an aqueous environment, lipid molecules can spontaneously self-assemble into specifically ordered lyotropic liquid-crystalline phases to bury their hydrophobic tails in the interior and expose their hydrophilic heads to the aqueous medium. Generally, there are numerous intrinsic factors that control the shape of the resulting phospholipid-based structures like the nature and the size of the lipid head group, the length and degree of unsaturation of the hydrocarbon chains and the extrinsic factors like the temperature, pH and the concentration.^[13,14] There are many examples of lipid-based structures such as, monolayers, micelles (Figure 1.2a), reverse micelles (Figure 1.2b), bilayers (Figure 1.2d) and hexagonal phases (Figure 1.2e).

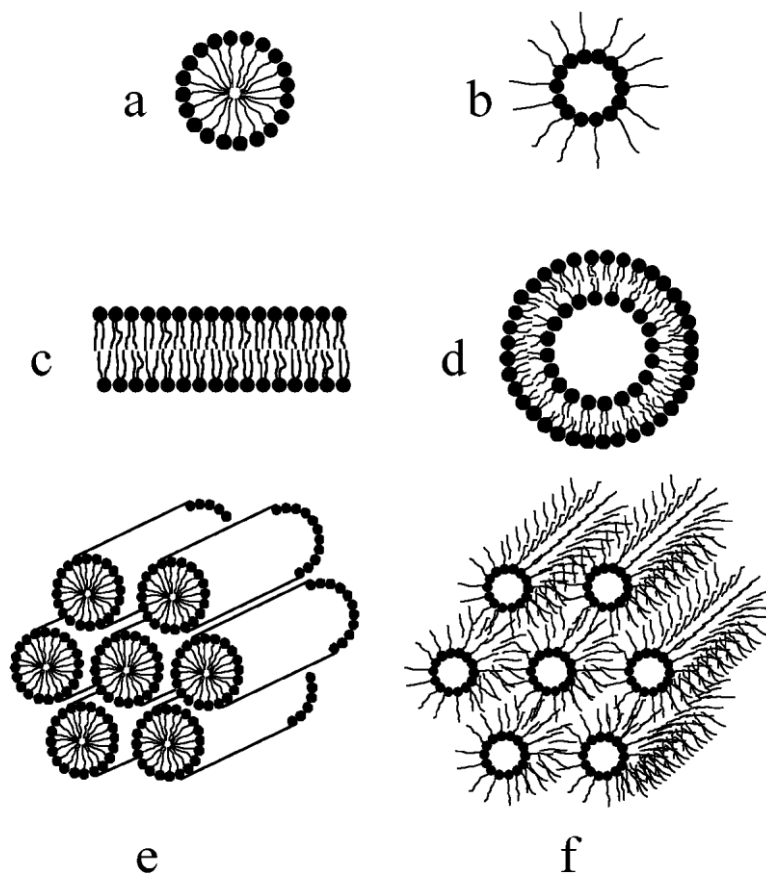


Figure 1.2: Common lamellar and non-lamellar packing arrangements of lipids in aqueous environment. (a) micelle, (b) inverse micelle, (c) lamellar bilayer, (d) bilayer vesicle, (e) hexagonal, (f) inverse hexagonal.^[15]

Most lipids that form spherical micelles have charged head groups leading to a large head group area. In contrast, amphiphiles with small head group area or bulky hydrocarbon chains cannot fit into such small aggregates to pack into micellar structure but, instead form bilayers. Under certain conditions, the formation of curved bilayers (vesicles) becomes more favorable than the formation of infinite planar lipid bilayers. This arises from the elimination of the energetically unfavorable edges of the vesicle at a finite rather than infinite number of aggregation, which is also entropically favored.^[16,17] Thus, as long as lipids are in a closed spherical bilayer, they can maintain areas at their optimal values, which means that vesicles would be the preferred spatial orientation in this case. In addition, lipid bilayers are considered as the major building blocks of biological membranes which, together with membrane proteins and cholesterol, control the shape of the cell and many other functions like storage of compounds, ions transport, cell fusion and metabolism.^[15]

In cells, lipids are featured by various spatial arrangement and motional freedom by adopting different fluid and solid phases with respect to the surrounding environment. Moreover, one of the most important characteristics of cells that allows a given substance to pass through the membrane only with selective permeability is the capacity of the lipid bilayer to keep various environments between external and internal region.^[15,18]

As mentioned previously, the degree of fatty acid saturation affects the mobility of lipids. However, the temperature is another factor that can highly influence their fluidity within the bilayer.^[19] When the temperature changes, the physical state of the phospholipid bilayer changes as well from a two-dimensional rigid crystalline (or gel) to a liquid state or vice-versa. This change of state is called a phase transition. There are several factors that directly influence the phase transition temperature (T_m) including hydrocarbon length, unsaturation, charge and head group species.^[20] For instance, as the hydrocarbon length increases, *Van der Waals* interactions become stronger and the membrane-permeability decreases, requiring more energy to disrupt the ordered packing and thereby, the T_m increases.^[21] Conversely, introducing a *cis*-double bond into the acyl group requires much lower temperatures to induce an ordered packing arrangement.^[18]

As indicated in Figure 1.3, at a temperature below T_m , phospholipids exist in a gel phase and present low fluidity and low permeability. As a result, hydrophobic tails in the interior of the lipid bilayer pack together more tightly. At a temperature above T_m , the phospholipids are highly fluid but less permeable. At a temperature equal to T_m , both the fluidity and the

permeability of the lipid bilayer, increase slightly. This phenomenon is attributed to the presence of highly permeable interfacial areas between coexisting gel ($<T_m$) and fluid ($>T_m$) bilayer domains.^[15]

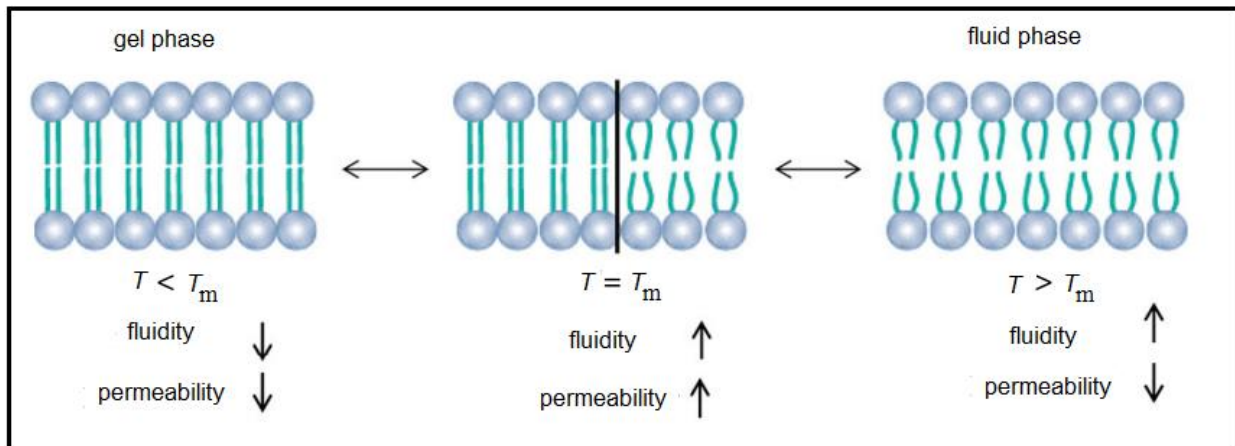


Figure 1.3: Schematic representation of the influence of temperature on phospholipid bilayer fluidity and permeability.^[22]

1.2 Membrane Proteins

Biological membranes contain mainly phospholipids and proteins, conferring them unique physical and chemical properties. Membrane proteins contribute to diverse and critical cellular functions such as cell adhesion, energy transduction, signaling, cell recognition and transport of ions and other small molecules.^[23] Protein complexes are stabilized within the cell membrane by various chemical forces, such as hydrogen bonds, hydrophobic, electrostatic and *Van der Waals* forces.^[1,24] This mostly depends on the local dielectric environment of protein atoms, which means by way of spatial arrangement of proteins in membranes.^[25,26]

1.2.1 Protein-Lipid Interactions

To ensure the solubility of proteins in membranes, polarity of the lipid phase should match the polarity of the embedded proteins. In this regard, the membrane fluidity must be strictly adjusted in various cells and in various environmental conditions by regulating the lipid components. Thus, the functionality required for structural flexibility of membrane proteins

can be maintained even at highly anisotropic lipid environments.^[27] The complement of proteins linked to a membrane varies depending on the cell type and subcellular location. Generally, membrane proteins can be classified into two broad categories, integral proteins and peripheral proteins.^[28] This classification is mainly based on the protein interactions and functions within the membrane.

While integral proteins cross the entire phospholipid bilayer with structures that embed from one side of the membrane to the other side, peripheral proteins are bound indirectly to the membrane by interacting with integral membrane proteins or directly by interacting with polar head groups of lipids. Integral membrane proteins present a large part of biological membranes ranging from 20-80%.^[29] The transmembrane-spanning domains of these special proteins contain a straight or tilted stretch of about 20 amino acids with hydrophobic side chains that interact with the inner part of the membrane followed by distinct clusters of aromatic and charged residues on both sides that have a specific affinity to the membrane-water interface. α -Helices, multiple β -strands and β -helices are the most conspicuous membrane-spanning domains known to date that can fulfill the requirements need for a hydrogen bond prospect of a polypeptide main chain to be saturated inside a hydrophobic environment. The α -helical proteins are abundantly found by approximately 25-30% of the genes of all sequenced organisms in all types of cellular and intracellular membranes.^[31] Whereas, the β -barrels are encoded by less than 3% of bacterial genes and mainly exist in outer membranes of bacteria, mitochondria and chloroplasts.^[31,32] Besides, single- and double-stranded β -helices are known from membrane polypeptides with alternating L- and D-residues like gramicidin A, B and C.^[28]

In order to obtain detailed information about the interactions between proteins and lipid bilayer, relatively simple model membranes have been used, in which structural parameters can be systematically altered. Thus, useful information derived from these model systems depend critically on the choice of proteins and lipid compositions. Indeed, there are many examples of α -helical peptides that have been designed to gain insight into adaptations of proteins to their environmental membranes. Especially those proposed by Killian et al. consisting of sequences with alternating alanine and leucine residues as hydrophobic stretch flanked by either polar lysine residues (KALP peptides) or tryptophan residues (WALP peptides).^[34,7] These synthetic peptides have been applied to show the direct influence on the membrane morphology to various model membranes with different acyl chain length and to

precisely explore the effect of altering their hydrophobic length relative to the bilayer thickness. These phenomena are readily explained by the concept of hydrophobic mismatch arising from a difference between the hydrophobic thickness of lipid membranes and the length of transmembrane protein segments. Also, hydrophobic mismatch is thought to play an important factor controlling membrane protein insertion and folding,^[35] protein activity^[36] and aggregation.^[37] Many experimental and theoretical studies have revealed that two types of hydrophobic mismatch can occur: first, a positive mismatch, in which the hydrophobic part of a transmembrane protein is too large to match the hydrophobic bilayer thickness and second, a negative mismatch, in which the length of the peptide segment is shorter than the hydrophobic bilayer thickness.^[23,35] As a result of these two cases, the peptides as well as the lipid bilayer may give different responses to relieve the energetic constraints imposed by the hydrophobic mismatch. From the lipid side, the thickness of the overall bilayer might be affected with concomitant alterations in phase properties, or a lateral phase segregation can be promoted.^[37,38] On the protein side, the elastic energy of mismatch may favor aggregation,^[39,40] lateral sorting and/or structural reorganizations.^[41,42] The plausible mechanisms that can be adopted by either proteins and lipid bilayers are schematically depicted in Figure 1.4.

Thus, in case of a positive hydrophobic mismatch (Figure 1.4, left), the proteins might oligomerize in the membrane to minimize the exposed hydrophobic area, they could tilt to reduce their effective hydrophobic length or vary the backbone conformation. Lipids in turn could modulate the bilayer thickness by stretching their acyl chains or even assemble into another type of aggregates by disrupting the bilayer organization.

In case of a negative hydrophobic mismatch (Figure 1.4, right), proteins could aggregate or change their backbone conformation. Furthermore, a deformation of their side chain orientation can occur. In addition, peptides with insufficient length of hydrophobic stretch might not incorporate into the membrane but, instead tend to localize on the lipid surface. Alternatively, lipids could reduce the effective bilayer thickness by disrupting the bilayer organization or disordering their hydrocarbon acyl chains to form an inverted non-lamellar structure.^[7]

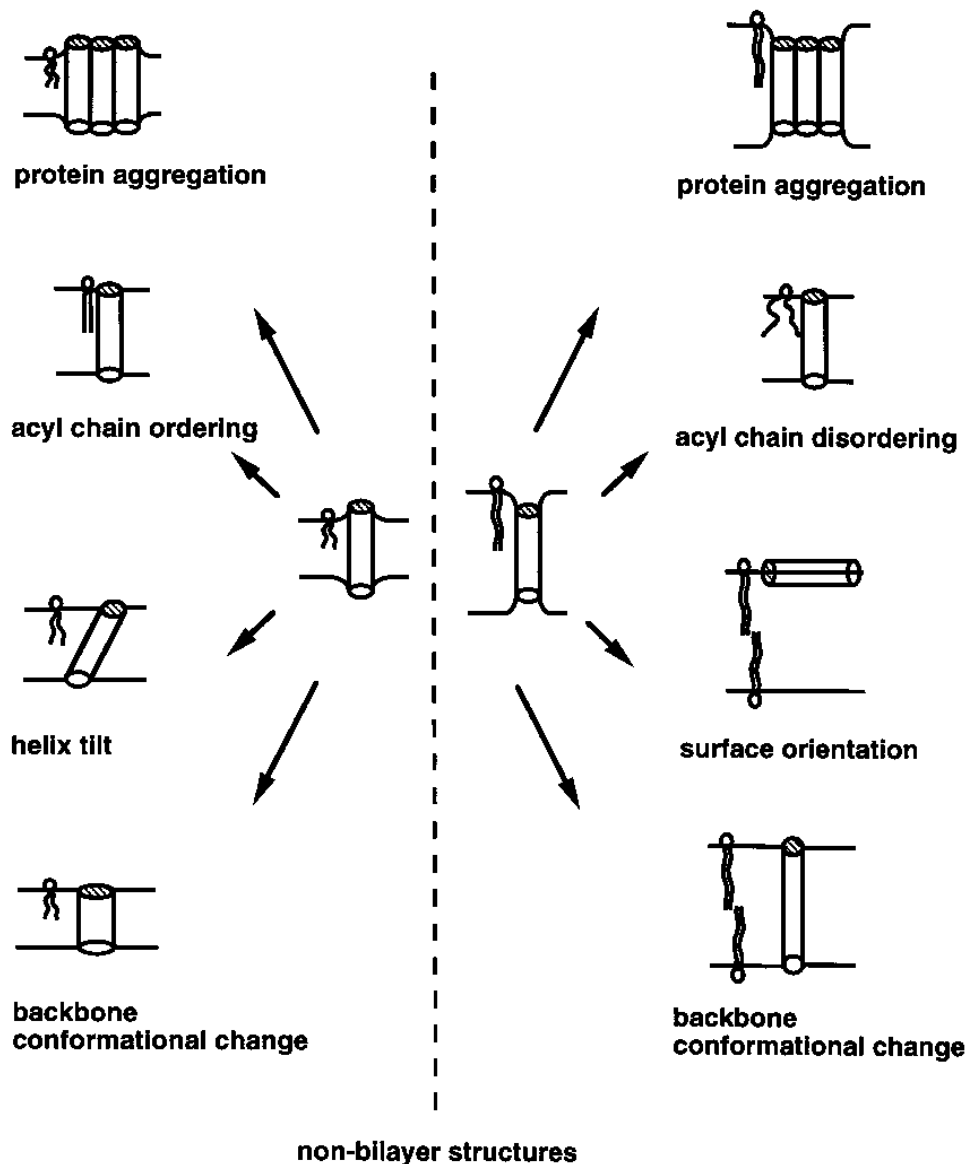


Figure 1.4: Schematic illustration of some possible consequences arising from positive hydrophobic mismatch (left) and negative hydrophobic mismatch (right).^[35]

Interestingly, it has been indicated that a difference of about 7 Å for a positive hydrophobic mismatch and more than 13 Å for a negative hydrophobic mismatch could be tolerated, presumably, because of the alternative possibility of tilting.^[35] Such a helix tilt can significantly influence the functional activities of membrane proteins as has been extensively reported for bacteriorhodopsin.^[42]

1.2.2 Protein-Protein Interactions

Helix-helix interactions are intrinsic to virtually every cellular process. In nature, 80% of proteins exist as oligomeric complexes to perform their biochemical functions, rather than remaining as individual species.^[43] Based on energetic considerations, the possible driving forces for interactions between transmembrane helices are packing effects, such as interhelical polar interactions including hydrogen bonds and ion pairs as well as *Van der Waals* interactions between closely packed helices.^[44] A study proposed by Popot and Engelman and then elaborated by White and coworkers has revealed that the process of protein assembly within the membrane can be simplified in terms of two energetically distinct stages, the so-called “two-stage model” (Figure 1.5).^[45,46]

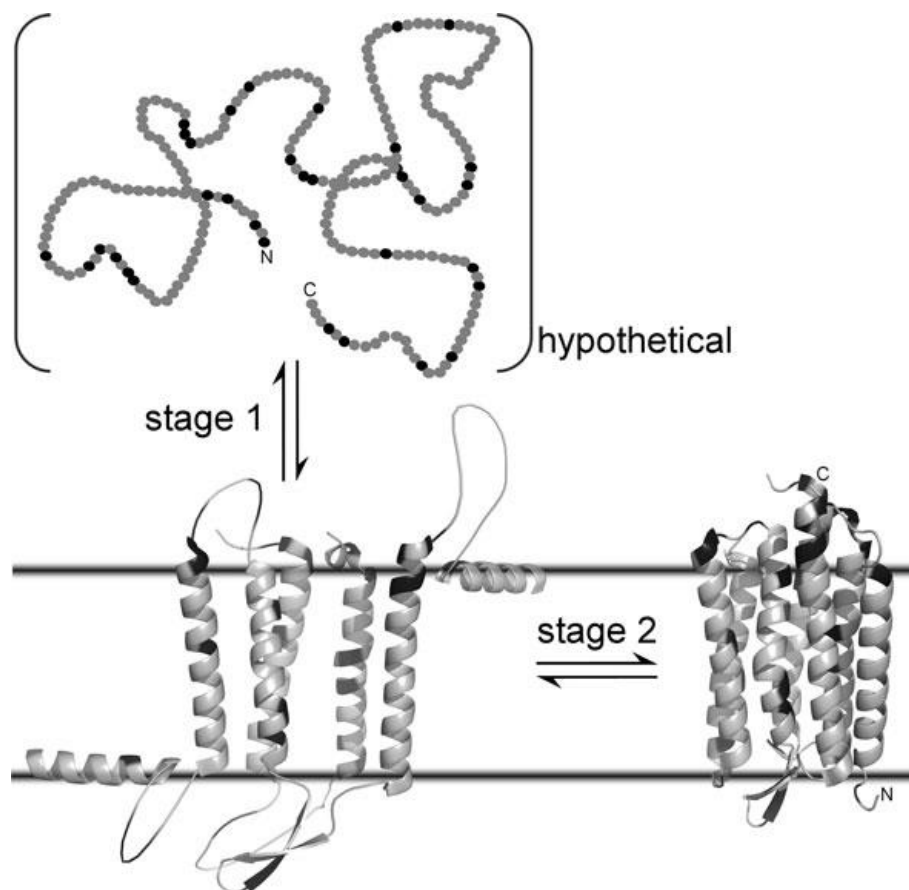


Figure 1.5: Example of the two-state model of membrane protein folding using bacteriorhodopsin from *Halobacterium salinarum* (231 residues). In the first stage, the preformed helix inserts into the bilayer followed by the second stage, in which the helices associate to form the native folded structure.^[1]

In the first stage, the protein is transferred from water to the apolar region of the bilayer driven by the hydrophobicity of its apolar side chains. Whereas, aromatic and positively charged residues tend to localize near the bilayer head group regions and thereby, contribute to the appropriate orientation of the protein within the biological membrane. After inserting in the membrane environment, the second stage consists of stabilizing the protein's helical conformation by satisfying its backbone energy *via* amide-carbonyl hydrogen bonds. Then, the protein can be able to assemble through the coalescence of helices to form the tightly native tertiary structure. In this stage, the possible diffusion of the helices within the plane of the membrane bilayer will be limited due to the presence of links between the helices meaning that the unfavorable entropic term in the free energy of association is minimized, which is for example the case of disulfide bridges in soluble proteins.^[48]

Although this two-stage model provides valuable conceptual frameworks for understanding the actual kinetic process of protein insertion and folding as it occurs *in vivo*, the features that govern the subsequent association of the inserted helices are controversial and remain poorly understood.^[49] Thus, in recent years numerous simple transmembrane protein model segments have been developed to address the general properties that promote helix-helix association, such as the presence of apolar, charged or aromatic residues.^[50,51] Compared with the composition of proteins in general, the apolar side chain residues in transmembrane α -helices exhibit the most prevalent species and play an essential role for function, conformational specificity and thermodynamic stability of the entire protein.^[52,53] To this end, several examples displaying the role of hydrophobic side chain residues in a transmembrane domain have been reported. Interestingly, Engelman and his group have explored the primary GxxxG motif^[47] as a model transmembrane helix composed of solely apolar and small amino acids. This discovery has steered attention to the importance of *Van der Waals* interactions in transmembrane protein folding and has also enabled understanding of the specific dimerization of the whole motif family, which includes the SxxxS,^[54] SxxxSxxxG^[55] or FxxGxxxG motifs.^[56]

Beside the fact that buried apolar residues appear to relatively provide a sufficient force for proteins folding, polar motifs are expected to drive association in membranes. The low-dielectric environment displayed by the hydrocarbon core of a lipid bilayer conveniently results in strong electrostatic interactions.^[1] As a result, the formation of a hydrogen bond within transmembrane proteins is expected to be notably more stable than in aqueous-soluble

proteins since in the hydrophobic region of the lipid membrane, dehydration of the two interacting groups is not required to form a stable hydrogen bonding.^[57] Substantially, Hu and coworkers have found out that placing the polar Asn residues at four buried α positions in a two-stranded coiled coil seems to contribute to conformationally stabilizing the coiled coil peptides *via* formation of hydrogen bond forces between Asn residues side chains.^[58] Similarly, Engelman et *al.* as well as Degrado et *al.* have demonstrated that other polar motifs, such as Asp, Glu, Gln or His appear to be fundamental for folding, proton translocation activity and other biological functions.^[50,59]

Aromatic side chains in turn can be essential for *Van der Waals* forces, hydrophobic and weak polar interactions.^[60,61] In fact, Phe residues can enhance transmembrane domain interactions when it is placed at position $i-3$ of a GXXXG motif.^[56] Furthermore, it has been found that Trp and Tyr prefer to localize at the termini of many membrane proteins close to the hydrophobic-hydrophilic region, where they are thought to vertically anchor the protein in the lipid bilayer by interacting with the membrane head groups.^[55,62]

2 Artificially Folded Molecular Structures

2.1 Foldamers

In nature biological macromolecules (mainly proteins and nucleic acids) are in charge of carrying out sophisticated chemical tasks, such as catalysis, directed flow of electrons, specific binding and controlled crystallization of inorganic phases.^[3] In particular, proteins are considered as very interesting biological polymers since they play a key role in many biological processes and have a strong tendency to adopt specific and tight conformations. The process of protein folding can be classified into four major levels of organization (Figure 2.1).

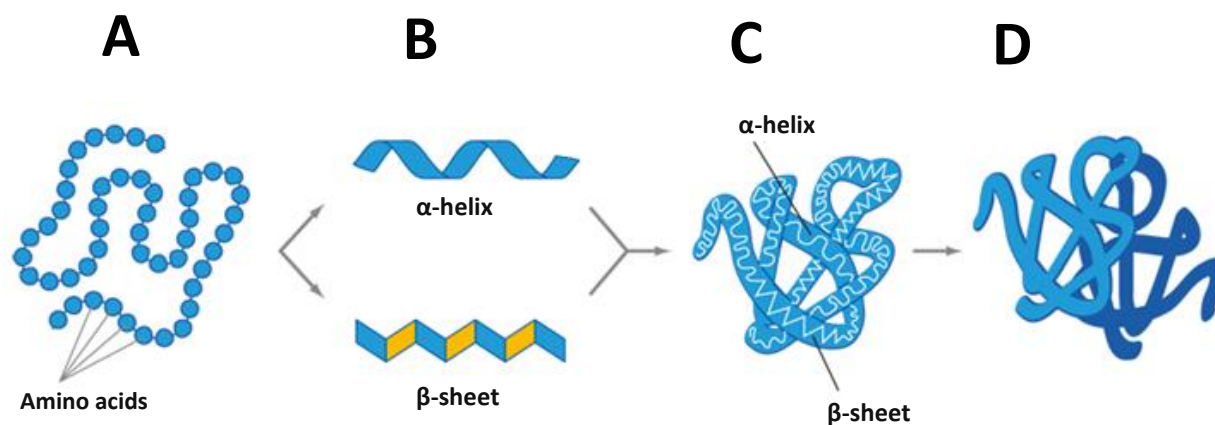


Figure 2.1: The four recognized levels of protein structures including A) primary, B) secondary, C) tertiary and D) quaternary structures. (Image modified from OpenStax Biology's by National Human Genome Research Institute).

Primary structure: the linear sequence of amino acids linked together by peptide bonds, forming a polypeptide.

Secondary structure: locally folded structure formed within a polypeptide due to interactions between atoms of the backbone resulting in a defined directionality in all cases. The most common types of secondary structures are the α -helix and β -sheet.

Tertiary structure: the overall three-dimensional structure of a polypeptide that arises from interactions between the amino acid side chains. At this level of organization, the proteins

include a much broader range of intermolecular contacts such as disulfide bonds, hydrophobic interactions and ionic bonds.

Quaternary structure: the global shape resulting from the aggregation of multiple folded polypeptides which form the final functional protein.

More recently, a fifth structural hierarchy (quinary structure) has been reported by Edelstein for interactions within helical arrays found for sickle cell hemoglobin fibers or tubulin units in microtubules.^[71]

The correct arrangement of biological macromolecules in a specific tridimensional disposition is highly required in order to generate their “active site”. Thus, elucidating the relationship between the folding pattern and the activity of biopolymers may allow the *de novo* design of biomimetic polymers with interesting conformational and functional propensities.

Artificially folded molecular architectures or foldamers are defined as oligomers with a strong tendency to fold into specific compact conformations, stabilized by non-covalent interactions between non-adjacent residues in solution.^[3,63] In the past decades, the design and synthesis of a variety of foldamers and their corresponding building blocks have been the interest of many research groups. However, producing polymers with high molecular weight that can mimic thoroughly the sophisticated functions and structures of bio-macromolecules is still limited.

There are several important principles that govern the design of foldamers with suitable properties such as (i) the modification of an existing peptide by modulating either the amino acid side chains or the backbone itself, (ii) the insertion of constraints to elucidate the rules that govern the mechanisms of proteins folding^[64] and (iii) the evolution of patterns to stabilize the secondary structure of short chains.^[65,66]

According to the nature of their single monomer unit, foldamers can be grouped into two major types as elucidated in Figure 2.2: “Aliphatic foldamers” that contain saturated carbon chains between the amide and carbonyl groups and “aromatic foldamers” that reveal aromatic moieties within their backbone.^[119] The intact synthesis and functions of these unnatural polymers may provide significant applications in pharmaceuticals and nanomedicine material sciences.

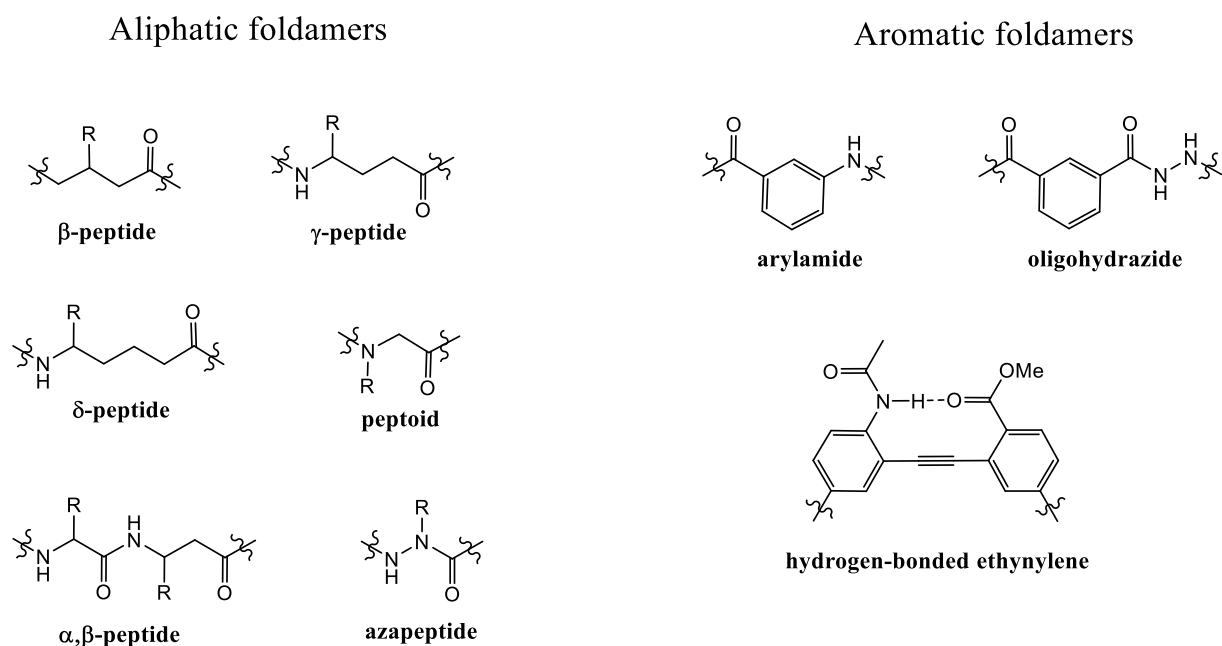


Figure 2.2: Examples of foldamer backbones.^[119]

2.2 β -Peptides

At present, the family of β -peptides is considered as most desirable mimics of natural peptides compared to other aliphatic foldamers. Kovacs *et al.* have reported the first model of the helical structure of β -peptides composed of a poly(β -L-aspartic acid) in solution.^[72] They proposed that the helical conformation of this β -polypeptide chain consists of 3.4 residues per turn and an axial translation of 1.58 Å. Over the next decades, structural and synthetic investigations of many research groups, especially the pioneering works of the Seebach and the Gellman group, have laid a solid foundation for a better understanding of the folding behavior of β -peptides in solution and in solid state.^[67-70]

β -Peptides are unnatural polymers made up solely of β -amino acids that differ from their natural α -amino acids counterparts by one additional methylene group either between the carbonyl groups and the α -carbon atoms (β^3) or between the α -carbon and nitrogen atoms (β^2) (Figure 2.3A).^[73] The C_β -substituted β -amino acids can be formed by homologation^[68,74] or by other known synthetic routes.^[75,76] The addition of one more carbon atom into the polyamide backbone can be translated into the introduction of one extra torsion angle resulting in more degrees of conformational freedom (Figure 2.3B).

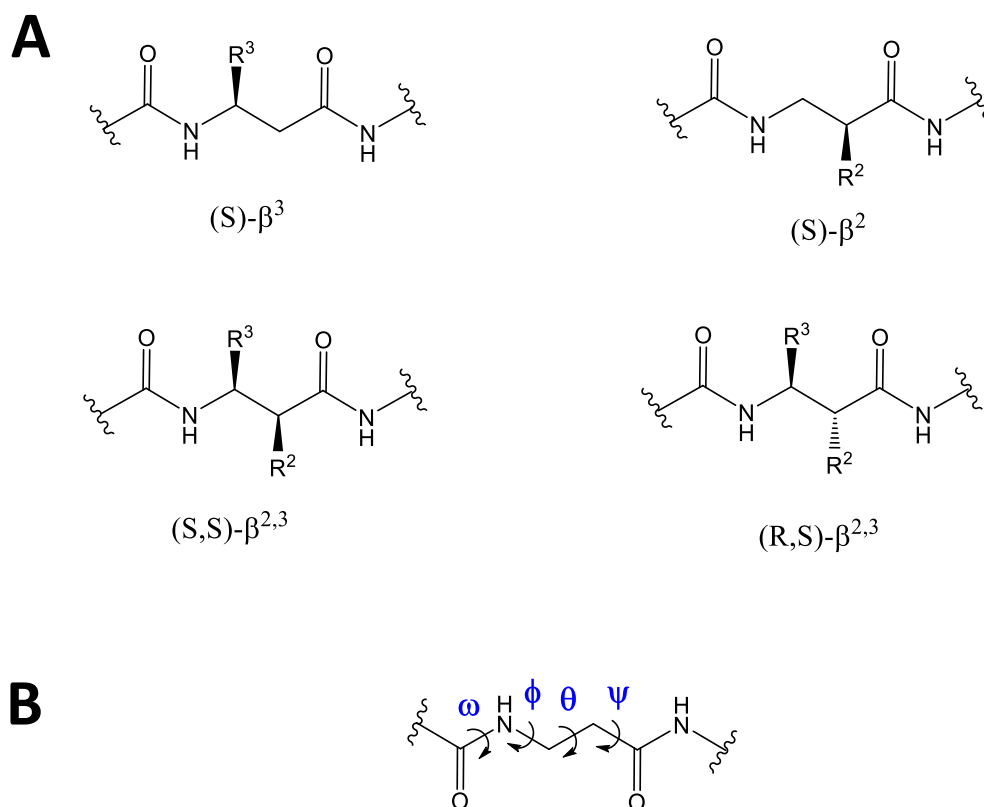


Figure 2.3: General constitution of A) designation of the substitution pattern of β -amino acid residues and B) the backbone torsions.

It is especially interesting and might be even surprising that β -peptides are able to form conformations characteristically similar to those occurring in natural peptides and proteins. Indeed, based on the high flexibility of glycine-rich peptides, it is expected that β -peptides possess higher conformational flexibility due to the introduction of additional C-C bonds and thereby, the formation of ordered conformations is entropically disfavored. In contrast to this anticipated aspect, β -peptides showed a high ability to form a rich variety of regular conformational states. Concerning α -peptides, the formation of stable α -helical secondary structures required at least a chain length of 15 α -amino acids.^[77] In the case of β -peptides, one can expect that even higher number of stretches would be required to form stable secondary structures due to their high number of possible conformers. However, β -peptides are able to show stable secondary structures even when the chain lengths contain as few as six amino acids.^[78] As highlighted previously, β -peptides adopt a wide array of distinctive secondary structural motifs including helices, hairpins and parallel sheets.^[79] According to the nature of their units, β -peptides are able to adopt different helical secondary structures,

among which the 14-helix, 12-helix, 10/12-helix, 10-helix and the 8-helix (Figure 2.4). The nomenclature of β -helical conformations varied widely in the literature. Herein, the nomenclature is based on the number of the atoms in the hydrogen-bonded ring.^[95]

The overall helical parameters of β -peptides differ significantly in many aspects from the ones of the α -helix, such as the radius, the number of residues per turn and the overall dipole (Figure 2.5 and Table 2.1).

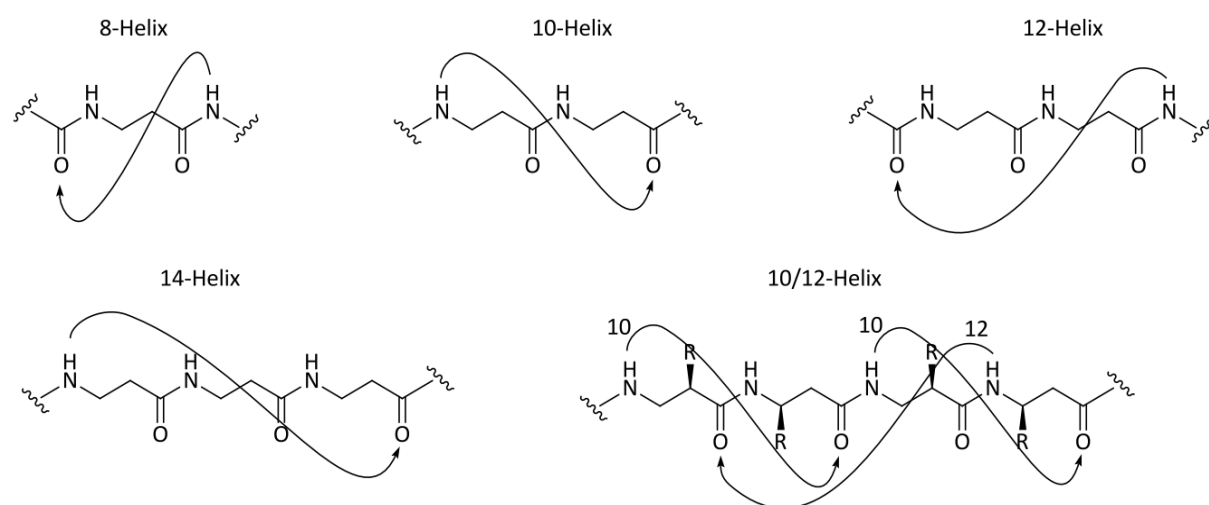


Figure 2.4: Possible intramolecular hydrogen-bond arrangements in β -peptides.^[3]

2.2.1 14-Helical Secondary Structure:

The 14-helical secondary structure is one type of the β -peptide conformations, which is stabilized by a hydrogen bond between an amide proton (N-H) at residue i and a main chain carbonyl (C=O) at residue $i+2$, creating a series of intercatenated 14-membered rings.^[1] Furthermore, the extended backbone length in the case of the 14-helix changes the array of side chains around the helical axis giving a rise to 3 residues per turn, compared to 3.6 residues in the case of the α -helix. Unlike the more widely splayed arrangement found in α -helix, this integer phase results in side chains that are stacked almost directly atop one another in three linear sides with side chains aligned at 120° intervals when viewed from top of the helix axis (Figure 2.5).

Similar to α -peptides, the intramolecular hydrogen bonds in β -peptides are stabilized by the presence of amide bonds; however, in the case of the 14-helix the amide carbonyl and NH groups project toward the N- and C-terminus, respectively, which result in a net macro-dipole opposite to that of the α -helix.

In terms of chirality, the 14-helix composed of L- β^3 -amino acids tends to be left-handed, rather than the typically right-handed configuration found in natural α -helical structures.

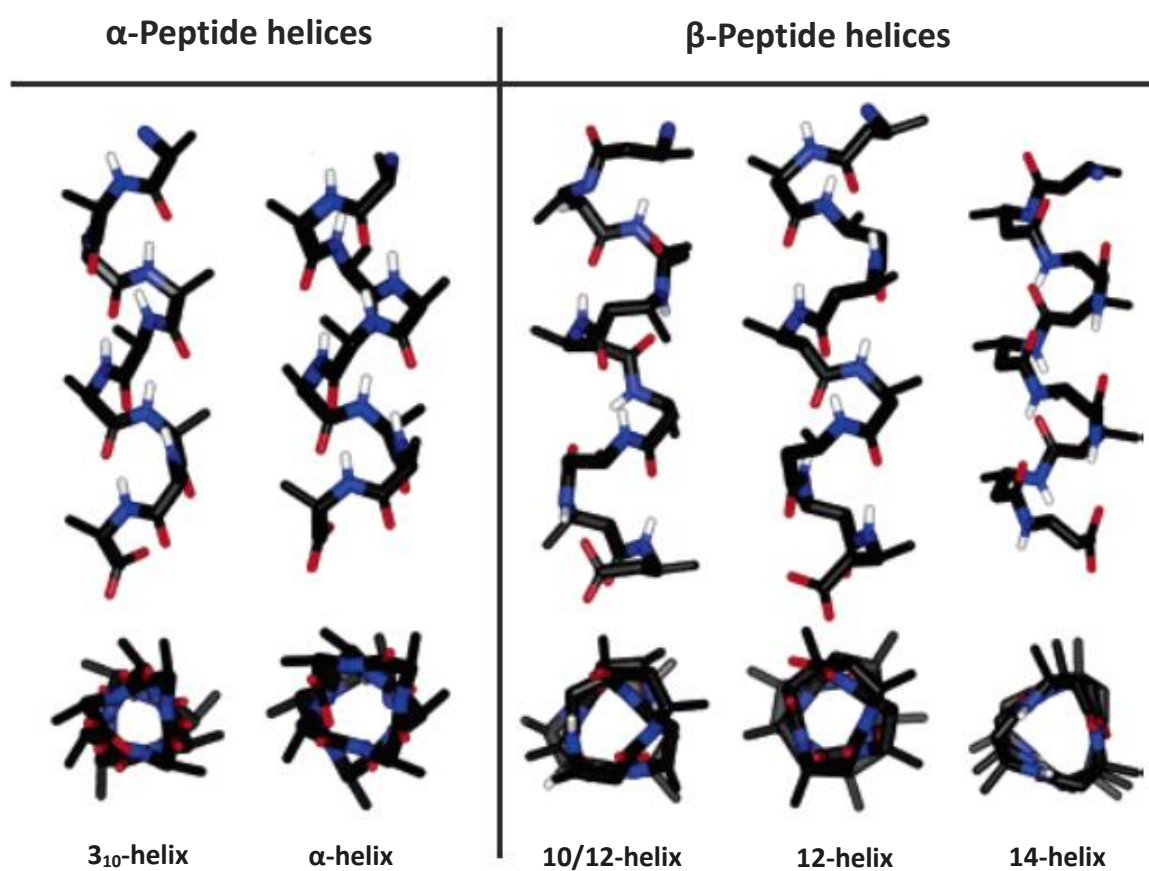


Figure 2.5: Lateral and top views of ideal α - and β -peptide helices. Carbon atoms are shown in black, oxygens in red, nitrogens in blue, amide hydrogens in white and other hydrogen atoms have been omitted for clarity.^[2]

Gellman's and Seebach's groups have been especially interested in studying the essential interactions contributing to the stability of β -peptide secondary structures based on different strategies. On the one hand, Gellman's group has focused on conformationally constrained residues that limit the degree of freedom between C_α and the C_β bonds by introducing cyclic β -amino acids such as the six-membered ring *trans*-2-aminocyclohexane carboxylic acid

(ACHC)^[83-86] and the five-membered ring *trans*-2-aminocyclopentanecarboxylic acid (ACPC).^[70,87-89] On the other hand, Seebach's group has pursued the design of β -peptides based on sequences with minimal conformational restrictions that display more resemblance to the natural α -peptides.

Table 2.1: Torsional angles and helical parameters of α -helix, 14-helix and 12-helix.

Structure	residue/turn	rise (Å)	radius (Å)	pitch (Å)	φ (°)	θ (°)	ψ (°)	ω (°)
α -helix ^[80]	3.6	1.5	2.2	5.4	-57	-	-47	180
14-helix ^[81]	3.0	1.6 (1.7) ^[90]	2.7	5 (5.2)	-134.3	60	-139.9	180
12-helix ^[82]	2.5 (2.7)	2.1 (2.2)	2.3	5.6 (5.9)	95.0	-94.3	103.0	-180

Gellman and coworkers showed that the oligomer **1** (Figure 2.6) with six ACHC units strongly favors the 14-helical conformation in solid state as well as in solution as indicated by crystallographic and NMR studies.^[83,84]

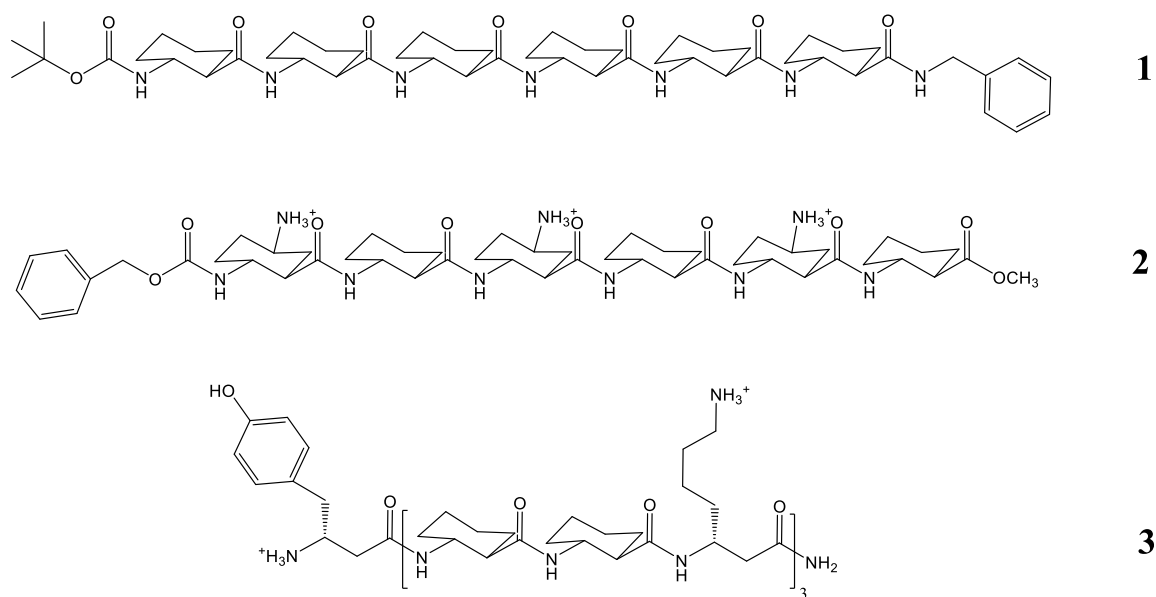


Figure 2.6: β -Peptide oligomers **1-3** were designed to achieve the formation of the 14-helix.

However, due to the high hydrophobicity of these residues, the utility of β -peptides containing a large proportion of ACHC in a biological context is very limited. To address this limitation and improve the solubility of these residues in aqueous media, one additional amino moiety has been inserted to the cyclic ring of ACHC resulting in the formation of DCHC (*R,R,R*-2,5-diaminocyclohexanecarboxylic acid) (oligomer **2**).^[92] Furthermore, they have reported a 10-residue β -peptide formed from the hydrophobic ACHC and the polar β^3 -Lysine rich sequence (oligomer **3**). These amphiphilic 10-residue β -peptide tends to adopt a stable 14-helix and forms soluble aggregates in a tetramer-hexamer size range in a buffered solution at pH 8 as judged by sedimentation equilibrium data.^[6]

Likewise, several studies from Seebach and his group have shed light on the rules governing the stability of the 14-helix. In 1996, they reported the first helical β -peptide consisting of six residues, which can characteristically fold into a 14-helix as assessed by CD, NMR and X-ray crystal-structure analysis (oligomer **4**).^[93]

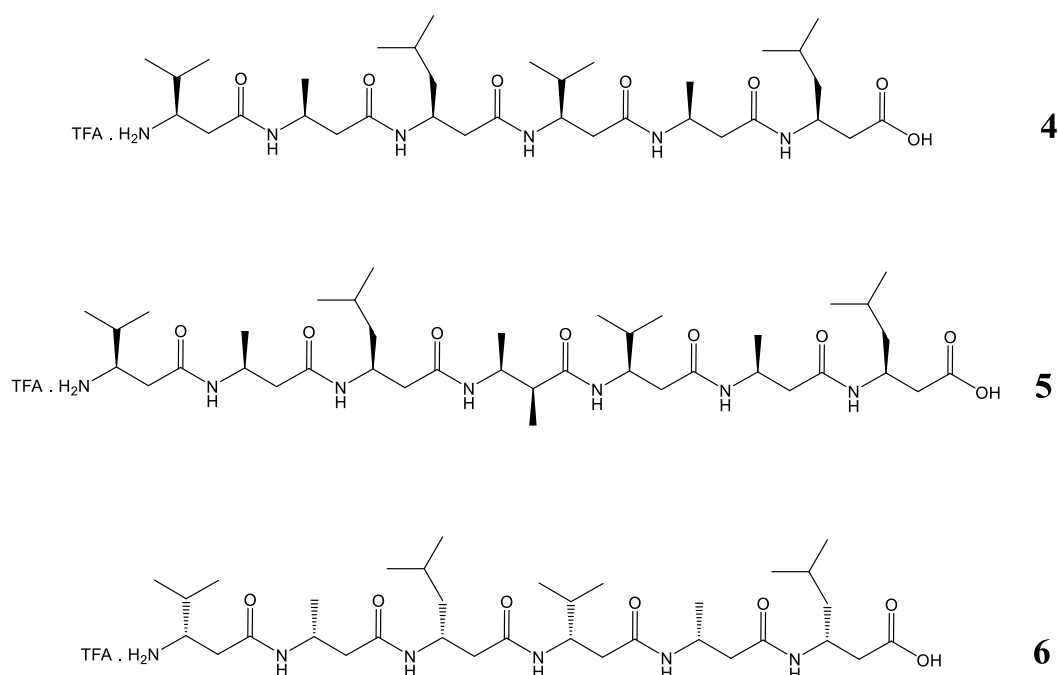


Figure 2.7: β -Peptide oligomers **4-6** composed of β -amino acids that fold into a 14-helical structure.

Subsequently, they synthesized a series of β -peptides derived from the oligomer **4** in order to explore the structural characteristics that control the stability of the 14-helix including oligomers **5** and **6** (Figure 2.7). In the case of oligomer **5**, they added the residue $\beta^{2,3}$ -Alanine

($\beta^{2,3}$ -Ala) in the central position of the sequence, whereas in the case of oligomer **6** they altered the stereochemistry of the β -amino acids.^[67,94]

The 14-helix is a very distinctive conformation since the residues projected from the positions i and $i+3$ are quite near to each other (4.8 Å) and nearly parallel to one another, which is similar to the β -sheet structure among conventional peptides (Figure 2.5). Consequently, the geometry of the 14-helix is considered as a key element to increase the extent of its stability by introducing covalent and non-covalent interactions between the side chain juxtapositions.^[95] In 2001, Seebach demonstrated that the formation of salt-bridges within a water-soluble β -heptapeptidic helix by introducing two pairs of β^3 -homomornithine and β^3 -homoglutamic acid residues having an opposite charge can enhance the stability of the 14-helical conformation in methanol as indicated by NMR structural data and CD analysis (oligomer **7**).^[98] Independently, Cheng *et al.* have reported that the electrostatic interactions between the side chains of acyclic β -residues at position i and position $i+3$ can be used to increase the stability of the 14-helix of a 15-mer β -oligomer **8** in water.^[99]

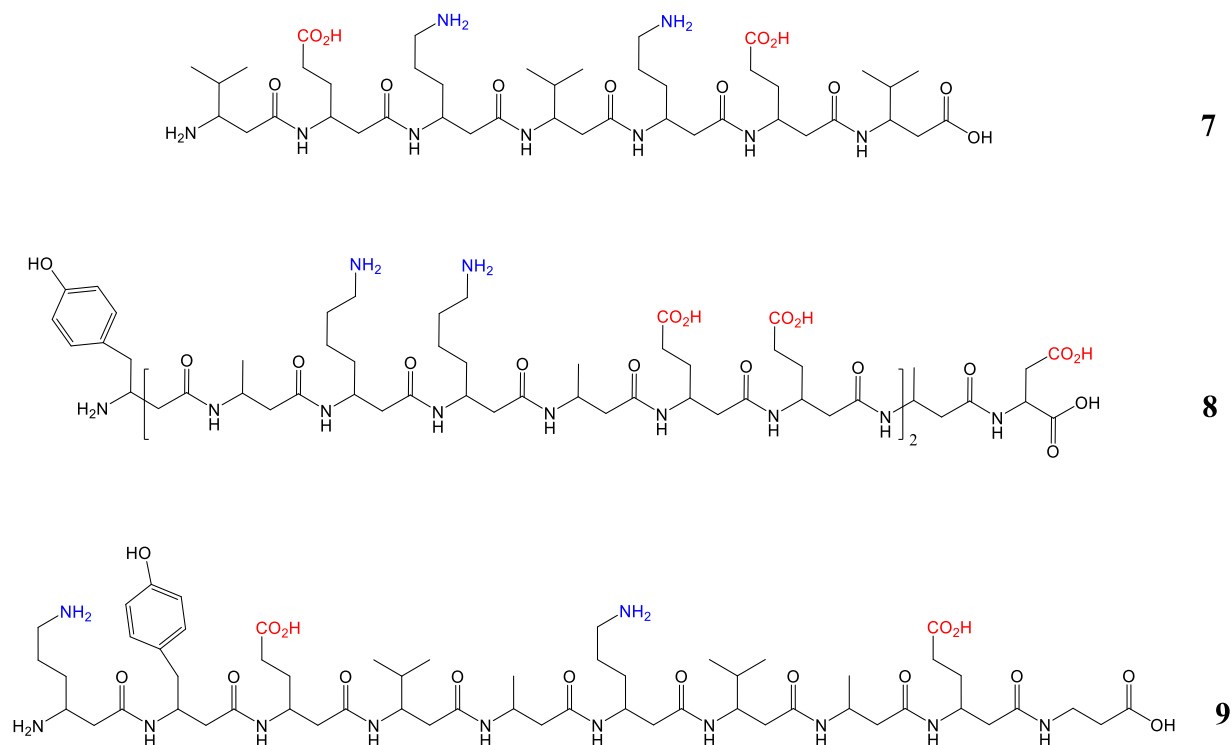


Figure 2.8: β -Peptide oligomers **7-9** were designed to explore the stability of the 14-helix.

In comparison between the oligomers **7** and **8** (Figure 2.8), Seebach's β -peptide **7** (with 7 residues) is shorter than Cheng's β -peptide **8** (with 15 residues) and contains a less number of salt-bridges, thus it is not surprising that the latter is more stable as evidenced by CD spectroscopy. Additionally, it was demonstrated from both oligomers **7** and **8**, that changing the salt concentration or pH value of the buffer can significantly decrease the overall structure of the 14-helix, suggesting the powerful role of electrostatic interactions in stabilizing the 14-helix. Thereafter, Hart *et al.* have demonstrated that the extent of 14-helicity in β -undecapeptides can be increased in a different but complementary manner by replacing charged amino acids to minimize the overall macro-dipole of the 14-helix in water (oligomer **9**).^[100]

Another impact of side-chain pattern on the conformation preference in the case of the 14-helix has been addressed by Ruepling and coworkers, indicating that the disulfide bridge between two cysteine side chains in positions i and $i+3$ strongly stabilize the 14-helix.^[96] In the same way, DeGrado and coworkers have shown that stapling two 14-helices together *via* a disulfide bond showed a greater degree of 14-helicity relative to their monohelical counterparts by cooperatively stabilizing the secondary structure *via* a hydrophobic interaction interface between the covalent dimer (Figure 2.9).^[97]

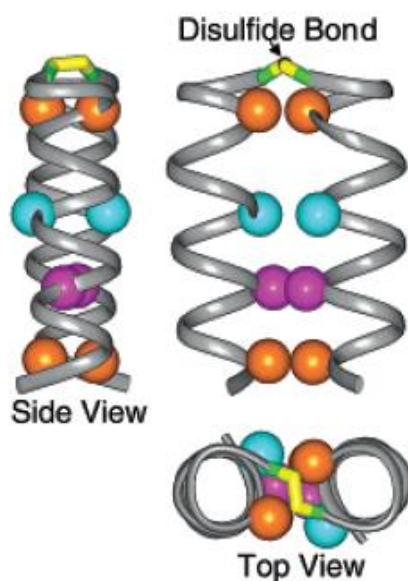


Figure 2.9: schematic illustration of a disulfide-crosslinked parallel β -helical bundle with polar amino acids (colored spheres) that interact at the helical interface.^[97]

2.2.2 12-Helical Secondary Structure:

Gellman et *al.* have demonstrated that the cyclohexyl AHC can stabilize the θ torsional angle to a value of about $\pm 60^\circ$, which can precisely stabilize the 14-helical conformation. However, using the cyclopentyl ring of ACPC instead of AHC biases θ toward higher values rendering a novel helical shape, the 12-helix, as the most appropriate helical conformer (Figure 2.10).^[70]

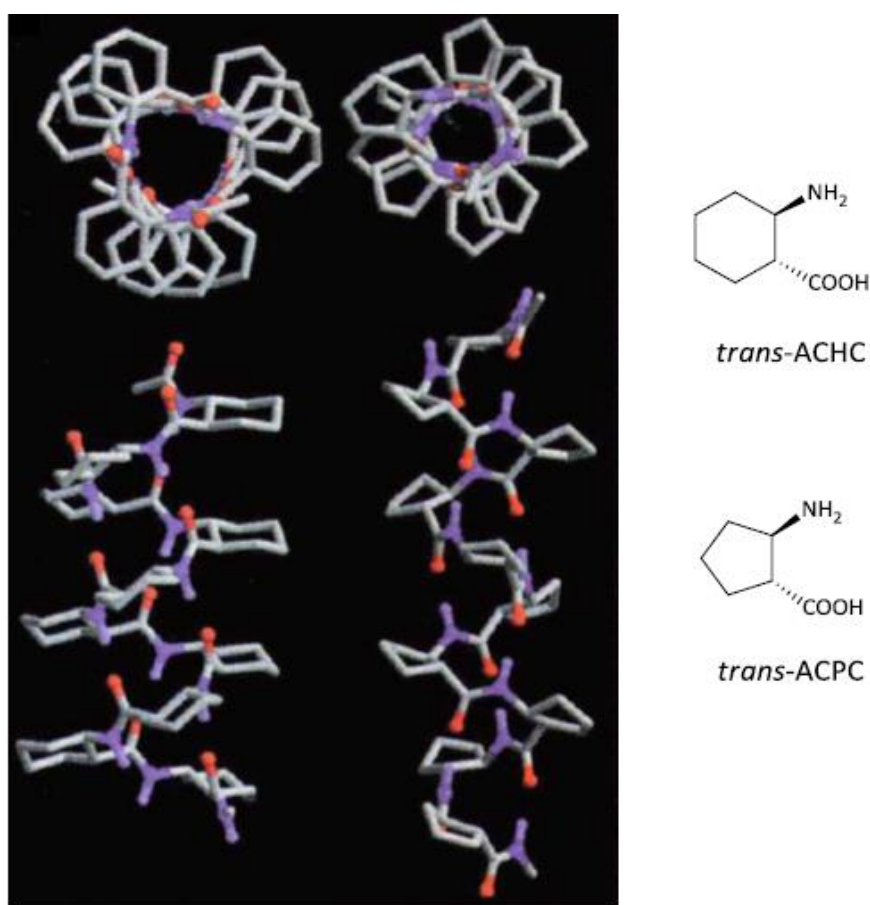


Figure 2.10: Top and perpendicular views of the 14-helix decamer consisting of *trans*-AHC (left) and the 12-helix decamer consisting of *trans*-ACPC (right).^[70]

The 12-helix is stabilized by hydrogen bondings between the backbone amides at positions i and $i+3$. It consists of approximately 2.5 residues per turn and exhibits the same dipole moment as the α -helix, with amide protons exposed from the N-terminus of the helix (Figure 2.5 and Table 2.1). In organic solvents, the 12-helical conformation of a β -peptide containing as few as six ACPC residues is very stable. However, β -peptides composed solely of these apolar residues are not soluble in aqueous solutions. To overcome this problem, additional

pyrrolidiny amino acid *trans*-3-aminopyrrolidine-4-carboxylic acid (APC) was introduced to the β -peptides along with ACPC building blocks (oligomers **10-12**).^[101]

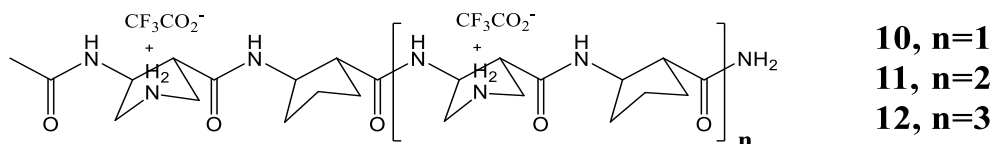


Figure 2.11: Chemical structure of oligomers **10**, **11** and **12**.

Using CD spectroscopy, it has been shown that a sequence containing as few as four ACP residues can fold into a 12-helical conformation in aqueous solution. Moreover, the propensity of the heterocyclic APC residues to fold into 12-helix is as high as their carbacyclic ACPC analogues.

2.2.3 Other Conformations of β -Peptides:

Besides the more prevalent 14-helix and 12-helix, Seebach and his group have demonstrated that a short β -peptide with six alternating β^2 - and β^3 -amino acids can adopt a 10/12-helical motif (Figure 2.4).^[68] In opposite to the uniform alignment of amide bonds in the case of the 14- and the 12- helical axis (Figure 2.5), the 10/12 helix is featured by an intertwined network of 10- and 12- membered hydrogen-bonded rings. Additionally, this helix shows two types of amide bond orientations, resulting in a nullified macro-dipole moment. In addition to the well-defined helices described above, other helical structures have also been detected in β -peptides, including 10-, 8-, 16-, 18- and 20-helix.

More recently, Fleet et al. have investigated a β -hexapeptide, in which the peptide backbone was constrained by monomers with four-membered oxetane rings (Figure 2.12A). The two-dimensional NMR studies with molecular mechanics conformational analysis reveal that this β -hexapeptide tends to fold into a well-known left-handed helical conformation stabilized by 10-membered hydrogen-bonded rings.^[102]

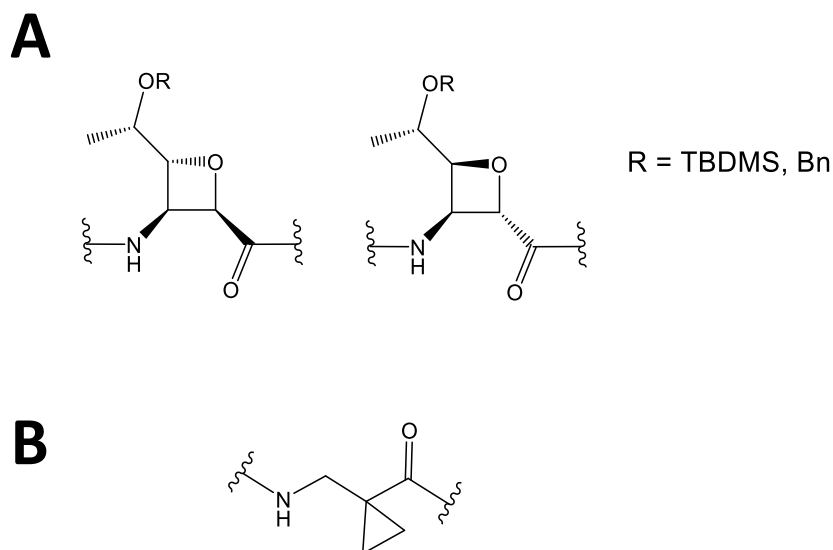


Figure 2.12: Molecular structure of A) oxetane ring β -amino acids and B) 1 (aminomethyl)cyclopropanecarboxylic acid.

Additionally, the 8-helical conformation was determined by Abele *et al.* for short oligomers containing a chain of the achiral monomer 1-(aminomethyl) cyclopropanecarboxylic acid as detailed by X-ray crystal structural data (Figure 2.12B).^[112] The obtained results indicate that longer oligomers of this type might adopt regular eight-membered ring hydrogen bonds that would be characterized by approximately two residues per turn.

Apart from the known helical conformations, β -peptide foldamers are also able to adopt sheet-like secondary structures. For example, a β -polypeptide composed of solely β -alanine residues can be crystallized as an extended sheet-like structure^[104]; however, it showed a disordered structure in solution.^[105]

As presented in Figure 2.13, sheet conformations of β -peptides can be mainly divided into two types, in which the residue adopts either an anti C_{α} - C_{β} or a gauche C_{α} - C_{β} torsion angle. Similar to β -sheets formed by α -peptides, β -peptide sheet formed by amino acids with gauche C_{α} - C_{β} torsion angles would lack a net dipole since the backbone carbonyls alternate in direction along each strand. However, this is not the case for β -peptide sheets formed by anti C_{α} - C_{β} torsion angles because all the carbonyls in the backbone are oriented in nearly the same direction, hence, giving a net dipole for the resulting sheet.^[106]

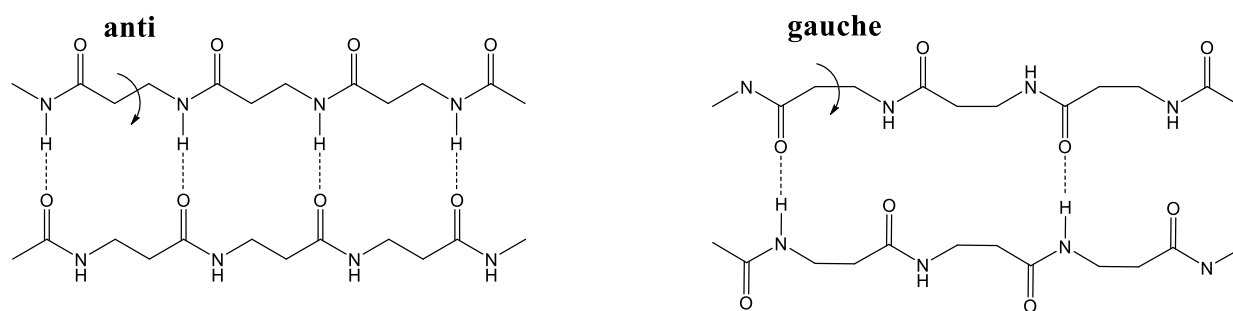


Figure 2.13: The two types of antiparallel β -peptide sheet structures in which the residues adopt either an anti C_{α} - C_{β} torsion angle (left) or gauche C_{α} - C_{β} torsion angle (right).

2.3 Biological Functions of β -Peptides

Due to their controllable structural motifs, β -peptides are ideal biomimetic polymer scaffolds that allow the design of sequences with promising activities and highly interesting in diverse biomedical applications. Especially the 14-helix provides an appropriate patterned backbone that has been widely used by many research groups as a target to arrange amphiphilic sequences. In fact, Seebach and co-workers have shown that there is a correlation between the ability of β -peptides to fold into stable 14-helical foldamers in methanol and their inhibitory effect on sterol and lipid absorption.^[107] They introduced first-generation models of short amphiphilic 14-helices capable of mimicking the biological activity of natural peptides by inhibiting cholesterol and fat uptake in human colonic carcinoma cells. Despite having less potent inhibitory effect compared to their α -peptide analogues, these bioactive β -peptides consist of a much smaller number of residues and are targeted to a specific receptor-mediated process. Besides, it has been demonstrated that β -peptides are stable towards proteolytic degradation *in vitro* as well as *in vivo*,^[93,108,109] and they have the ability to penetrate cell membranes to be localized within the cell nuclei.^[110-113] Thereby, β -peptides should be considered as promising new-generation therapeutic models in the medicinal viewpoint.

Understanding the effect of hydrophobic/hydrophilic balance, chain length and helix-forming potential is highly important to optimize the selectivity and the affinity of α -helical antibacterial peptides.^[114] In a similar way, the design of β -peptides with graded amphiphilicity and helix stability would be interesting in order to allow optimization of their affinity and selectivity. Taking the advantageous geometry of the 14-helix into account, DeGrado *et al.* have described the design of positively charged β -peptides that have the ability to mimic the

activities of a class of biological membrane-active peptide toxins and antibiotics (Figure 2.14).^[115]

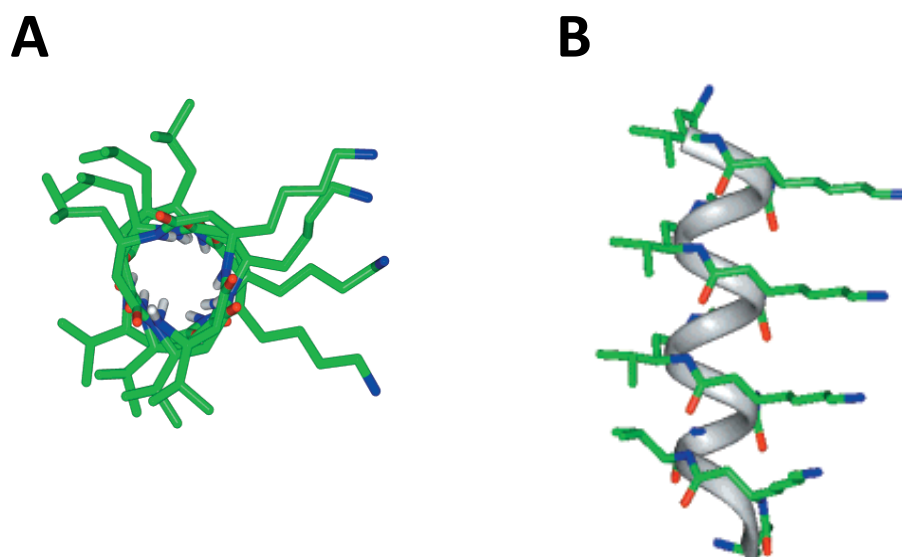


Figure 2.14: A) The top^[115] and B) the side^[116] views of an amphiphilic β -peptide containing β^3 -Val, β^3 -Leu and β^3 -Lys. Carbon atoms are shown in green, nitrogens in blue, and oxygens in red.

The biological activities of these β -peptides were tested using human erythrocytes as models for mammalian cells and *Escherichia coli* as models for bacteria. The data have shown that these compounds were capable of suppressing bacterial cell growth by disrupting the structural integrity of their phospholipid membranes. Although these β -peptide first-generation models were reasonably active with IC_{50} values in the minimal micromolar range, they generally showed poor discrimination between bacteria *versus* mammalian cells. In further studies, they have optimized the hydrophobicity of these β -peptides by changing the hydrophobic β^3 -Val and β^3 -Leu by the less hydrophobic β^3 -Ala, which resulted in significantly improved selectivities and potencies.^[116]

In the same way, the design of antimicrobial β -peptides that can form 12-helical conformations rather than 14-helices was possible by using the oligomer **13** (Figure 2.15), which contains both, positively charged APC and hydrophobic ACPC residues.^[117] These β -peptides are highly potent and very specific towards bacteria, exhibiting an excellent activity against four bacterial species including two pathogens, which are resistant to common antibiotics.

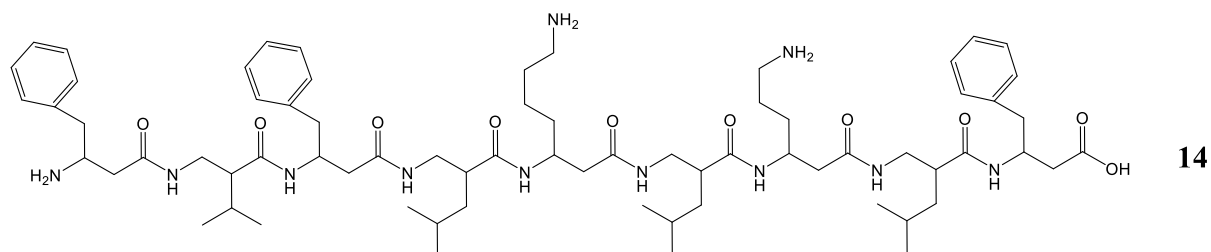
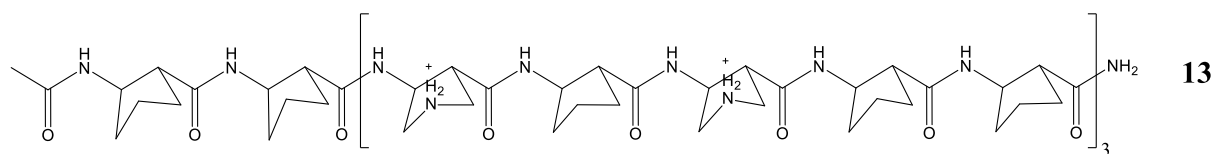


Figure 2.15: β -Peptide oligomers **13** and **14** were designed to investigate the biological activity of the 12-helix in the case of the oligomer **13** and the 10/12 helix in the case of the oligomer **14**.

Regarding the 10/12 helix, the bioavailability of β -peptides formed by alternating β^2 - and β^3 -amino acids is expected to be notably enhanced due to the lack of a net macro-dipole moment. Thus, Seebach and his group have revealed that the β^2/β^3 -nonapeptide (oligomer **14**) can adopt an amphiphilic right-handed 10/12/10-helix, showing a remarkable antibacterial activity towards some of the investigated micro-organisms.^[118]

3 Design and Synthesis of β -Peptides

3.1 Design of β -Peptides

Transmembrane (TM) proteins are abundantly found in nature and account for about 20-30% of the open reading frames of the exemplary genomes.^[121,122] However, the three-dimensional structure of membrane proteins is still poorly understood. It has long been recognized that helix-helix interactions play a key role in stabilizing membrane proteins.^[45] In this regard, several studies pointed out the importance of tight packing and specific residues to better investigate helical association of membrane proteins.^[123,124]

Recently, β -peptides are of major interest in the field of self-organizing systems due to their tendency to form side-chain-controllable compact conformations and by virtue of the wide range of their potential applications in the medicinal domain.^[68,125-128] Using the special pattern of β -peptides, the major goal of this study is to better understand the function and the mobility of transmembrane proteins by electrostatically stabilizing their tertiary structures using non-covalent interactions. Generally, the stability of a protein tertiary structure depends strongly on the number, size and arrangement of its residues. Therefore, the judicious choice of amino acids allows the formation of helices with well-defined conformations that can be used as templates for directing the spatial arrangement of peptides.

The unique side chain alignment of the 14-helical secondary structure was exploited by several researchers to orient the formation of helical bundles (see section 2.2). This helix is obtained by using β -amino acids having lateral substituents in β -position or by using the cyclic AHC amino acid.^[127] On the other side, the β -peptide 12-helix merits a particular attention as it bears some similarity to the natural α -helix commonly formed by conventional peptides.^[11] All these convenient characteristics suggest that both 14- and 12-helices might be reasonable platforms for molecular recognition. Hence, the choice of the sequences in this study is based on the formation of stable 14- and 12-helices as they can offer rigid and well-known patterns. For this purpose, the sequences **P0** and **P5** were designed to achieve the formation of 14- and 12-helix, respectively (Figure 3.1). Subsequently, these two sequences were used as initial references to design other sequences bearing residues that can create an additional force to drive helix-helix assembly in a regular way. Taking into account that these β -peptides will be used as TM model proteins, the transmembrane-buried part of these sequences was mostly

composed of hydrophobic amino acids. However, many TM proteins in nature might contain polar amino acids that contribute to helix-helix interactions, co-factor binding, etc.^[120]

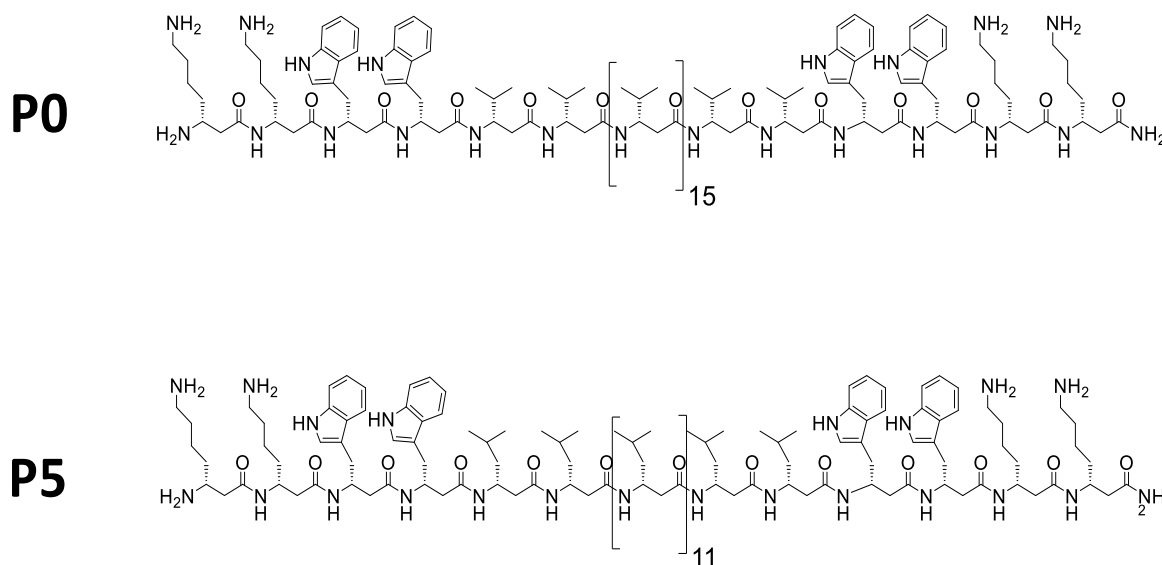


Figure 3.1: Molecular structure of the β -peptides **P0** and **P5**.

3.1.1 Structural Design of the 14-Helix

The oligomer **P0** was basically designed to promote the formation of 14-helical backbone. This structure would display a well-explained scaffold that can be used to incorporate recognition units, which in turn would instigate the helices association driven by hydrogen bonding. As illustrated in Figure 3.1, the membrane-spanning region of **P0** possesses a long chain containing 19 residues of hydrophobic β^3 -valines (β^3 -Val) followed by the presence of two β^3 -tryptophans (β^3 -Trp) and two β^3 -lysines (β^3 -Lys) at each end of the sequence.

The choice of β^3 -Val was guided by the notion that these residues can efficiently enhance the extent of β -peptides to fold into a stable 14-helical motif. Indeed, studies from several research groups demonstrate that the use of these aliphatic side chains induces the 14-helicity in different aqueous solutions.^[100,115,131,132] Furthermore, the length of the hydrophobic stretch of β -peptide **P0** was adjusted to match the apolar region of the lipid model system used in this study, which composed of 1-palmitoyl-2-oleoyl-*sn*-glycero-3-phosphocholine, POPC (Figure 3.2) .

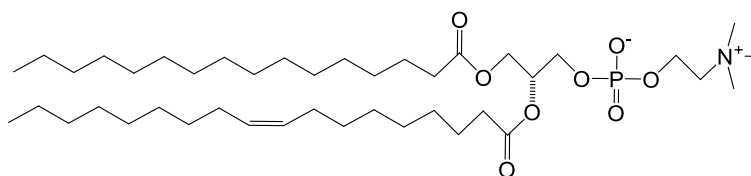


Figure 3.2: Chemical structure of POPC (1-palmitoyl-2-oleoyl-*sn*-glycero-3-phosphocholine).

The interfacial region of **P0** was further enriched by the addition of two aromatic side chains β^3 -Trp. This was inspired from the structure of Gramicidin A (gA), a small Trp-flanked ion channel that has been broadly explored in membrane environment.^[23,52,133,134] Generally, the indole side chain of Trp appears to localize in the interface of the membrane.^[137] On the one hand, it consists of a hydrophobic aromatic ring that might be preferentially positioned in the apolar region of the lipid bilayer. The amide group linked to the aromatic ring of Trp confers polarity and considerable dipole moment to the overall side chain and thereby, it is expected to be localized in the more polar environment at the polar-apolar region.^[34] These versatile molecular properties of Trp render it as an ideal amphiphilic residue to anchor and stabilize the peptide in the membrane-water interface since its indole N-H-moiety exhibit a great electrostatic potential for cations- π interactions and capable of hydrogen bond donation.^[135] Since most biological events occur in aqueous media, it was highly desirable to add polar amino acids in order to increase the solubility of **P0** in aqueous solutions. Thus, two molecules of β^3 -Lys were attached to flank the hydrophobic stretch of **P0** on both N- and C-terminus. This polar amino acid has a relatively long and flexible aliphatic side chain that is ended with a positively charged amine. The flanking β^3 -Lys side chains are expected to extend into the polar interface around the lipid phosphate group or more precisely towards the water-membrane interface.^[34,136]

In summary, the particular choice of the molecular composition of **P0** implies that this foldamer has the ability to show a 14-helical secondary structure, which offers a well-designed scaffold by containing three spatial streaks stacking almost directly atop one another (Figure 3.3 right).

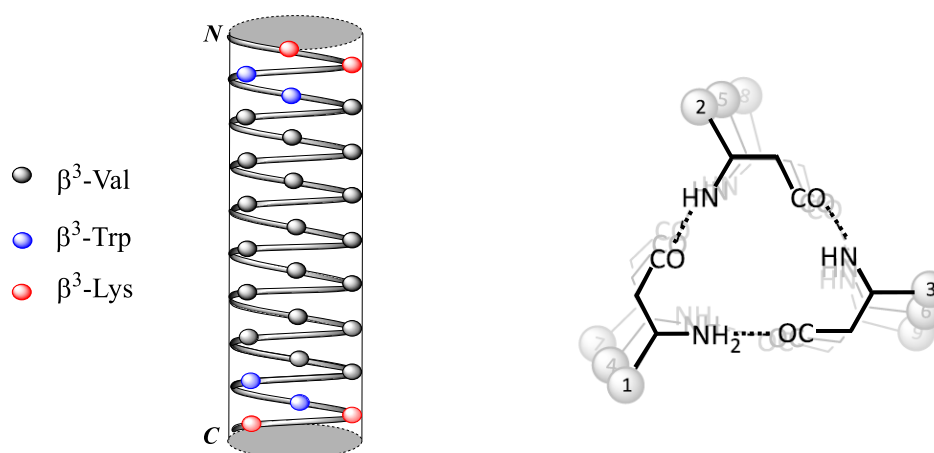


Figure 3.3: Left) Schematic illustration of **P0** and right)^[138] top view of the 14-helix.

The advantageous structure of 14-conformations is expected to form an appropriate helical-wheel representation to specifically introduce residues capable of creating covalent and non-covalent interactions that can successively mediate the association of the transmembrane helices.

Interhelical hydrogen bonds within TM proteins are thought to play a dynamic role by improving the stability and the specificity of TM helices association.^[59] However, structural contributions of polar residues in the membrane are less well understood. Interestingly, studies from DeGrado and Engelman have demonstrated that the insertion of residues with polar side chain such as Asn, Gln, Asp or Glu can strongly promote helix-helix association of α -helices in both micelles and biological membranes *via* side chain-side chain hydrogen bonding.^[49,50,59] Based on the same concept, we have specifically placed the polar β^3 -glutamines (β^3 -Gln) within the foldamer **P0** to investigate whether the interhelical hydrogen bond created by the side chains of these residues can drive organized self-assembly of the 14-helices. For this reason, the buried β^3 -Val molecules across one linear side of **P0** were specifically substituted at positions i and $i+3$ by one, two and three β^3 -glutamines (β^3 -Gln) resulting in the formation of the β -sequences **P1**, **P2** and **P3**, respectively (Figure 3.4).

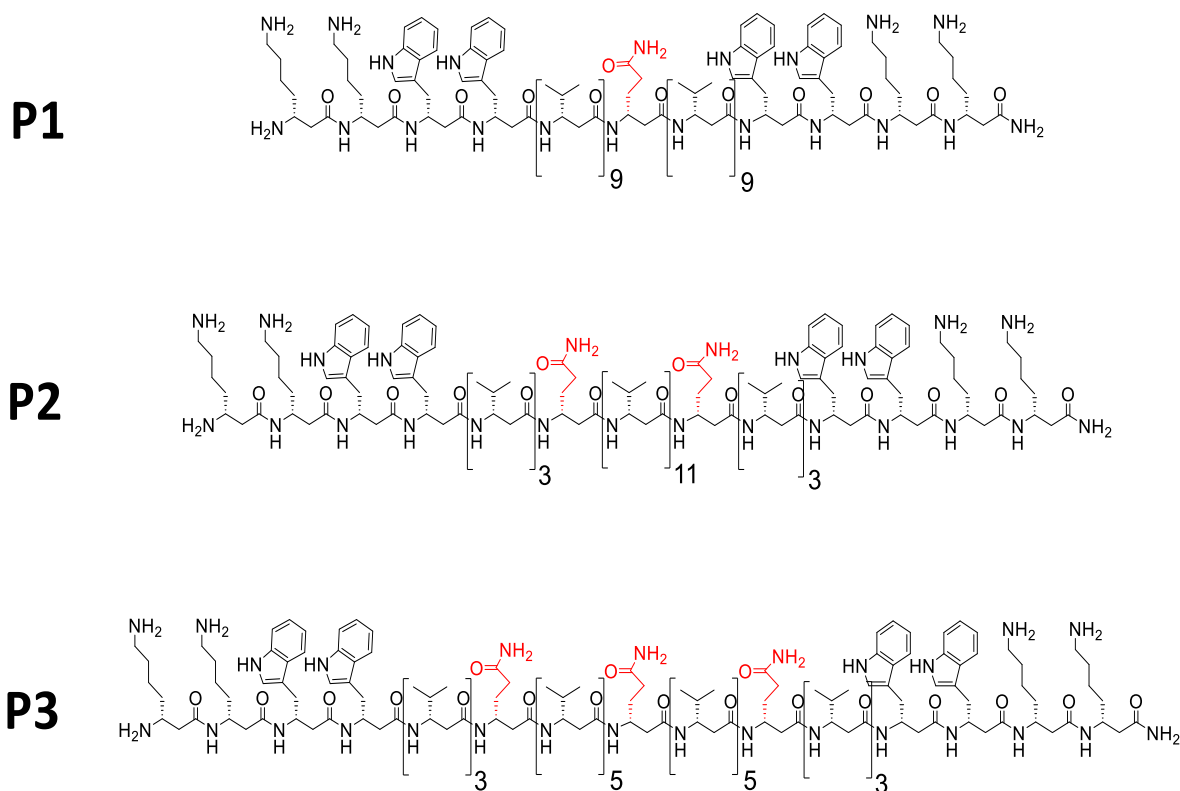


Figure 3.4: Molecular structure of the helices **P1** (with one β^3 -Gln), **P2** (with two β^3 -Gln), **P3** (with three β^3 -Gln).

The polar Gln residue is among the amino acids containing a side chain that can characteristically act as both hydrogen bond donor and acceptor, resulting in homo-aggregation of the helices (Figure 3.5).

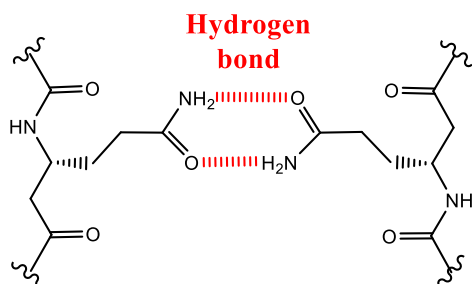


Figure 3.5: Hydrogen bonding resulted from interactions between the polar side chains of the β^3 -Gln.

Similarly, it has been also demonstrated that including polar asparagines (Asn) within the helices can result in their self-assembly due to hydrogen bond interactions. ^[49,50,59] However,

the side chain of Gln is more flexible than Asn by having one additional CH_2 -moiety rendering the former more suitable choice in this study.

Additionally, the inclusion of β^3 -Gln was performed in such a way to fulfill a symmetrical distribution of these residues within the 14-helices with the aim to facilitate hydrogen bonding interactions in either parallel or anti-parallel mode of oligomerization (Figure 3.6).

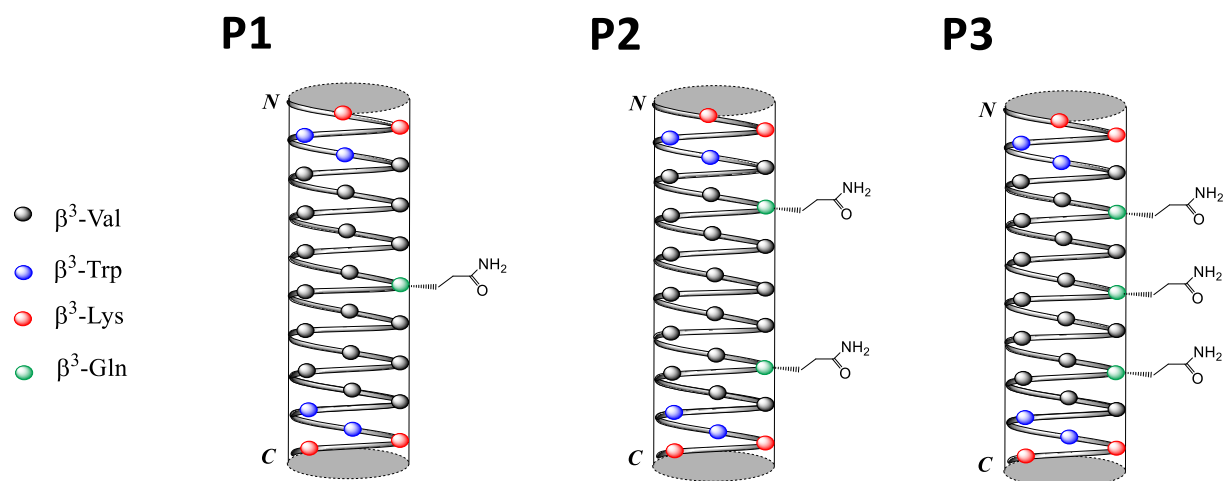


Figure 3.6: Schematic illustration of the helices **P1** (with one β^3 -Gln), **P2** (with two β^3 -Gln) and **P3** (with three β^3 -Gln).

The concept of high organization of the 14-helical backbone can be further extended by positioning recognition units not only in one side of the 14-helix but also in two sides. To this end, two sides of the sequence **P0** were subsequently functionalized by substituting two molecules of the buried β^3 -Val in each side with the polar residues β^3 -Gln, generating the sequence **P4** (Figure 3.7).

The architecture of the helix **P4** can easily facilitate the formation of hydrogen bond between β^3 -Gln side chains across turns of the helix, which might be featured by creating a system with higher order aggregates. Nevertheless, the exact number of the subunits existing in the same oligomer strongly depends on the distribution of β^3 -Gln residues, the overall geometry of the helix and the parallel anti-parallel orientation mode of the helices.

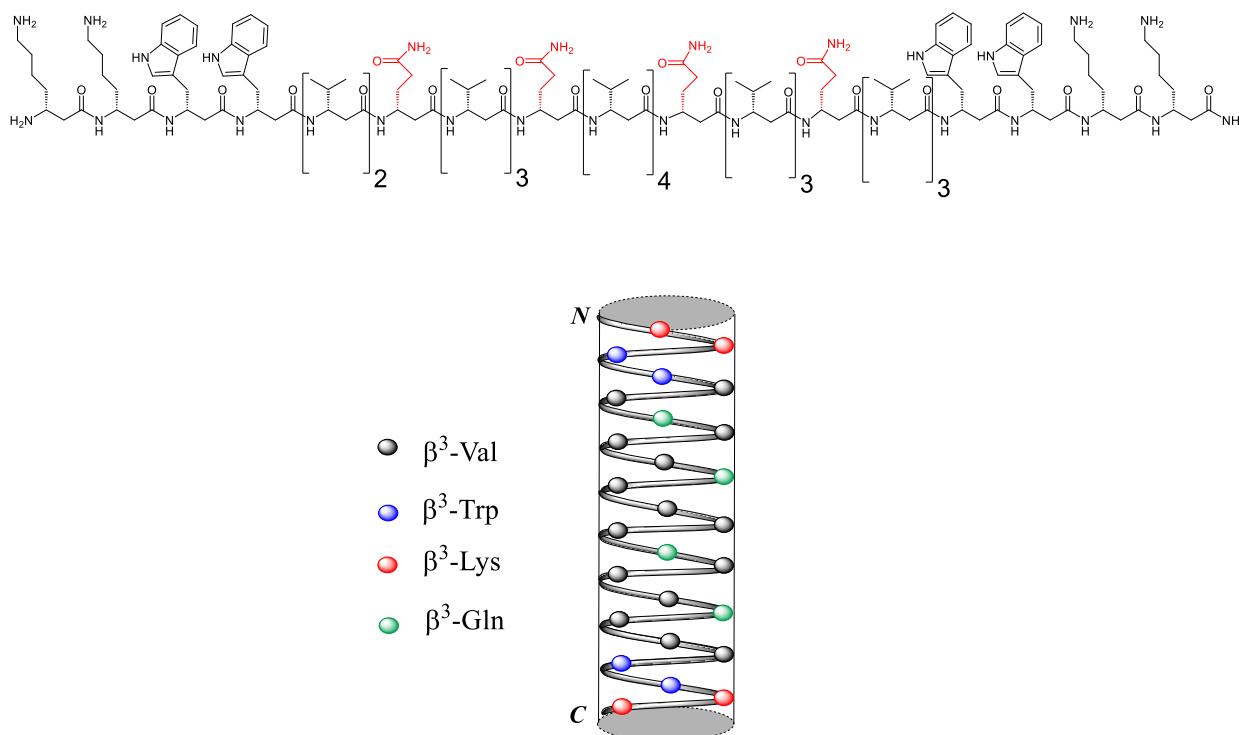


Figure 3.7: Top) Molecular structure of **P4** containing four β^3 -Gln and bottom) Schematic illustration of the helix **P4**.

3.1.2 Structural Design of the 12-Helix

In analogy to **P0**, the β -peptide **P5** was designed to fold into a 12-helical conformation. It is well known that the structural conformation of the 12-helix differs widely from that of the 14-helix in many aspects (see section 2.2). For instance, in the case of the 12-helical secondary structure, the length of the helix is greater than that of the 14-helix and therefore, it was required to decrease the number of the amino acids forming the hydrophobic stretch of the helix to match the apolar region of the lipid bilayer POPC. Thus, 15 hydrophobic β^3 -leucines (β^3 -Leu) amino acids were sufficient to form the hydrophobic core of the β -peptide **P5**.

In contrast to β^3 -Val, it has been observed that the use of β^3 -Leu tends to decrease the stability of the 14-helical secondary structure^[2] and, instead increases the tendency of the β -peptides to fold into 12-helical conformations.^[132,139] Keeping the same concept as in the case of **P0**, β^3 -Trp and β^3 -Lys were positioned to flank the hydrophobic stretch of **P5** (Figure 3.8 left).

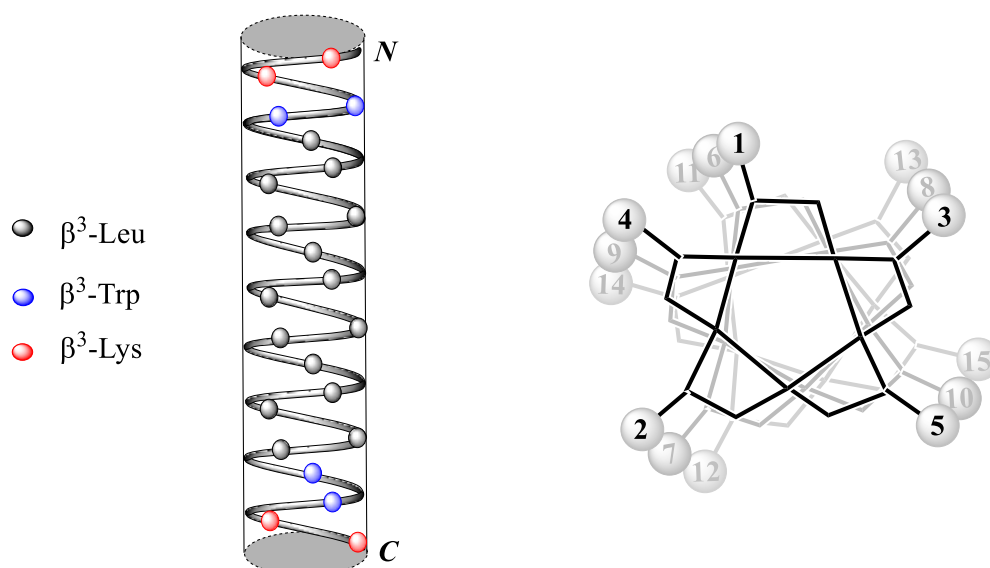
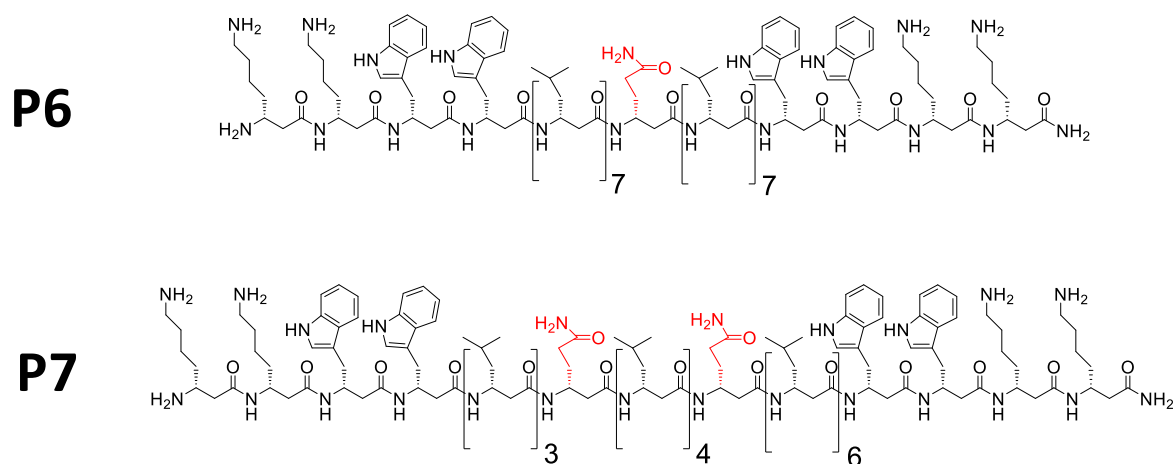


Figure 3.8: Left) Schematic illustration of **P5** and right) projection along the 12-helical axis assuming 2.5 residues per turn.

The conformational properties of the 12-helix restrict the placement of functional groups at specific sites along the helix, which render the inclusion of β^3 -Gln residues more challenging since the three-dimensional arrangement of this helix is more splayed in the space compared to the 14-helix by having approximately 2.5 residues per turn (Figure 3.8B).^[130] For this reason, one, two and three β^3 -Leu were substituted within the helix **P5** at positions i and $i+5$ (every two turns) to generate the helices **P6**, **P7** and **P8**, respectively (Figure 3.9).



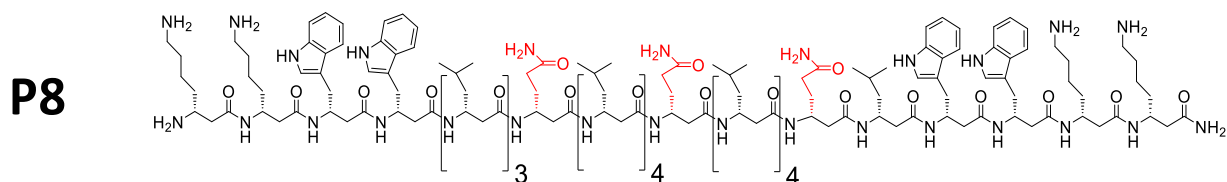


Figure 3.9: Molecular structure of the helices **P6** (with one β^3 -Gln), **P7** (with two β^3 -Gln), **P8** (with three β^3 -Gln).

Undesirably, the architecture of the 12-helical scaffold prevents the symmetrical distribution of β^3 -Gln amino acids within the helix, which means that hydrogen bond interactions within the β^3 -Gln side chains along the 12-helices might be limited by the parallel orientation of the sequences (Figure 3.10).

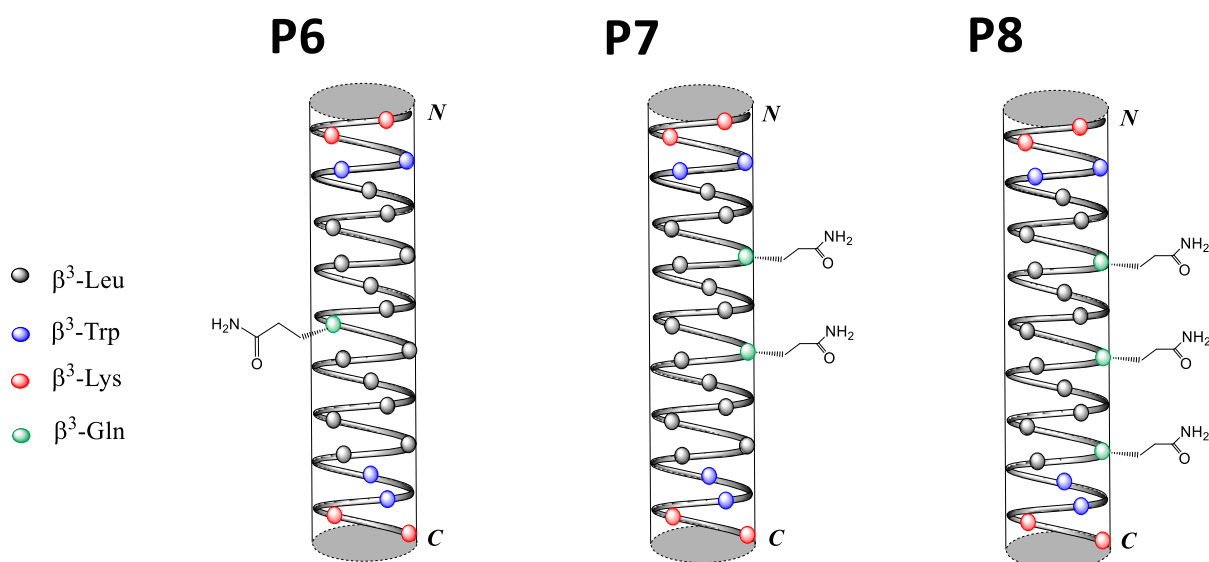


Figure 3.10: Schematic illustration of the helices **P6** (with one β^3 -Gln), **P7** (with two β^3 -Gln) and **P8** (with three β^3 -Gln).

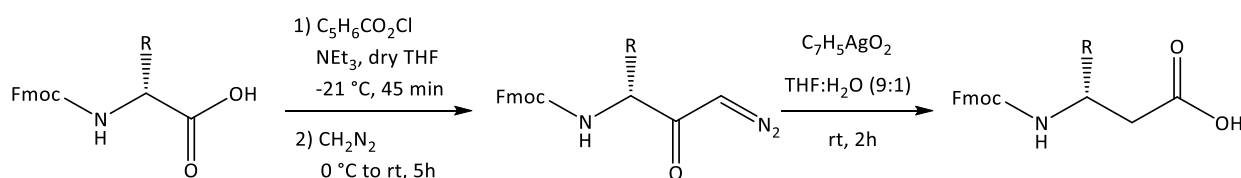
3.2 Synthesis of β -Peptides

3.2.1 Synthesis of D- β^3 -Amino Acids

D- β^3 -Amino acids were readily prepared in very good yields from their D- α -amino acid counterparts through *Arndt-Eistert* homologation.^[78,138,150,151] This method leaves the stereocenter at the α -carbon intact and precisely inserts a CH_2 -group into the amino acid backbone.

Thus, the resulting D- β^3 -amino acids were enantiomerically pure and no racemization has been observed. As a first step, the D- α -amino acids were reacted with isobutyl chloroformate to obtain the activated esters. Then, the diazoketones were afforded by the subsequent nucleophilic attack of diazomethane (added as an ethereal solution) at the activated carbonyl centers as presented in Scheme 3.1. Finally, Wolff rearrangement was catalyzed by adding silver benzoate to the diazoketones, giving rise to the finale D- β^3 -amino acids after releasing N₂-group.

The D- β^3 -Lys, D- β^3 -Trp and D- β^3 -Gln were orthogonally protected with different protecting groups to avert undesirable side reactions.



Scheme 3.1: Synthetic approach for the preparation of D- β^3 -amino acids from their D- α -amino acid counterparts using *Arndt-Eistert* reaction.

3.2.2 Synthesis of β -Peptides

The β -peptides have been synthesized manually using a microwave-assisted Fmoc-solid-phase peptide synthesis (SPPS).^[2,89,132,142] Usually, both the synthesis and purification of β -peptides that contain approximately more than 10 residues in length can be difficult, especially in the case of very hydrophobic β -sequences. Nevertheless, the method adopted in this study allowed the preparation and the purification of the target foldamers by modifying some conditions during the β -peptides synthesis. Thus, two different methods have been adopted, first for β -peptides containing a large amount of β^3 -Val and second for β -peptides containing a large amount of β^3 -Leu. A schematic representation for the stepwise synthesis of β -peptides containing β^3 -Val using MBHA rink amide resin (loading capacity of 0.57 mmol/g) is shown in Figure 3.11.

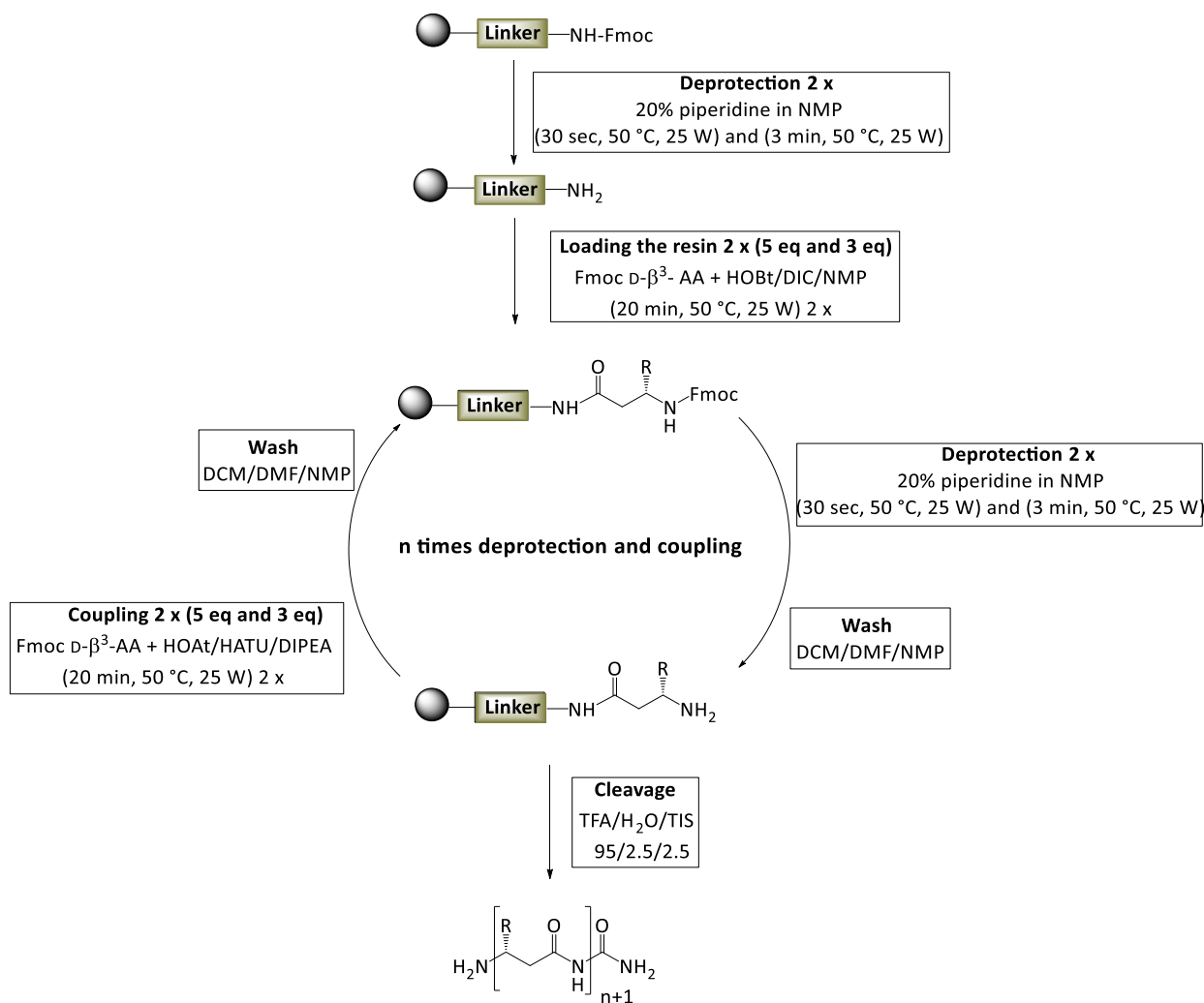


Figure 3.11: Stepwise Fmoc-based solid-phase peptide synthesis (SPPS) for β -peptides on MBHA resin amide resin.

The synthesis of these sequences began with loading the resin with D- β^3 -Fmoc-Lys(Boc)-OH followed by removing the Fmoc-protecting group under basic conditions using 20% piperidine in NMP. Subsequently, the next coupling was performed twice (20 min in each) after pre-activating the ester of the desired D- β^3 -amino acid with a mixture of HATU/HOAt/DIPEA at 50 °C. The procedure of deprotection and coupling was successively repeated until the desired chain length was reached. Finally, the β -peptide was cleaved from the resin under acidic conditions using a cocktail of TFA/H₂O/TIS (95%/2.5%/2.5%).

β -Peptides containing a large amount of D- β^3 -Leu are more hydrophobic and prone to aggregate easily, leading to incomplete reactions during the synthesis especially after the fifth or the sixth residue.^[143,144] Thus, different conditions have been pursued in this study to overcome the problem of aggregation due to the high hydrophobicity of the sequences

containing D- β^3 -Leu: (i) the rink amide MBHA resin was replaced by the less apolar NovaPEG rink amide LL resin (loading capacity of 0.18 mmol/g), which has been used in many cases for the synthesis of very hydrophobic sequences,^[148,149] (ii) after coupling the sixth residue, the use of DBU (1,8-Diazabicyclo[5.4.0]undec-7-ene) along with piperidine was essential to efficiently remove the Fmoc-protecting group.^[142,144] Therefore, a mixture of 10% DBU and 10% piperidine in NMP was used as a deprotecting solution, (iii) coupling at higher temperature can interrupt interactions causing the aggregation in many cases for very hydrophobic peptides,^[145,146] however, the very high temperature might lead to undesirable side reactions.^[147] Herein, the temperatures during the peptide elongation was elevated up to 75 °C, (iv) after the sixth amino acid, the coupling time was elongated to 30 min, instead of 20 min, and (v) during the synthesis of all the β -peptides (including β -peptide containing D- β^3 -Val), NMP was selected as a solvent for each step to dissolve the D- β^3 -amino acid because most peptide building blocks and reagents are well soluble in NMP.^[140,141] Using the previous conditions, the synthesis of β -peptides containing a large number of hydrophobic β^3 -Leu residues was possible.

In order to measure FRET, the donor NBD (4-chloro-7-nitrobenzo-2-oxa-1,3-diazol) and the acceptor TAMRA (5(6)-carboxytetramethylrhodamine) were selected as pair of fluorophores and attached to the last β^3 -Lys at the N-terminus in all synthesized β -peptides (Figure 3.12). For this reason, a third β^3 -Lys was added to the N-terminus of the β -peptides in order to maintain the relative solubility of these sequences in aqueous media.

Labeling β -peptides was accomplished on resin using DIPEA and PyBOP (in the case of the acceptor TAMRA) in NMP, over night and at room temperature.

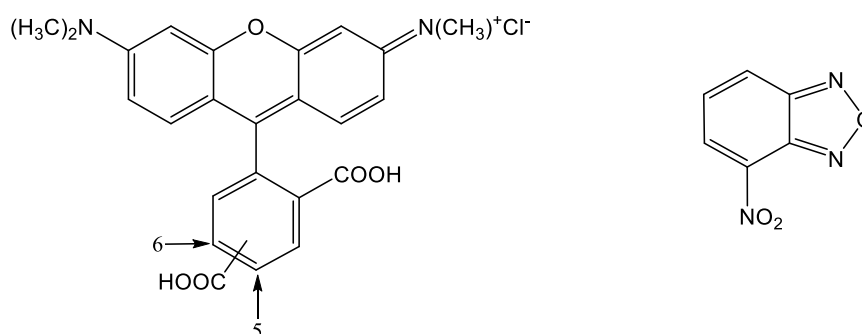


Figure 3.12: Chemical structure of NBD (right) and TAMRA (left).

Finally, the obtained β -oligomers were purified with HPLC using a C18 reversed-phase column and characterized by mass spectrometry. Table 3.1 represents the sequences of all synthesized transmembrane β -peptides as well as their fluorescent labeled-analogues prepared for FRET measurements.

Table 3.1: The synthesized β -peptides as well as their fluorescent analogues and β -peptides lacking fluorophores.

Sequence	Name
H-hLys ₂ -hTrp ₂ -hVal ₁₉ -hTrp ₂ -hLys ₂ -NH ₂	P0
H-hLys(NBD)-hLys ₂ -hTrp ₂ -hVal ₁₉ -hTrp ₂ -hLys ₂ -NH ₂	P0_D
H-hLys(TAMRA)-hLys ₂ -hTrp ₂ -hVal ₁₉ -hTrp ₂ -hLys ₂ -NH ₂	P0_A
H-hLys ₃ -hTrp ₂ -hVal ₁₉ -hTrp ₂ -hLys ₂ -NH ₂	P0_U
H-hLys ₂ -hTrp ₂ -hVal ₉ -hGln-hVal ₉ -hTrp ₂ -hLys ₂ -NH ₂	P1
H-hLys(NBD)-hLys ₂ -hTrp ₂ -hVal ₉ -hGln-hVal ₉ -hTrp ₂ -hLys ₂ -NH ₂	P1_D
H-hLys(TAMRA)-hLys ₂ -hTrp ₂ -hVal ₉ -hGln-hVal ₉ -hTrp ₂ -hLys ₂ -NH ₂	P1_A
H-hLys ₃ -hTrp ₂ -hVal ₉ -hGln-hVal ₉ -hTrp ₂ -hLys ₂ -NH ₂	P1_U
H-hLys ₂ -hTrp ₂ -hVal ₃ -hGln-hVal ₁₁ -hGln-hVal ₃ -hTrp ₂ -hLys ₂ -NH ₂	P2
H-hLys(NBD)-hLys ₂ -hTrp ₂ -hVal ₃ -hGln-hVal ₁₁ -hGln-hVal ₃ -hTrp ₂ -hLys ₂ -NH ₂	P2_D
H-hLys(TAMRA)-hLys ₂ -hTrp ₂ -hVal ₃ -hGln-hVal ₁₁ -hGln-hVal ₃ -hTrp ₂ -hLys ₂ -NH ₂	P2_A
H-hLys ₃ -hTrp ₂ -hVal ₃ -hGln-hVal ₁₁ -hGln-hVal ₃ -hTrp ₂ -hLys ₂ -NH ₂	P2_U

H-hLys ₂ -hTrp ₂ -hVal ₃ -hGln-hVal ₅ -hGln-hVal ₅ -hGln-hVal ₃ -hTrp ₂ -hLys ₂ -NH ₂	P3
H-hLys(NBD)-hLys ₂ -hTrp ₂ -hVal ₃ -hGln-hVal ₅ -hGln-hVal ₅ -hGln-hVal ₃ -hTrp ₂ -hLys ₂ -NH ₂	P3_D
H-hLys(TAMRA)-hLys ₂ -hTrp ₂ -hVal ₃ -hGln-hVal ₅ -hGln-hVal ₅ -hGln-hVal ₃ -hTrp ₂ -hLys ₂ -NH ₂	P3_A
H-hLys ₃ -hTrp ₂ -hVal ₃ -hGln-hVal ₅ -hGln-hVal ₅ -hGln-hVal ₃ -hTrp ₂ -hLys ₂ -NH ₂	P3_U
H-hLys ₂ -hTrp ₂ -hVal ₂ -hGln-hVal ₃ -hGln-hVal ₄ -hGln-hVal ₃ -hGln-hVal ₃ -hTrp ₂ -hLys ₂ -NH ₂	P4
H-hLys(NBD)-hLys ₂ -hTrp ₂ -hVal ₂ -hGln-hVal ₃ -hGln-hVal ₄ -hGln-hVal ₃ -hGln-hVal ₃ -hTrp ₂ -hLys ₂ -NH ₂	P4_D
H-hLys(TAMRA)-hLys ₂ -hTrp ₂ -hVal ₂ -hGln-hVal ₃ -hGln-hVal ₄ -hGln-hVal ₃ -hGln-hVal ₃ -hTrp ₂ -hLys ₂ -NH ₂	P4_A
H-hLys ₃ -hTrp ₂ -hVal ₂ -hGln-hVal ₃ -hGln-hVal ₄ -hGln-hVal ₃ -hGln-hVal ₃ -hTrp ₂ -hLys ₃ -NH ₂	P4_U
H-hLys ₂ -hTrp ₂ -hLeu ₁₅ -hTrp ₂ -hLys ₂ -NH ₂	P5
H-hLys(NBD)-hLys ₂ -hTrp ₂ -hLeu ₁₅ -hTrp ₂ -hLys ₂ -NH ₂	P5_D
H-hLys(TAMRA)-hLys ₂ -hTrp ₂ -hLeu ₁₅ -hTrp ₂ -hLys ₂ -NH ₂	P5_A
H-hLys ₃ -hTrp ₂ -hLeu ₁₅ -hTrp ₂ -hLys ₂ -NH ₂	P5_U
H-hLys ₂ -hTrp ₂ -hLeu ₇ -hGln-hLeu ₇ -hTrp ₂ -hLys ₂ -NH ₂	P6

H-hLys(NBD)-hLys ₂ -hTrp ₂ -hLeu ₇ -hGln-hLeu ₇ -hTrp ₂ -hLys ₂ -NH ₂	P6_D
H-hLys(TAMRA)-hLys ₂ -hTrp ₂ -hLeu ₇ -hGln-hLeu ₇ -hTrp ₂ -hLys ₂ -NH ₂	P6_A
H-hLys ₃ -hTrp ₂ -hLeu ₇ -hGln-hLeu ₇ -hTrp ₂ -hLys ₂ -NH ₂	P6_U
H-hLys ₂ -hTrp ₂ -hLeu ₃ -hGln-hLeu ₄ -hGln-hLeu ₆ -hTrp ₂ -hLys ₂ -NH ₂	P7
H-hLys(NBD)-hLys ₂ -hTrp ₂ -hLeu ₃ -hGln-hLeu ₄ -hGln-hLeu ₆ -hTrp ₂ -hLys ₂ -NH ₂	P7_D
H-hLys(TAMRA)-hLys ₂ -hTrp ₂ -hLeu ₃ -hGln-hLeu ₄ -hGln-hLeu ₆ -hTrp ₂ -hLys ₂ -NH ₂	P7_A
H-hLys ₃ -hTrp ₂ -hLeu ₃ -hGln-hLeu ₄ -hGln-hLeu ₆ -hTrp ₂ -hLys ₂ -NH ₂	P7_U
H-hLys ₂ -hTrp ₂ -hLeu ₃ -hGln-hLeu ₄ -hGln-hLeu ₄ -hGln-hLeu ₁ -hTrp ₂ -hLys ₂ -NH ₂	P8
H-hLys(NBD)-hLys ₂ -hTrp ₂ -hLeu ₃ -hGln-hLeu ₄ -hGln-hLeu ₄ -hGln-hLeu ₁ -hTrp ₂ -hLys ₂ -NH ₂	P8_D
H-hLys(TAMRA)-hLys ₂ -hTrp ₂ -hLeu ₃ -hGln-hLeu ₄ -hGln-hLeu ₄ -hGln-hLeu ₁ -hTrp ₂ -hLys ₂ -NH ₂	P8_A
H-hLys ₃ -hTrp ₂ -hLeu ₃ -hGln-hLeu ₄ -hGln-hLeu ₄ -hGln-hLeu ₁ -hTrp ₂ -hLys ₂ -NH ₂	P8_U

4 Structural Characterization

4.1 CD Spectroscopy

4.1.1 Theoretical Basis

Circular dichroism (CD) spectroscopy has been increasingly recognized as a valuable technique to reveal the secondary structures of proteins and peptides in different and predictable ways. For CD spectroscopy, the idea of circularly polarized light is considered as the most important physical/optical concept. Thus, the polarized beam of light is composed of right- (*R*) and left- (*L*) handed circularly polarized components, in which the difference in their absorption can be measured and quantified using the equation: $\Delta A = A_L - A_R$ (Figure 4.1).^[152,153] The theoretical background of CD spectroscopy and its application to study the types of molecules has been broadly covered in the literature.^[152,155-157]

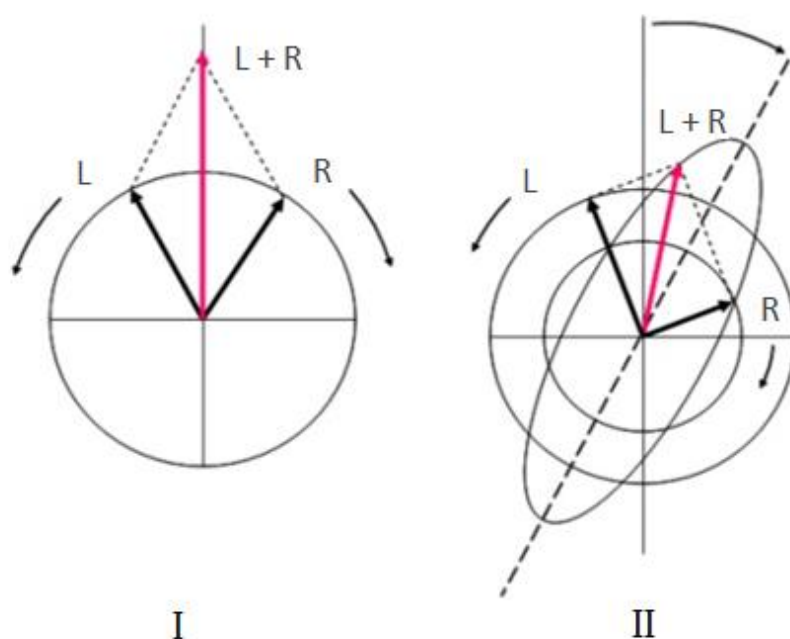


Figure 4.1: Left (*L*) and right (*R*) circularly polarized components of plane polarized radiation: (I) Linear polarized light can be viewed as a superposition of opposite circular polarized light of equal amplitude and phase; (II) different absorption of left- and right-handed polarized component leads to ellipticity (CD) and optical rotation (OR).^[153]

The CD spectrum in the far UV region (240-180 nm), corresponding to the absorption of the peptide bond (amide chromophore), can be examined to give information about regular conformational characteristics, such as α -helix and β -sheet. On the other hand, the CD spectrum in the near UV region (320-260 nm), which is correlated to the environments of aromatic side chains and displays the content of proteins tertiary structure.^[152] Nevertheless, several amino acid side chains (notably Tyr, Trp, Phe, His, and Met) can absorb light strongly in the far UV region (below 250 nm).^[154]

4.1.2 Secondary Structure of β -Peptides in Solution and within the Membrane

CD spectroscopy has been widely utilized to analyze various types of β -peptide secondary structures in different environments.^[78,95,142] In this study, the helicity of the synthesized β -peptides was analyzed using the same technique outside and inside artificial lipid membranes. It has been shown that β -peptides adopting left-handed 14-helix display a maximum near 195 nm and a minimum near 215 nm and vice versa for right-handed 14-helix. On the other hand, the experimental CD spectra of a 12-helical pattern have been diagnosed by showing a maximum near 200-205 nm and two minima near 220 nm and 190 nm. However, the magnitude of the ellipticities (θ) can be varied based on the helix content as well as the surrounding milieu.^[95,132] As it is the case for α -helices, the intensity of the CD spectrum for β -peptides appears to be length-dependent by showing more intense ellipticity as the helix is lengthened.^[115]

As it was previously described, the backbones of β -peptides **P0** and **P5** were consistently pre-organized to show 14- and 12-helical conformations, respectively (see section 3.1). As a first step, the secondary structures of these two β -peptides was investigated in 2,2,2-trifluoroethanol (TFE). The main concern over using TFE in this study is its ability to induce helical structure to the native conformation of peptides and proteins.^[158,159] The dielectric constant of TFE is about one third compared to that of water and more closely approximates to that of the interior of proteins, which would favorably strengthen the intramolecular hydrogen bonds and therefore stabilize the peptide secondary structure.^[160]

The results depicted in Figure 4.2 represent the CD spectra obtained from measuring the helicity of the sequences **P0** and **P5** in TFE at different temperatures and a concentration of 30 μ M. The CD spectrum corresponding to **P0** (Figure 4.2 top) shows a minimum at 193 nm, a

maximum at 210 nm and a zero crossing at *ca.* 202 nm. As it was expected, these bands characteristically display that **P0** tends to fold into a right-handed 14-helix. Basically, the right-handed configuration was obtained due to the presence of D- β^3 -amino acids derived from α -D-residues (β -peptides comprised of L- β^3 -residues derived from α -L-residues display opposite CD extrema).

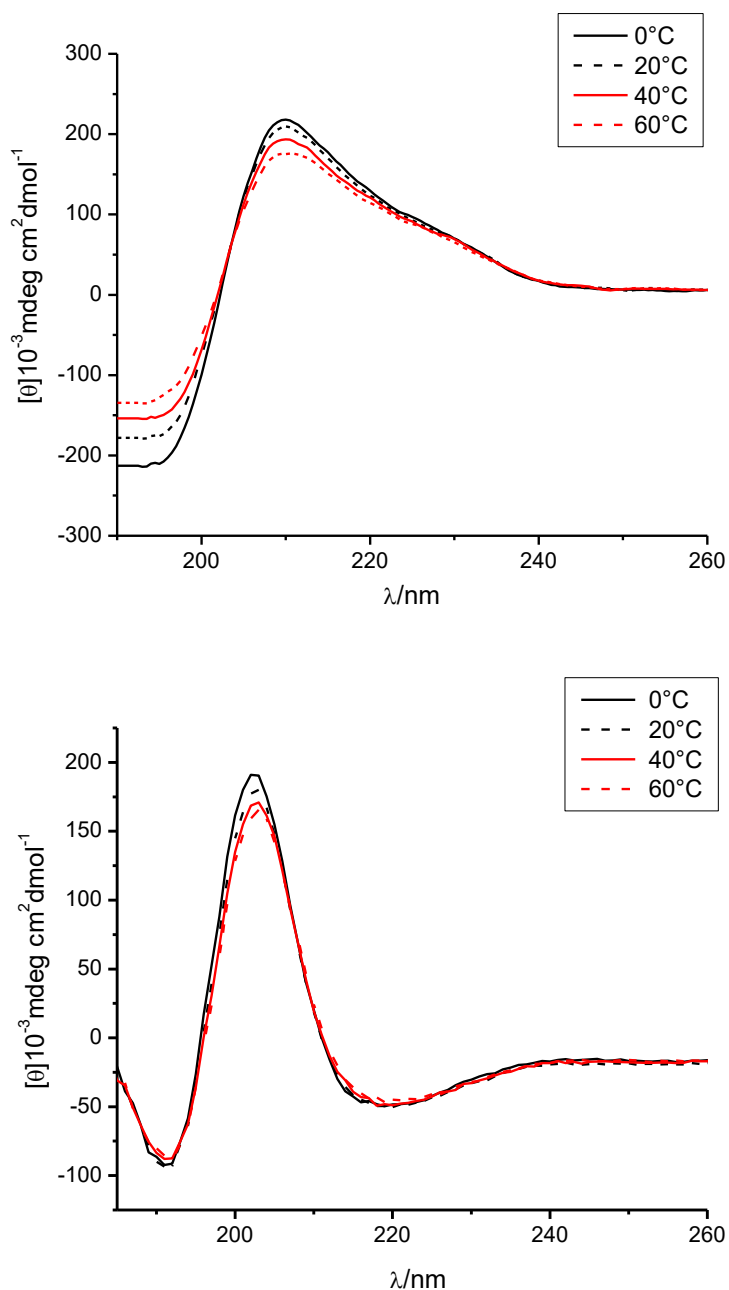


Figure 4.2: CD-spectra of β -peptides **P0** (top) and **P5** (bottom) in TFE at different temperatures and concentration of 30 μ M.

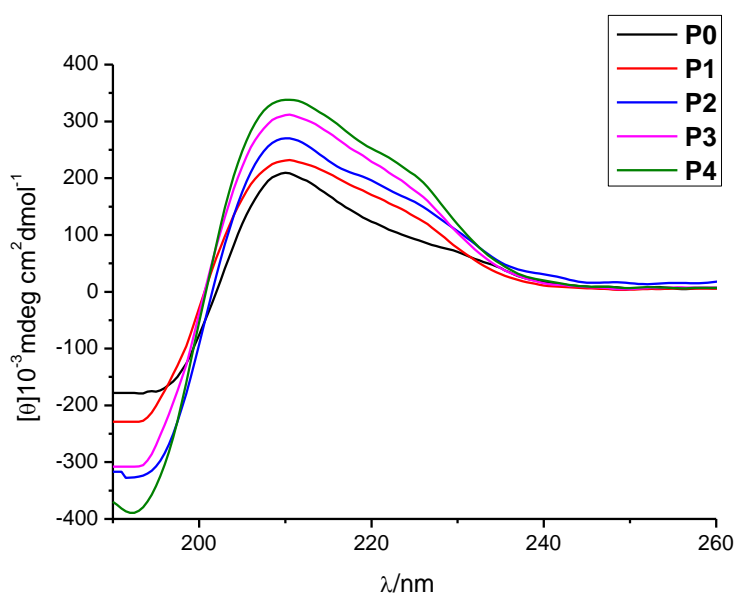
In contrast, **P5** exhibits a different CD spectrum from that of **P0** by showing three bands, a maximum at 202 nm and two minima at 219 nm and 191 nm (Figure 4.2 bottom). These values are more likely a signature for a left-handed 12-helix.

In conclusion, the dramatic variation between the CD spectra of **P0** and **P5** in TFE denotes that β^3 -Val and β^3 -Leu have very distinct secondary structural predilections, which is consistent with the view that β^3 -building blocks are quite malleable.^[132,139]

Additionally, the stability of both **P0** and **P5** patterns was further supported by recording CD spectra at different temperatures, showing that the structural characteristics of these helices were conserved even at high temperatures up to 60 °C (Figure 4.2).

In order to analyze the effect of introducing recognition units on the secondary structures, analogical CD spectroscopy experiments have been performed for all other β -peptides (bearing one or more β^3 -Gln) using the same conditions. The results from measuring CD spectroscopy of **P1**, **P2**, **P3** and **P4** (β -peptides containing β^3 -Val) are depicted in Figure 4.3 (top). It is clearly shown that these helices preferably maintain a neat 14-helical conformation by revealing similar bands compared to **P0** (Table 4.1).

Besides, Figure 4.3 (bottom) displays the helicity of **P6**, **P7** and **P8** (β -peptides containing β^3 -Leu). Similarly, the propensity of these helices to fold into a 12-helical secondary structure seems to be retained because of exhibiting identical bands as **P5** (Table 4.2).



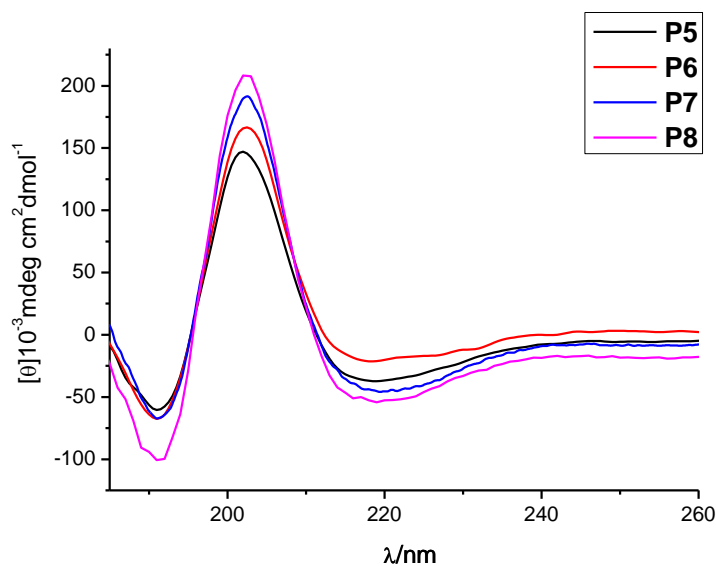


Figure 4.3: CD spectra of β -peptides **P0**, **P1**, **P2**, **P3** and **P4** (top) and **P5**, **P6**, **P7** and **P8**(bottom) in TFE at 20°C and concentration of 30 μ M.

Furthermore, the β -helical conformations of all β -peptides appeared to be stable as well at high temperatures up to 60 °C (Figure 1.S in the “Appendix”).

Table 4.1: Maximum and minimum wavelengths for **P0-P4** showing a right-handed 14-helix in TFE and POPC at room temperature.

	P0		P1		P2		P3		P4	
Medium	TFE	POPC	TFE	POPC	TFE	POPC	TFE	POPC	TFE	POPC
λ_{\max} (nm)	210	208.5	210.5	208.5	210	208	210.5	208	210.5	208.5
λ_{\min} (nm)	193	192	192.5	192	192	190.5	192	190.5	192	190.5
Conformation	Right-handed 14-helix									

The results from both 14- and 12-helices show a slight shift in the wavelength values from those existing in the literature, which is due to the different dielectric constant of the surrounding milieu.^[166]

Interestingly, all these results unambiguously confirm that varying side chains within the β -peptides can be tolerated in the context of reasonably preserving rigid helical conformations.

Table 4.2: Maximum and minimum wavelengths for **P5-P8** showing a left-handed 12-helix in TFE and POPC at room temperature.

	P5		P6		P7		P8	
Medium	TFE	POPC	TFE	POPC	TFE	POPC	TFE	POPC
λ_{\max} (nm)	202	204.5	202.5	205	202.5	204.5	202	205
$\lambda_{\min 1}$ (nm)	219	223	219.5	217.5	218.5	219.5	219	218
$\lambda_{\min 2}$ (nm)	191	196.5	191	196.5	191	198	191	196.5
Conformation	Left-handed 12-helix							

Several investigations from various research groups have indicated that the spectral properties of proteins can be influenced by the presence of aromatic side chains such as Trp and Tyr (tyrosine) even when they are present at the frayed ends of the helix.^[161,162,163] Generally, this influence can be detected in the CD spectra as an additional CD band in the 225-250 nm region. Indeed, the CD spectra of all the β -peptides in this study show a clear band near 225 nm since all the sequences contain four β^3 -Trp residues (see section 3.1).

From CD spectroscopy it has been confirmed that the β -peptides containing β^3 -Val fold into a 14-helix and thereby, their hydrophobic stretch can be assessed to be 31.6 Å, assuming an ideal 14-helical conformation with three residues per turn and a pitch of 5.0 Å. In a similar vein, the length of the hydrophobic region of β -peptides folding into a 12-helix can be estimated to be 33.6 Å, assuming an ideal 12-helical conformation with 2.5 residues per turn and a pitch of 5.6 Å. It is worth mentioning that the length of the hydrophobic stretch in both cases surpasses the hydrocarbon region of the artificial membrane POPC used in this study, which is $2D_C = 29.2$ Å at 20 °C.^[164] As a result of this phenomenon, which is known as positive hydrophobic mismatch, peptides as well as lipids can adopt different responses such as a change in their structural conformations (see section 1.2.1).^[35,165] Therefore, the stability of

the secondary structure for all β -peptides embedded within LUVs POPC was assessed by CD spectroscopy using 5:100 as peptide-to-lipid (P:L) ratio (Figure 4.4).

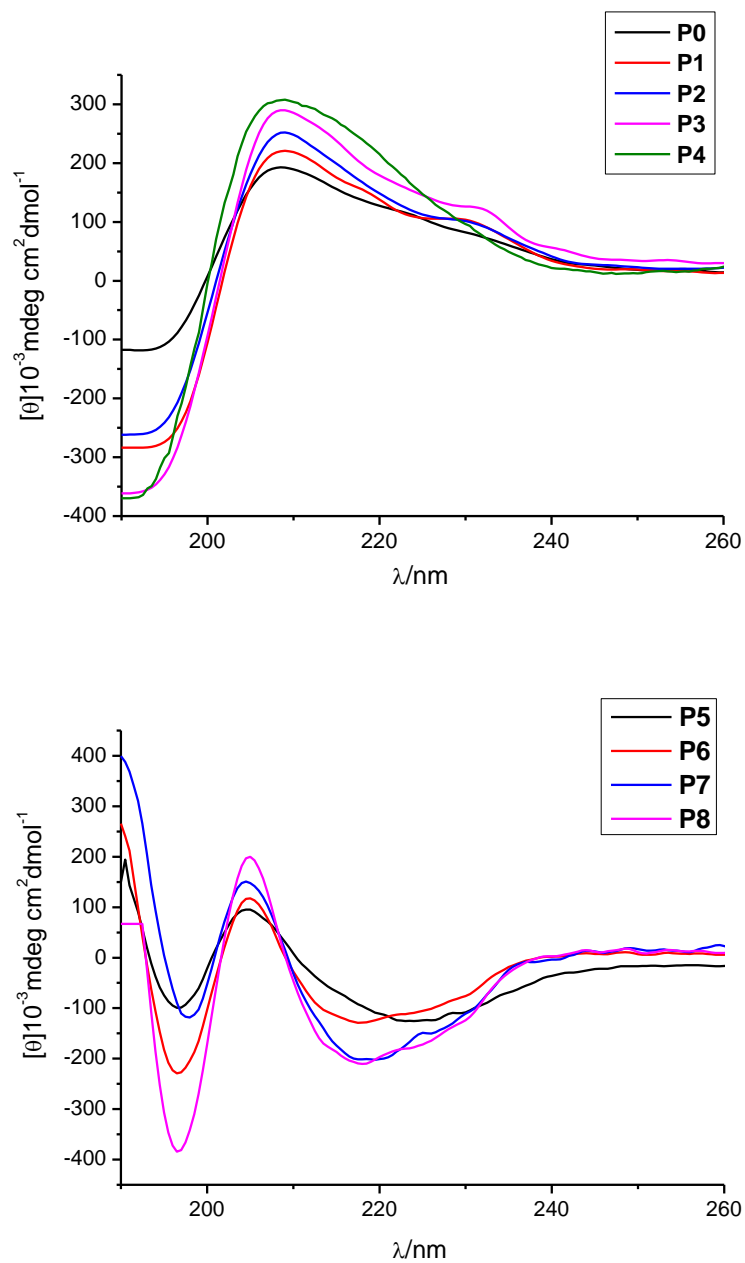


Figure 4.4: CD-spectra of β -peptides **P0**, **P1**, **P2**, **P3** and **P4** (top) and **P6**, **P7** and **P8**(bottom) within POPC LUVs as5:100 ratio at 20 °C.

The strong resemblance between the spectra of the β -peptides in TFE and within the lipid bilayer implies that the conformational preference of all the β -peptides was preserved, which greatly demonstrates the extreme stability of these sequences in various environments (Figure 4.4, Table 4.1 and 4.2).

4.2 Fluorescence Spectroscopy

4.2.1 Insertion of β -Peptides within the Membrane

Numerous studies have been conducted concerning the multiple role of Trp fluorescence to derive inferences with respect to changes in structural characteristics of proteins as well as their physical and dynamical properties.^[167-170] It is known that Trp residues are sensitive to subtle changes in their local environments, which can be clearly observed in the change of their fluorescence wavelength (λ_{\max}), ranging from about 308 nm to 355 nm.^[167] This distinctive property has been used to classify the position of Trp residues according to their surrounding in three discrete categories.^[171,172] One of these categories includes Trp molecules inside the protein in a low-polar environment with a wavelength maximum λ_{\max} less than 330 nm. The second category consists of the complete exposure of Trp residues to water with a wavelength maximum λ_{\max} at *ca.* 350 nm. The last category reflects the presence of Trp residues in the polar-apolar region near the membrane-water interface with a wavelength maximum λ_{\max} more than 330 nm. Basically, the change in Trp fluorescence wavelength is due to the difference between the dielectric constant imposed by the protein and the surrounding milieu, which strongly suggests that the orientation of Trp residues is highly correlated with the electric field direction.^[167,168]

Since all the synthesized β -peptides in this study contain β^3 -Trp, we used the fluorescence emission of these residues to gather an overview of β -peptides positioning within the membrane. The results shown in Figure 4.5 display an initial study about the β^3 -Trp fluorescence of the β -sequences **P0** and **P5** within the lipid bilayer composed of POPC using 1:600 ratio as well as in TFE at concentration of 30 μ M.

As shown in Figure 4.5 (top), the fluorescence emission maximum (λ_{\max}) of **P0** in TFE was detected at 348 nm, indicating the complete exposure of these residues to the polar environment (TFE in this case). However, after insertion of this peptide into the lipid bilayer,

the fluorescence emission maximum of β^3 -Trp was blue-shifted to be 342 nm, which reflects that these residues exist in a more hydrophobic environment in the lipid bilayer.

Likewise, the fluorescence emission (λ_{\max}) of **P5** in TFE shows a maximum at 347 nm (Figure 4.5 bottom), meaning that Trp molecules are in a polar environment. Besides, the fluorescence maximum of β^3 -Trp residues was blue-shifted to 341 nm when **P5** was integrated within the lipid bilayer, reporting that these residues are partially buried in the membrane interior.

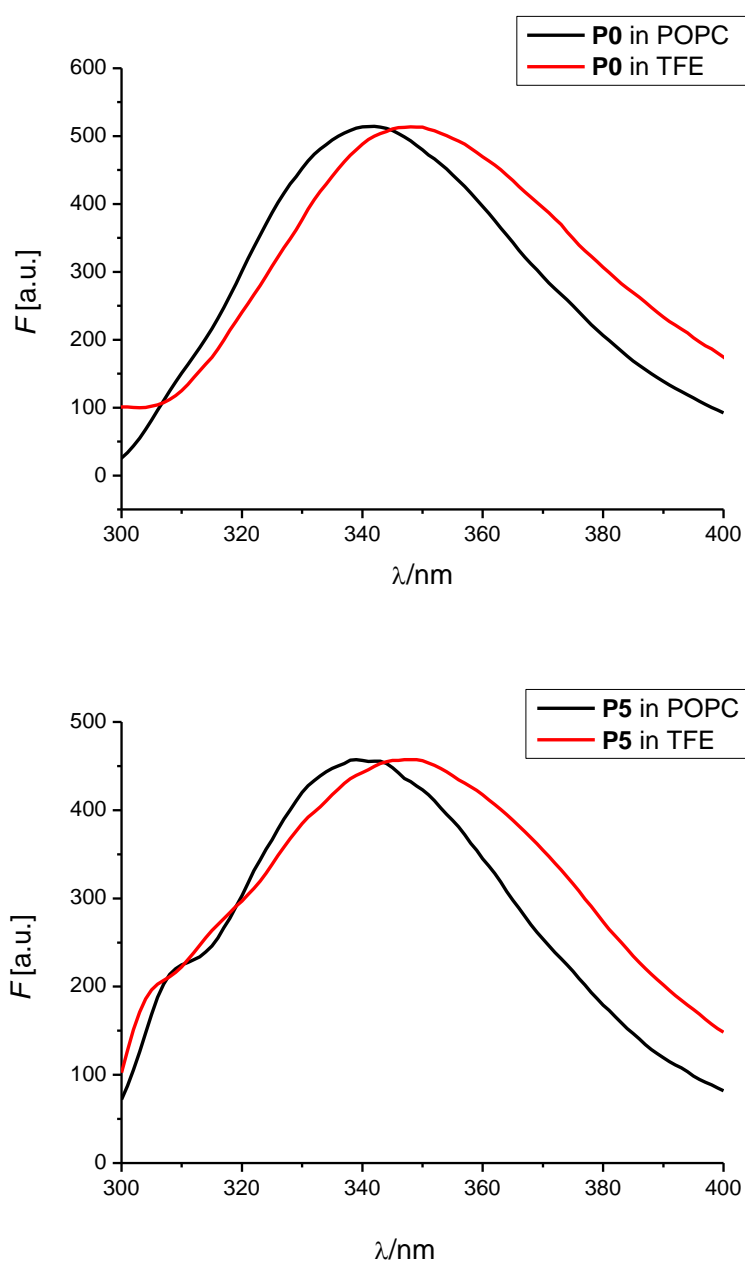


Figure 4.5: The β^3 -Trp fluorescence spectra of **P0** (top) and **P5** (bottom) within the lipid bilayer POPC LUVs using 1:600 ratio as well as in TFE at room temperature and concentration of 30 μ M.

In a similar way, Trp fluorescence measurements were performed for all other β -peptides either in TFE or in LUVs POPC (Figure 3.S in the “Appendix”). The results showed that the maximum of β^3 -Trp emission was blue-shifted in all cases after insertion of these sequences into the lipid bilayer, table 4.3 regroups all the obtained data.

Table 4.3: Fluorescence emission maxima of β^3 -Trp of the 14-helices (top) and the 12-helices (bottom) β -peptides determined in both TFE (concentration of 30 μ M) and within POPC vesicles (1:600 as peptide/lipid ratio) at room temperature.

14-Helix	P0		P1		P2		P3		P4	
Medium	TFE	POPC	TFE	POPC	TFE	POPC	TFE	POPC	TFE	POPC
λ_{\max} (nm)	348	342	349	339	349	339	349	339	347	340

12-Helix	P5		P6		P7		P8	
Medium	TFE	POPC	TFE	POPC	TFE	POPC	TFE	POPC
λ_{\max} (nm)	347	341	347	339	349	342	349	340

Generally, the blue shift in the emission maximum of the Trp molecules in all the cases confirms that the environment around the Trp, after inserting the β -peptides into the lipid bilayer, is more hydrophobic and that all the β^3 -Trp amino acids are localized near the water-membrane interface. Thus, these results suggest the transmembrane orientation of all the synthesized β -peptides within the POPC lipid bilayer.

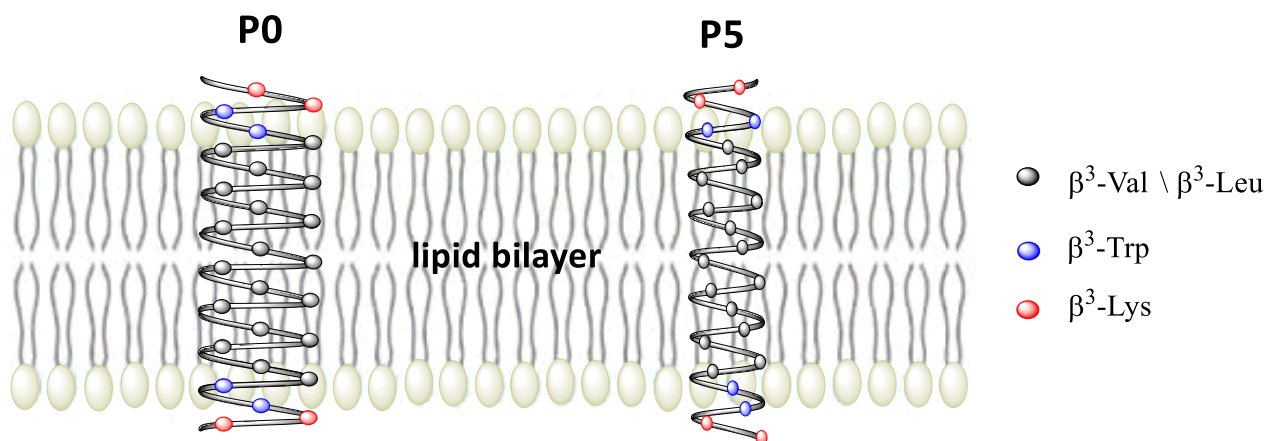


Figure 4.6: Schematic illustration of the β -sequences **P0** and **P5** positioning within the lipid bilayer composed of POPC.

4.2.2 Topological Insertion of β -Peptides into the Lipid Bilayer

Chemically modifying NBD-labeled lipids in both artificial and biological membranes by quenching the highly fluorescent NBD-probes using dithionite ions has been widely used to measure transverse-membrane asymmetry in vesicles and phospholipids translocase activity.^[174,183] In a similar way, membrane-impermeable dithionite ions can chemically reduce the NBD fluorophores attached to the N-terminus of peptides and thereby, selectively quench the fluorescent NBD-labeled analogues. This approach allows for precisely determining the preferable topological insertion of the peptides into the membrane and also the location of the N-terminus.^[177-179]

In aqueous media, the dithionite ions ($S_2O_4^{2-}$) exist in an equilibrium with the radical anions SO_2^- .^[180,181] These radicals are unable to penetrate the hydrophobic lipid bilayer and instead stay outside the vesicle, which causes a reduction of the electron-withdrawing nitro-group of the outer NBD molecules to non-fluorescent electron-donating amino-group by a single-electron transfer pathway (Figure 4.7). Accordingly, this procedure leads to the complete abolishment of NBD fluorescence and the formation of new non-fluorescent molecules (ABD).^[174]

This method has also been used to chemically modify the amino acid side chain of nitro-tyrosine derivatives without eliminating the biochemical functional properties of the protein.^[174,182]

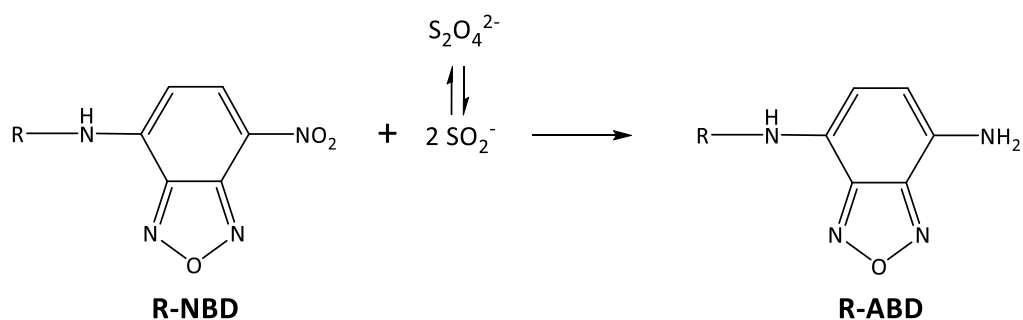
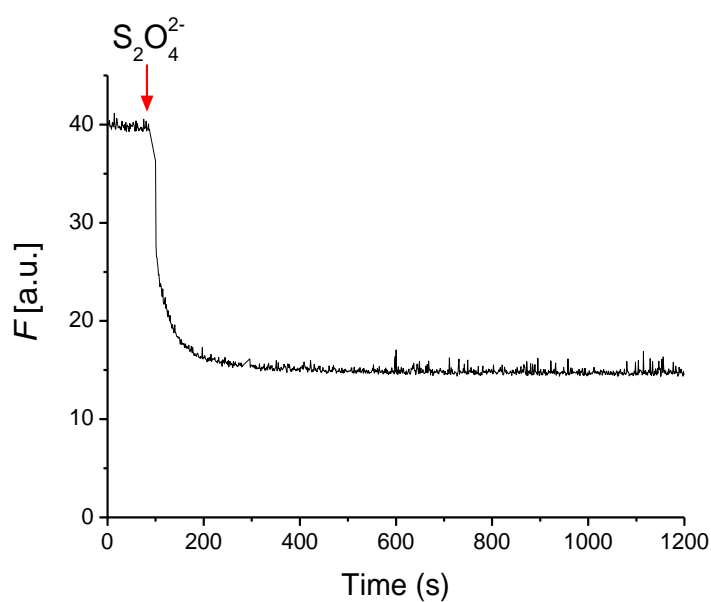


Figure 4.7: Reduction of 7-nitro2,1,3-benzoxadiazol-4-yl-labelled β -peptide (R-NBD) to 7-amin2,1,3-benzoxadiazol-4-yl-labelled β -peptide (R-ABD) with the membrane-impermeable dithionite ions.

Based on that concept, we probed a more suitable mode of insertion preferred by the β -peptides into the membrane by treating the outer leaflet of POPC liposomes containing fluorescently NBD-labeled probes with a freshly prepared sodium dithionite solution (Figure 4.8).



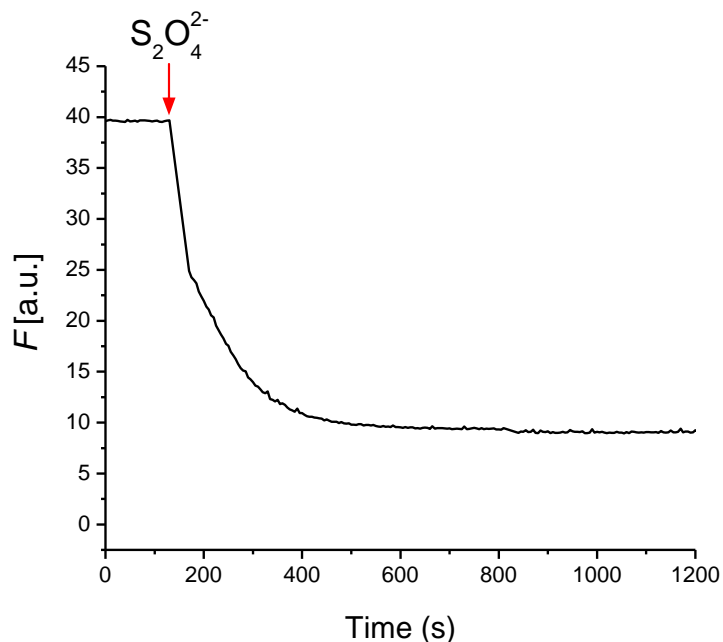


Figure 4.8: External addition of sodium dithionite solution to POPC LUVs containing 0.16 mol% fluorescent NBD-labeled **P0_D**(top)and **P5_D** (bottom). Fluorescence signal wavelength of NBD fluorophores was monitored at 533 nm for excitation wavelength at 450 nm.

The data depicted in Figure 4.8 show that the external addition of $S_2O_4^{2-}$ to LUVs containing 0.16 mol% of either fluorescent **P0_D** or **P5_D** causes a dramatic decrease in the intensity of NBD fluorescence by almost 64 % and 77 %, respectively, thus, indicating that the N-termini of about 64 % of **P0_D** and 77 % of **P5_D** are situated in the outer-leaflet of the vesicles. Consequently, the emission of the NBD fluorescence of about 36 % of **P0_D** and about 23 % of **P5_D** remain intact, indicating that the N-termini of 36 % of **P0_D** and 23 % of **P5_D** are located in the inner-leaflet of the vesicles.

These findings strongly demonstrate that the β -peptides are translocated across the lipid bilayer and form transmembrane helices with either an N-terminus inside or outside the lipid bilayer (see Figure 4.5 in the “Appendix”).

In some cases, a continuous decrease in the NBD-fluorescence might be subsequently observed, suggesting that the dithionite ions are tardily crossing the membrane. However, the permeability of dithionite and SO_2^- radicals can alter substantially with membrane lipid structure and protein composition.^[174]

4.3 Förster Resonance Energy Transfer Experiments

4.3.1 Theoretical Basis

In many biological research areas, the major interest is to precisely realise the location and the nature of interactions between particular molecular species. However, the usage of instruments with limited resolutions can often hamper the investigations to explore these phenomena. Fluorescence resonance energy transfer (more commonly referred to the acronym FRET) is a valuable technique that can permit the determination of intramolecular and intermolecular distances in the range of 10-100 Å, which is a sufficient distance for molecular interactions to take place.^[184-186] FRET is a distance-dependent physical process, by which a donor chromophore in an excited electronic state transfers its excitation energy to a nearby acceptor fluorophore in a non-radiative way through long-range dipole-dipole coupling.^[184,187-190]



where D and A represent the donor and the acceptor molecules in a ground state, respectively and D^* and A^* represent the first excited state of the fluorophores.

Since the excited acceptor can be converted into the ground vibrational level *via*vibrational relaxation, the inverse process is highly undesirable to occur. Consequently, the donor fluorophores are quenched while the acceptor fluorophores become excited, giving a rise to the emission of a fluorescent light under appropriate conditions.

The molecular processes underlying FRET are expounded in the Jablonski diagram (Figure 4.9). The theory that support the energy transfer is based on the concept of treating an excited chromophore as an oscillating dipole, which can undergo an exchange of energy with a second dipole containing identical resonance frequency.^[184] As a result, FRET analysis can be employed as an efficient molecular ruler, using a suitable donor and acceptor pair, for defining distances between labeled biomolecules.

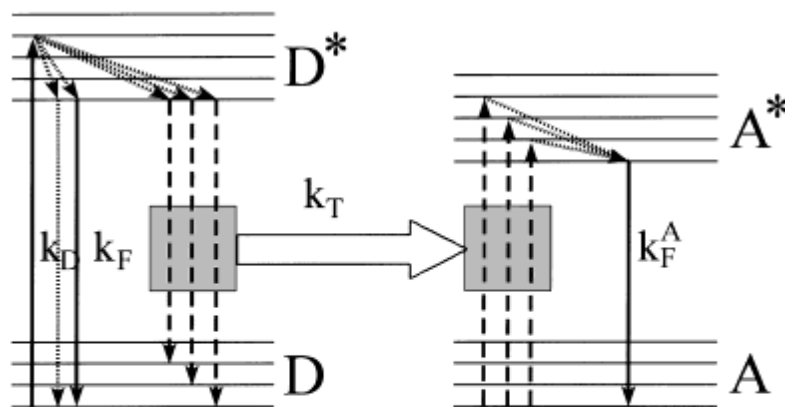


Figure 4.9: Jablonski diagram where K_F is the rate constant of the donor fluorescence emission and K_D is the sum of the rate constants of all other deexcitation processes of the donor.^[185]

In most cases, donor and acceptor are both fluorescent and the transfer of energy between them can be manifested through quenching the fluorescence of the donor and reducing its fluorescence lifetime, accompanied by raising the fluorescence emission of the acceptor. According to Förster theory,^[189] the rate of the energy transfer (K_T) process varies in proportion with the sixth power of the distance separating donor and acceptor molecules (R), given by the equation:

$$K_T = \left(\frac{1}{\tau_D}\right) \left(\frac{R_0}{R}\right)^6 \quad \text{eq. 2}$$

where τ_D denotes the donor lifetime in the absence of the acceptor and R_0 denotes the FÖRSTER or critical transfer distance between donor and acceptor when the transfer efficiency is 50%.^[186,191,192]

The efficiency of energy transfer (E) depends on the inverse sixth-distance between donor and acceptor (R) divided by the FÖRSTER radius (R_0) under the condition of 1:1 situation of donor:acceptor concentrations, which is defined as follows:

$$E = \frac{1}{1 + (R/R_0)^6} \quad \text{eq. 3}$$

E denotes the fraction of photons absorbed by the donor molecules that are transferred to the acceptor molecules. It is generally calculated using the relative fluorescence intensity of the donor in presence (F) and absence (F_0) of the acceptor:^[193]

$$E = 1 - \frac{F}{F_0} \quad \text{eq. 4}$$

Using the equations 3 and 4, the discrete distance R_0 between the fluorophores can be then calculated as follows:

$$E = R_0 \cdot \left(\frac{F}{F_0 - 1}\right)^{1/6} \quad \text{eq. 5}$$

Inside a lipid bilayer, the number of subunits in the peptide aggregate can be determined by using the dependence of the fluorescence of donor-labeled peptides on the mole fraction of acceptor-labeled peptides, according to a model defined by Adair and Engelman.^[194] Hence, no energy transfer is expected in the absence of an assembly process. This applied model was mainly based on four assumptions: labeling does not influence the association of the peptides, all peptides are located in the lipid bilayer, the interaction of the peptides is random, and one acceptor can quench all the donors within the same oligomer.

The measured fluorescence at any titration point can be represented in the following way:^[198]

$$F = f_D(N_D - N_Q) + f_Q N_Q \quad \text{eq. 6}$$

where f_D represents the molar fluorescence of unquenched donor, f_Q represents the molar fluorescence of quenched donor, N_D gives the total moles of donor and N_Q gives the moles of quenched donor. The value f_Q depends mainly on the actual quenching of various labeling isomers in population of donor and acceptor oligomers and their distribution, which enables to determine the average of the entire population.^[194] Thus, the fluorescence of the donor molecules in the absence of the acceptor molecules (F_0) is given by $f_D N_D$.

With a random number of donor and acceptor species in the oligomers, the relative fluorescence F/F_0 can be measured according to the equation 7:

$$\frac{F}{F_0} = 1 - \left(1 - \frac{F_Q}{F_D}\right) \frac{N_Q}{N_D} \quad \text{q. 7}$$

Based on equations 6 and 7, the measured relative fluorescence F/F_0 can be defined as the sum of the relative fluorescence of peptides in the monomeric state $(F/F_0)_m$ and those in the oligomeric state $(F/F_0)_o$.

$$\frac{F}{F_0} = \frac{n_m}{n_o} \left(\frac{F}{F_0}\right)_m + \left(1 - \frac{n_m}{n_o}\right) \left(\frac{F}{F_0}\right)_o \quad \text{eq. 8}$$

with

$$n_m = \frac{N_m}{N_{lipid}} \quad \text{eq. 9}$$

and

$$n_o = \frac{N_o}{N_{lipid}} \quad \text{eq. 10}$$

where N_m represents the number of peptides in the monomeric state, N_o represents the total number of peptides and N_{lipid} represents the total number of lipid molecules.

In addition, FRET can be statistically occurred in a vesicle without forming aggregates, which can be taken into account as has been described by Wolber and Hudson using the following approximation:^[192]

$$\left(\frac{F}{F_0}\right)_m = A_1 \exp\left(-K_1 \chi_A \frac{N_o}{A} R_0^2\right) + A_2 \exp\left(-K_2 \chi_A \frac{N_o}{A} R_0^2\right) \quad \text{eq. 11}$$

where A_1 , A_2 , K_1 , and K_2 are constants, $^{[10]}R_0$ is the FÖRSTER radius, χ_A the mole fraction of the acceptor and A is the surface area of one vesicle, which is assumed to be 62.7 \AA^2 in the case of POPC at $20 \text{ }^\circ\text{C}$.^[164]

Accordingly, various association states can be conceivable using FRET experiments. In the case of monomer-dimer equilibrium, the equation 8 can be written as:

$$\frac{F}{F_0} = \frac{n_m}{n_0} \left(\frac{F}{F_0}\right)_m + \left(1 - \frac{n_m}{n_0}\right) \left(\frac{F}{F_0}\right)_d \quad \text{eq. 12}$$

with

$$\left(\frac{F}{F_0}\right)_d = 1 - \chi_A \quad \text{eq. 13}$$

where $\left(\frac{F}{F_0}\right)_d$ is the relative fluorescence of peptides in the dimeric state.

In the same way, in the case of monomer-trimer equilibrium, the equation 8 can be written as:

$$\frac{F}{F_0} = \frac{n_m}{n_0} \left(\frac{F}{F_0}\right)_m + \left(1 - \frac{n_m}{n_0}\right) \left(\frac{F}{F_0}\right)_t \quad \text{eq. 14}$$

with

$$\left(\frac{F}{F_0}\right)_d = 1 - 2\chi_A - \chi_A^2 = (1 - \chi_A)^2 \quad \text{eq. 15}$$

where $\left(\frac{F}{F_0}\right)_t$ is the relative fluorescence of peptides in the trimeric state.

The dissociation constant K_D can be defined as:^[196,197,199]

$$K_D = \frac{(m \chi_P)^n}{(1-m)\frac{\chi_P}{n}} \quad \text{eq. 16}$$

where χ_P is the lipid-to-peptide ratio and n is the number of species in the oligomer. The value of K_D can be referred as a unit of peptide-to-lipid mole fraction (MF).

4.3.2 Self-Assembly of Transmembrane β -Peptides

The association state of fluorescently labeled β -peptides embedded in POPC LUVs at various peptide-to-lipid ratios and two different temperatures (20 °C and 60 °C) was addressed *via* FRET experiments. Thus, the dyes NBD and TAMRA were chosen as donor-acceptor pair and attached to the side chain of the last β^3 -Lys at the N-terminus of each β -peptide. These fluorophores have been successfully used to probe the oligomeric state of other peptides in membranes.^[197,199,201] Furthermore, this pair is distinguished by a FÖRSTER radius ranging from 5.1 - 5.5 nm depending on the composition of the lipid and the peptide.^[177,196] Thus, in this study, the value R_0 of this pair exceeds the inter-chromophore distance of all the synthesized β -peptides showing either 14- or 12-helical conformations expected for either parallel or anti-parallel mode of association. Generally, self-assembly of transmembrane proteins should result in a decrease of NBD fluorescence with a concomitant increase of TAMRA fluorescence.^[177,197] As previously described (see section 3.1), the β -sequences **P0** and **P5** were used as an initial model for designing other β -peptides bearing residues to impose helix-helix interactions and reinforce the formation of aggregates. Thus, these two sequences are expected to exist in a monomeric state within the membrane. To evaluate the thermodynamics of helix-helix association, FRET measurements were carried out at different peptide-to-lipid ratios by changing the concentration of POPC: 1:300 (1.65 mM POPC), 1:600 (3.30 mM POPC), 1:900 (4.95 mM POPC), and 1:1200 (6.60 mM POPC). The samples were prepared separately with increasing concentration of TAMRA-labeled β -peptides (ranging from 0.00 to 2.75 μ M) and keeping the concentration of NBD-labeled β -peptides constant at 2.75 μ M. The total concentration of the milieu was kept constant at 5.5 μ M by adding the corresponding non-labeled β -peptides. The correction of spectra was achieved by subtracting each spectrum from its corresponding vesicle suspension without fluorescently labeled species. The data were obtained for each β -peptide by plotting the relative fluorescence (F/F_0) of the donor in presence (F) to that in absence (F_0) of the acceptor as a function of mole fraction of the quencher TAMRA-labeled peptide χ_A .

4.3.2.1 Self-Assembly of 14-Helices

The possible aggregation of β -peptides showing 14-helical secondary structure was addressed by measuring FRET experiments using the same conditions described previously. The results are depicted in Figure 4.10.

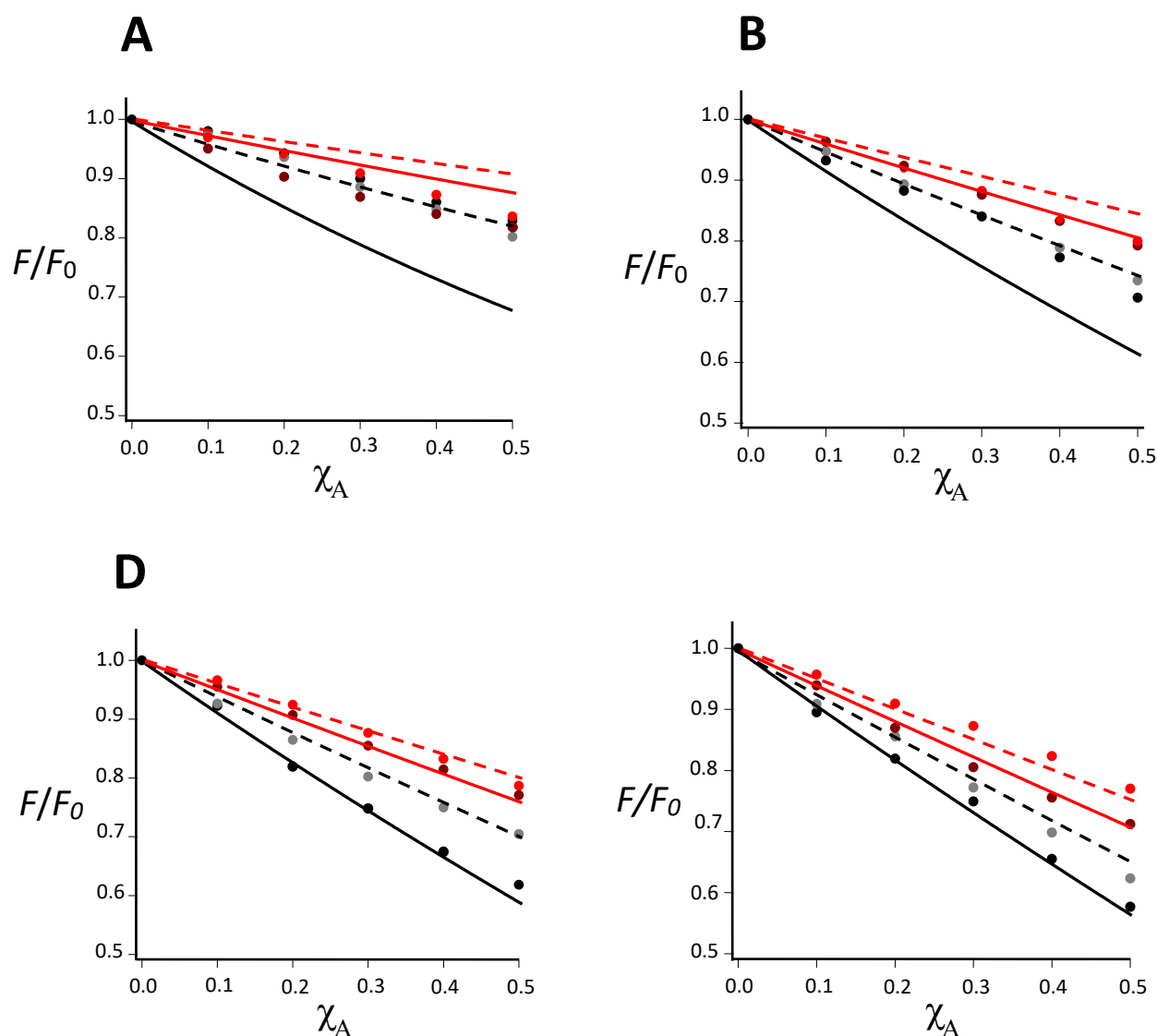


Figure 4.10: Relative emission of NBD-fluorescence (F/F_0) as a function of χ_A for β -peptides showing 14-helix at 1:300 (●), 1:600 (●), 1:900 (●), 1:1200 (●) peptide-to-lipid ratios and at 20 °C. For **P0** (A) only statistical FRET was assumed (100 nm LUVs POPC, $R_0 = 5.1$ nm). For **P1**(B), **P2**(C) and **P3** (D) a monomer-dimer equilibrium was assumed and fitted to the obtained data as shown in different lines (solid black line for 1:300, dashed black line for 1:600, solid red line for 1:900 and dashed red line for 1:1200).

In the case of **P0**, the data depicted in Figure 4.10A can be fitted to the theoretical formula of Wolber and Hudson^[192] leading to a value of $R_0 = 5.1$ nm by assuming only statistical FRET. This value matches the one cited in the literature and supports our expectation that **P0** exists as monomers in the membrane. For the three other β -peptides (**P1**, **P2** and **P3**), the inclusion of β^3 -Gln was based on the notion that these polar residues can promote self-assembly of the

peptides by creating hydrogen bonds between the helices. In addition, the positions of β^3 -Gln amino acids within these β -peptides were organized to accomplish a symmetrical sequential arrangement of these helices in order to enable their association regardless of the parallel or anti-parallel mode of association. Thus, the preorganization of these sequences is expected to strongly favor the formation of oligomers in the membrane and more precisely the formation of homo-dimers (Figure 4.11).

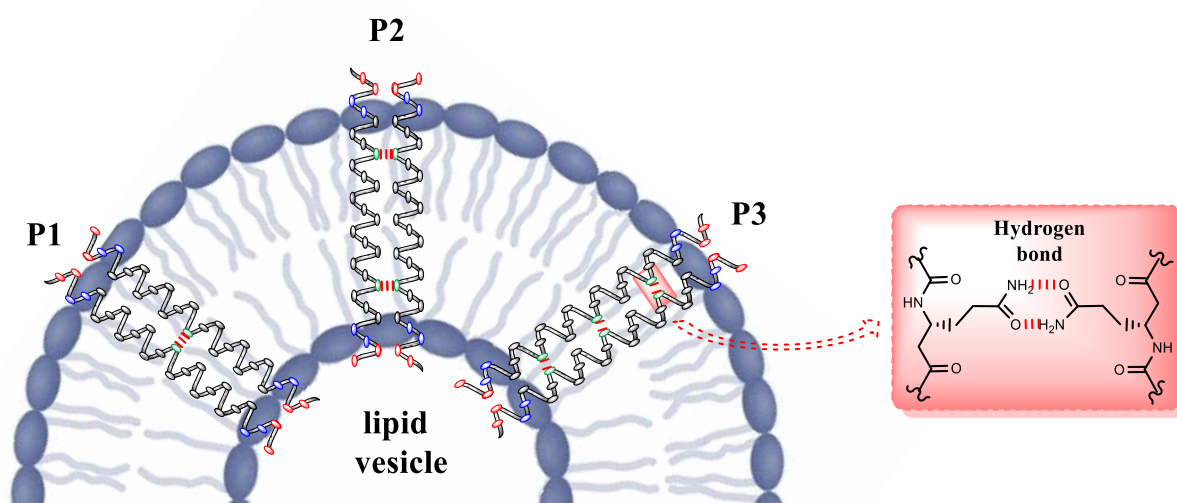


Figure 4.11: Schematic representation of self-dimerization of transmembrane 14-helices embedded in lipid bilayer composed of POPC. Red and blue positions in the β -peptides represent the positions of β^3 -Lys and β^3 -Trp, respectively whereas the black positions represent β^3 -Val functionalized with one, two and three β^3 -Gln (green positions) resulting the formation of **P1**, **P2** and **P3**, respectively (left). Hydrogen bonding resulted from polar side chains of β^3 -Gln residues (right).

The results of the FRET measurements for **P1**, **P2** and **P3** are shown in Figure 4.10B, C and D, respectively. Apparently, the data show an increase in quenching of the NBD-fluorescence over an increase of the concentration of the quencher TAMRA, which means that these β -peptides tend to aggregate with strong affinity toward the number of β^3 -Gln residues. The best fit for FRET data was obtained by assuming a monomer-dimer model for all the β -peptides with dissociation constants (K_D) of 0.0076 ± 0.002 MF for **P1** (Figure 1B), 0.0034 ± 0.0002 MF for **P2** (Figure 4.10C) and 0.0015 ± 0.0001 MF for **P3** (Figure 4.10D). On the one hand, **P2** with two β^3 -Gln and **P3** with three β^3 -Gln emerge a full dimeric state as indicated by the good fit of the monomer-dimer model to the data depicted for various peptide-to lipid ratios (Figure

4.10C and D). On the other hand, **P1** with one β^3 -Gln does not fully self-associate in the membrane as expounded by the too small FRET effect at ratio of 1:300 (solid black line in Figure 4.10B).

These overall results unequivocally prove that the polar β^3 -Gln residues have a significant effect on self-association properties of β -peptides with the concept that at least two β^3 -Gln are required within the helices to achieve a full-dimeric state. Recently, U. Rost from our group has investigated the possibility of aggregation in the case of asymmetrically introduced polar recognition units within β -peptides.^[151] The results have shown that these helices tend to assemble into homo-trimers unlike the formation of homo-dimers presented in this study. In the first case of study, U. Rost has investigated the aggregational state of the β -peptides within the DOPC lipid bilayer which has a hydrocarbon thickness of 26.8 Å.^[164] However, herein, the used POPC lipid system has a hydrocarbon thickness of 29.2 Å,^[164] which means that the hydrophobic mismatch induced by the difference between the hydrocarbon region of the two lipid bilayers and the apolar part of the β -peptides adopting the 14-helix (which is 31.6 Å) is different in the both case of study. This variation indicates that the β -peptides have different tendency to associate within different models of lipid bilayers since the hydrophobic mismatch can significantly influence the formation of aggregates.^[206] Therefore, this could be a possible explanation for the formation of dimers in this study rather than trimers that have been observed in the former case.

It is expected that an increase in the temperature can break the hydrogen bond interactions between the helices and, thereby, nullify the dimeric character of **P2** and **P3**. Thus, FRET experiments for these two β -peptides were performed at 60 °C while keeping other conditions unchanged (Figure 4.12).

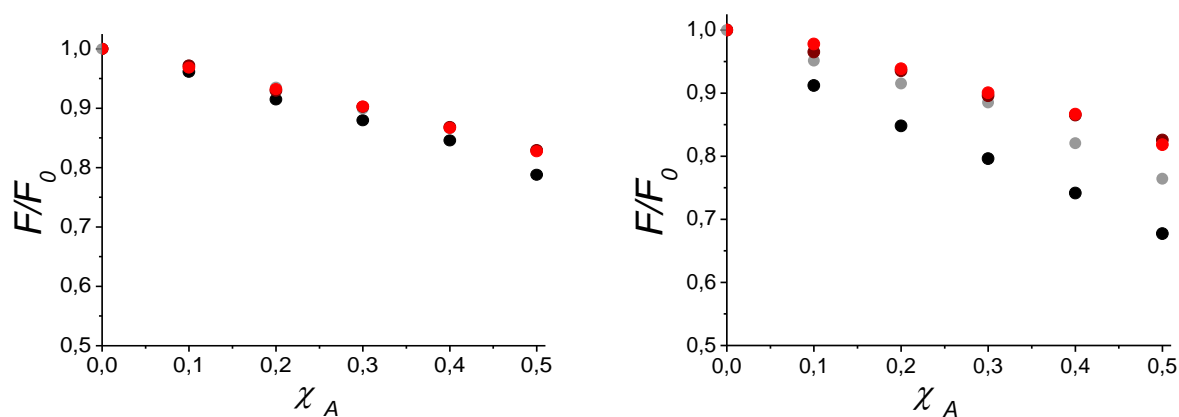
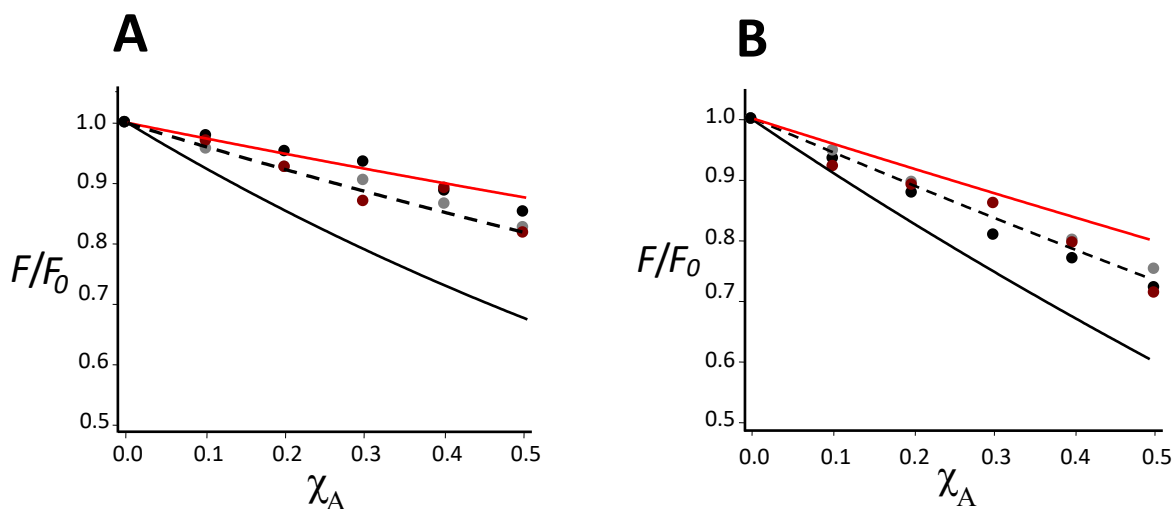


Figure 4.12: Relative emission of NBD-fluorescence (F/F_0) as a function of χ_A for **P2** (top) and **P3** (bottom) at 60 °C and 1:300 (●), 1:600 (●), 1:900 (●) and 1:1200 (●) as peptide-to-lipid ratios.

At 60 °C, **P2** exhibits a complete segregation from dimers to monomers as presented in Figure 4.12 (top). In contrast, **P3** did not fully dissociate by sustaining the dimeric character at ratio of 1:300 (Figure 4.12 bottom). These results suggest that **P3** has greater propensity to form more rigid dimers due to the presence of a third β^3 -Gln, which means more interactions between the transmembrane helices.

4.3.2.2 Self-Assembly of 12-Helices

In the same way, analogical FRET studies were performed to gain insight into the prospect of self-association of β -peptides showing a 12-helical secondary structure. The obtained results are depicted in Figure 4.13.



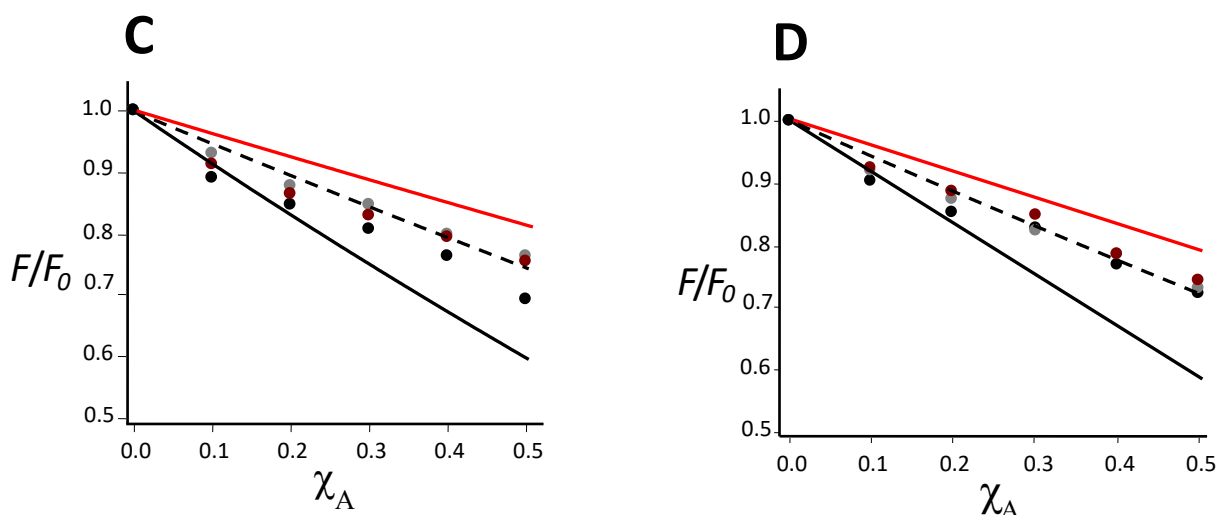


Figure 4.13: Relative emission of NBD-fluorescence (F/F_0) as a function of χ_A for β -peptides showing 12-helix at 1:300 (●), 1:600 (●), 1:900 (●) peptide-to-lipid ratios and at 20 °C. For **P5** only statistical FRET was assumed (100 nm POPC LUVs with $R_0 = 5.1$ nm). For **P6** (B), **P7** (C) and **P8** (D) a monomer-dimer equilibrium was assumed and fitted to the obtained data as shown in different lines (solid black line for 1:300, dashed black line for 1:600 and solid red line for 1:900).

As it is the case for the 14-helix, the 12-helical conformation was systematically predesigned to achieve an orderly association of the sequences across the membrane by reconstituting the helices with one, two and three β^3 -Gln, respectively (see section 3.1). However, the possibility of these helices to form aggregates is limited by their mode of insertion into the membrane as well as the side chain alignments of their residues.

Initially, **P5** was structurally designed as an initial backbone without imposing any interaction that can cause self-assembly of the helices. Thus, it is expected to exist as monomers within the lipid bilayer. Figure 4.13A depicts the data obtained from measuring FRET analysis for **P5** in POPC at 20 °C and at different peptide-to-lipid ratios (same conditions as described previously). According to theoretical description of Wolber and Hudson, only statistical FRET measurement was assumed for **P5** leading to a value of $R_0 = 5.1$ nm.^[192] This value is in a good agreement with the literature and indicates that **P5** was effectively found to be monomeric in the membrane.

For **P6**, **P7** and **P8**, a monomer-dimer equilibrium was assumed and fitted to the FRET data as shown in figure 4.13B, C and D, respectively. The results clearly indicate that the monomer-dimer model does not appropriately fit to the obtained FRET data in all cases. These findings

undoubtedly mean that there is no trend of these helices to form regular aggregates by exhibiting a very weak association relative to that of β -peptides showing 14-helix. Consequently, it could be a reflection that more likely random interactions occur between the helices. Since in this study the β^3 -Gln residues have been introduced based on the concept that the helices might self-associate in a parallel fashion, one plausible explanation could be that they prefer to associate in the membrane as anti-parallel bundles. This preference would constrain the interactions between the β^3 -Gln side chains in the case of β -peptides showing 12-helix. To overcome this restriction, the positions of β^3 -Gln amino acids can be altered in order to achieve a direct contact between their side chains in the case of an anti-parallel orientation of the sequences.

Another reason for the random interactions could be that the additional forces arising from β^3 -Gln side chains might not be sufficient to drive the 12-helices to self-assemble. Thus, the addition of more β^3 -Gln across the 12-helix can be a solution by creating more hydrogen bonds and thereby, increasing the possibility of interactions between the β -peptides. However, the addition of a large amount of these polar residues can lead to the binding of β -peptides on the membrane surface, which is certainly undesirable in this kind of study.

4.3.3 Higher Order Aggregates of β -Peptides

Designing a complex with a high molecular weight and suitable functional properties is of major interest in the field of biomacromolecular chemistry. Recently, self-assembly of subunits based on hydrogen bond interactions has considerably been studied.^[207]

It was shown that the selective introduction of β^3 -Gln residues within the helices has led to the homo-dimerization of the β -peptides showing 14-helix. These results are promising for further investigating whether these helices are able to show a complex inside the membrane with higher order aggregates. Thus, it is conceivable that the reasonable positioning of β^3 -Gln residues within the 14-helical backbone might drive the helices to show a well-defined self-assembled complex. For this reason, the oligomer **P4** was precisely designed by introducing two β^3 -Gln on two sides of the 14-helix as presented in Figure 4.14(See section 3.1.1).

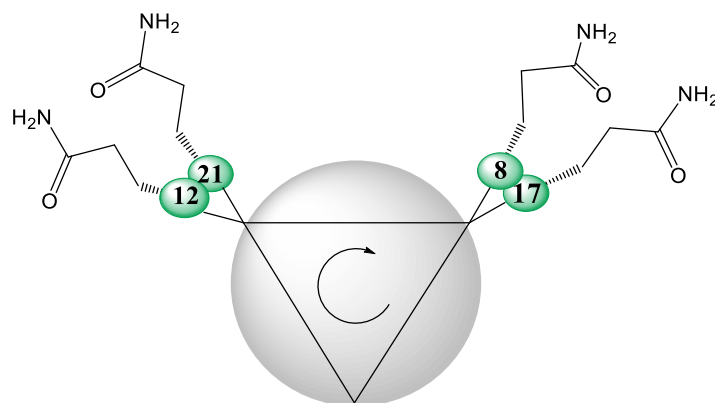


Figure 4.14: Top view of the right-handed 14-helix **P4** distributed with two β^3 -Gln amino acids on two sides at different positions as indicated in the figure.

The architecture of this peptide is expected to highly promote the formation of higher order aggregates by creating more non-covalent interactions between the polar side chains of the adjacent helices.

To analyze self-assembly of **P4** in LUVS composed of POPC, FRET experiments have been employed keeping the same conditions as previously described for other β -peptides (see section 4.3.2). Figure 4.15 illustrates the relative fluorescence of the NBD-labeled peptides (F/F_0) plotted against the molar fraction of TAMRA-labeled species (χ_A).

It is expected that in the case of the oligomer **P4**, the FRET data show a higher decrease in the NBD-fluorescence upon raising the concentration of TAMRA-labeled species than that resulted from the dimers **P2** and **P3**. Indeed, the results depicted in Figure 4.15 exhibit a significant high FRET effect upon reaching equal concentrations of donor and acceptor species of approximately 72% (for 1:300 ratio), 60% (for 1:600 ratio) and 52% (for 1:900). This means that the extent of FRET between **P4** oligomers is greater than that of all other β -peptides including the ones that have shown the formation of dimers.

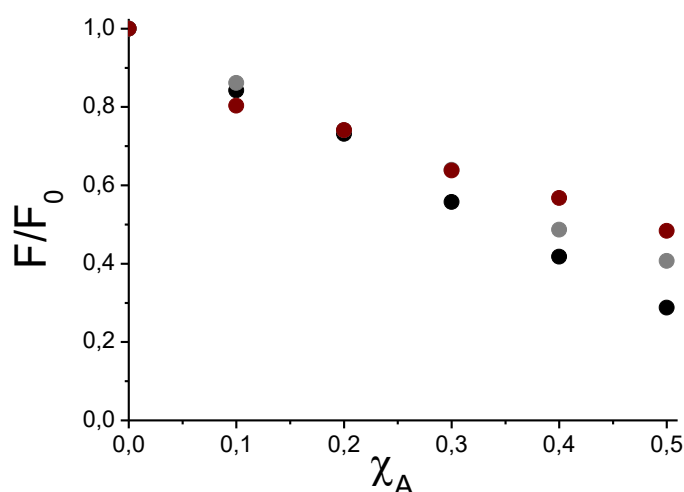


Figure 4.15: Relative emission of NBD-fluorescence (F/F_0) as a function of χ_A for **P4** at 1:300 (●), 1:600 (●), 1:900 (●) peptide-to-lipid ratios and at 20 °C. The concentration of the NBD-labeled peptides was kept constant at 2.75 μM while varying the concentration of the TAMRA-labeled peptides from 0 μM to 2.75 μM . The concentration of the overall peptide was kept at 5.5 μM by adding the corresponding non-labeled peptides.

This result suggests that **P4** tends to form a higher order aggregates within the same complex. It is noteworthy that FRET experiments in this case are considered as a limited technique to define the exact number of subunits forming the complex, which renders this method more qualitative than quantitative. In this context, other methods such as ultra-centrifugation or fluorescence microscopy might assist to determine the accurate information concerning the order of the aggregates.

4.3.4 Helix Orientation of Transmembrane β -Sequences within the Lipid Bilayer

The measurement presented herein aimed at obtaining clearer perception of the structural adaptations of β -peptides inside the membrane by determining the mode of assembly of the membrane-associated aggregates. Thus, the fluorescence of NBD-labeled species within POPC liposomes was monitored.

It is known that the fluorescence of NBD molecules can be self-quenched at higher concentrations.^[200,201] Thus, in the case of a close contact between the N-termini of β -peptides as assumed in a parallel orientation, it is expected that the fluorescence of their NBD-labeled analogues decreases or is abolished because of self-quenching upon increasing the

concentration of the NBD-probes. Otherwise, if the N-termini of β -peptides are far from each other as it is the case in an anti-parallel orientation, an increase in fluorescence of their NBD-labeled analogues will be observed. Based on this concept, we examined the orientation mode of β -sequences **P3** and **P8** by the intensity of their fluorescently NBD-labeled analogues **P3_D** and **P8_D**, respectively, as a function of peptide mol% in POPC LUVs at 25 °C (Figure 4.16 and Figure 2.5 in the “Appendix”).

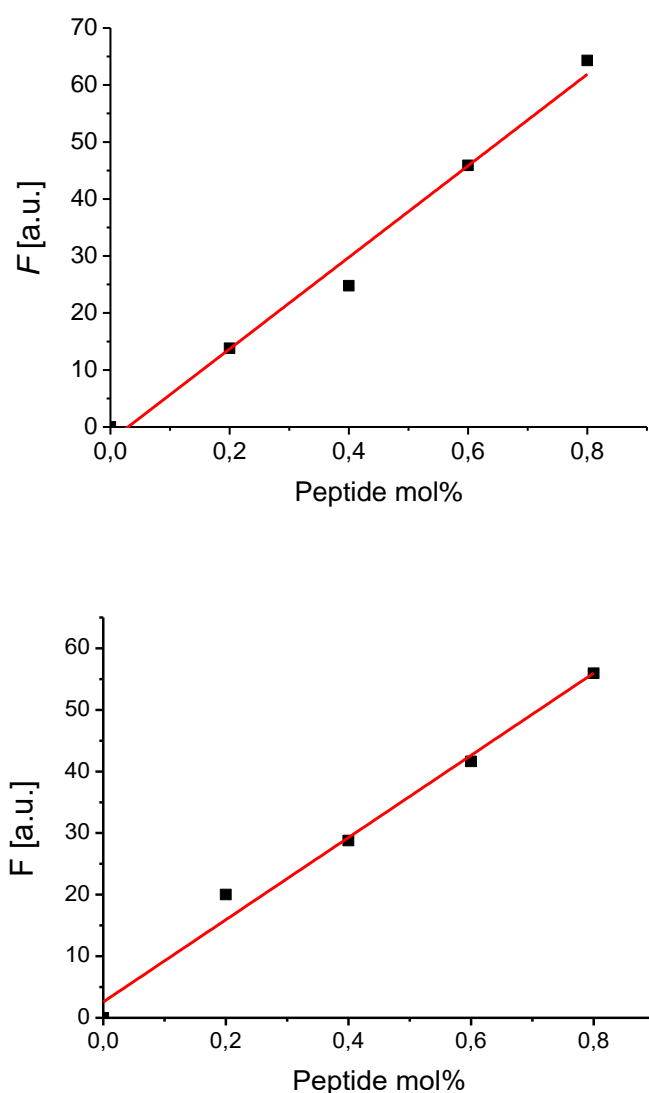


Figure 4.16: Fluorescence intensities of NBD-labeled β -peptides **P3_D** (top) and **P8_D** (bottom) defined as a function of peptide mol% in POPC LUVs at 25 °C.

The data plotted in Figure 4.16 show a remarkable increase in the intensity of the NBD fluorescence upon increase of the concentration of fluorescent NBD-labeled analogues in both cases, **P3_D** (Figure 4.16 top) and **P8_D** (Figure 4.16 bottom) (see also Figure 2.S in the “Appendix”). These results mightily denote that no self-quenching has been occurred and therefore, the β -sequences **P3** and **P8** adopt anti-parallel strand orientation within the membrane.

It is interesting to note that the characteristic of anti-parallel strand orientation has been also found for β -peptides functionalized with nucleobases in aqueous solution.^[4,127] More generally, anti-parallel trends of adjacent helices are preferred over parallel trends in known structures of natural membrane proteins.^[202,203] Thus, the present study might confirm that the non-natural β -peptides tend to assemble in anti-parallel strands, too, as has been found for biological proteins. One reasonable explanation for this anti-parallel association arises from the macro-dipole moment of the peptides. Although dipole-dipole interactions might be relatively weak, they are strong enough to orient the helices into an anti-parallel packing in the absence of stronger and/or specific helix association forces.^[204-206]

Overall, these findings might explain the reason of the random interactions that has been found between the 12-helices, suggesting that they form anti-parallel aggregates within the membrane and that the side chains of the β^3 -Gln are far away from each other, which prevent the formation of hydrogen bonds.

5 Conclusion

Non-covalent interactions are thought to play a crucial role in many biological functions, such as enzyme catalysis, protein-protein and protein-nucleic acid binding.^[1] Thus, specific physicochemical modifications of a given backbone can represent one approach to discern the role of these non-covalent forces in biological processes. However, the precise experimental delineation of chemical factors, which might control both the chemical selectivity and the biological reactivity remains difficult. Recently, designing peptidomimetics that adopt discrete tertiary structures and have the ability to penetrate the membrane is of great importance. In particular, β -peptides have been used as attractive model systems to mimic the biological functions of natural peptides. These non-natural polymers are characterized by rigid and well-known helical conformations and they show the ability to remain stable towards enzymatic degradation.^[2,109]

In this study, the self-assembly of a novel series of β -peptidic helices that can specifically fold into 14- and 12-helices across membranes has been investigated. Thus, polar residues have been precisely introduced into the β -peptides to drive a regular arrangement of adjoining helices through non-covalent interactions. Initially, the design of these foldamers was based on the apparent malleability of β^3 -acyclic residues to adopt discrete conformations. In this regard, β -peptides containing a long sequence of either β^3 -Val or β^3 -Leu have been strategically synthesized to induce the formation of stable 14- and 12-helices, respectively. These sequences were further enriched by the presence of β^3 -Trp residues to maintain interactions with the interfacial region and to explore the position of proteins within the membrane. Moreover, the sequences were flanked by β^3 -Lys residues to enhance the solubility in aqueous media.

β^3 -D-Amino acids derived from their natural D-amino acid counterparts have been successfully obtained *via* Arndt-Eistert homologation in very good yields. Worth mentioning, the synthesis of β -peptides containing a large amount of hydrophobic residues can be problematic, especially, after coupling the sixth amino acid. Therefore, a new synthetic methodology using manual microwave-assisted Fmoc-SPPS has been developed to successfully synthesize the desired sequences, mainly those containing a large number of the hydrophobic β^3 -Leu units.

After the synthesis and purification, the helicity of the respective sequences has been characterized using CD spectroscopy. The data have shown the formation of a right-handed 14-helix for β -peptides containing β^3 -Val residues and left-handed 12-helix for β -peptides containing β^3 -Leu residues. These two conformations are broadly described in the literature and used by several research groups, which suggest that they might be reasonable folding patterns for molecular recognition. Taking into account the differences between the structural backbones of the 14- and the 12-helices, the polar β^3 -Gln residues have been introduced in several positions across turns of the helices to create hydrogen bonds and thereby, to drive self-association of the β -peptides.

To ensure the stability of the secondary structure of the sequences bearing β^3 -Gln residues, CD spectroscopy has been employed either in solution or within POPC liposomes. The results display that the β -peptides preferably maintain their helicity, which demonstrate that the β^3 -Gln units are well-tolerated in several positions along the helices.

To confirm the insertion of β -peptides into the lipid bilayer, the intrinsic tryptophan fluorescence of β^3 -Trp amino acids inserted near the ends of the sequences was utilized. Thus, a blue-shift in the tryptophan fluorescence has been observed in all cases reflecting the presence of β^3 -Trp residues in the interface region of the membrane. Thereby, these findings signify that the transmembrane β -peptides are existing within the membrane.

In collaboration with Prof. Dr. Claudia Steinem, self-association of the β -peptides across membranes has been monitored by FRET analysis at various peptide-to-lipid ratios. In the case of β -peptides adopting 14-helix, FRET data have shown the formation of aggregates in a monomer-dimer equilibrium with strong affinity towards the number of β^3 -Gln residues. On the other hand, for β -peptides adopting 12-helix no clear trend to form regular aggregates was observed, which indicate that a more random interhelical interactions occur. One reason for the random interactions could be that no sequential equilibrium was adjusted between the helices.

The formation of homo dimers for β -peptides adopting 14-helix were promising for further investigate the possibility of designing higher-order assemblies. Thus, two sides of the 14-helix have been reconstituted with two β^3 -Gln molecules to form hydrogen bonds between more than two helices. The FRET data from measuring self-assembly of this oligomer indicated that the relative fluorescence of donor-labeled species was decreased significantly, more than that

observed in the case of dimers, while increasing the concentration of acceptor-labeled probes. These findings suggest the formation of higher order aggregates.

In conclusion, β -peptides adopting either 14- or 12-helix were successfully synthesized and served as suitable scaffolds to organize a well-defined three-dimensional spatial arrangement of the helices within the membrane through hydrogen bonds. Especially, the 14-helices with three side chain alignments can be used as the most favorable scaffold to form defined aggregates.

The assembly of transmembrane β -peptides can be further extended by inserting different recognitions units to the peptide backbone in order to reinforce the aggregation of the helices by various types of interactions like base pairing or electrostatic interactions. The resulting β -peptides bundles can lead to the formation of selective artificial transmembrane peptides with interesting biological functions, such as the formation of pore channels that play a crucial role in transport of ions and other small molecules.

6 Experimental Part

6.1 General Synthetic Methods and Materials

Solvents

Technical solvents were distilled prior to use and other solvents of highest grade were available and were used without additional purification (EtOAc, pentane, MeOH, DCM, CHCl₃, DMF, NMP, TFE, diethyl ether, acetonitrile). The solvents were obtained from *Carl Roth Ltd*, *GL Biochem*, *Novabiochem*, *Alfa Aesar*, *Iris Biotech GmbH*, *Merck*, *VWR International Ltd*, *Sigma Aldrich* and *Fisher Scientific*. Dry solvents were stored over molecular sieves of 4 Å. Piperidine was obtained from *Riedel de Haen* and used as supplied. For HPLC purification, MeOH was available as HPLC-grade and ultra-pure water (Mili-Q-H₂O) was processed using a *Simplicity system* of *Millipore* (Bredford, UK).

Reagents

The protected amino acids, fluorophores, reagents and resins for solid phase peptide synthesis (SPPS) were purchased from *Sigma Aldrich* (Taufkirchen, Germany), *Fluka* (Taufkirchen, Germany), *VWR International* (Fontenay-sous-Bois, France), *Grüssing GMBH* (Filsum, Germany), *ABCR* (Karlsruhe, Germany), *Merck* (Darmstadt, Germany), *Acros Organics* (Geel, Belgium), *Alfa Aesar* (Karlsruhe, Germany), *TCI* (Zwijndrecht, Belgium), *Applichem* (Darmstadt, Germany), *Fluorochem* (Hadfield, UK), *GL Biochem* (Shanghai, China) and *Carl Roth GMBH* (Karlsruhe, Germany). Lipids were obtained from the *Avanti Polar Lipids* (Alabaster, USA), *Bachem* (Bubendorf, Germany) and *Sigma Aldrich* (St. Louis, USA).

Reactions

All reactions containing air- and moisture-sensitive reagents were carried out under an inert flow of argon gas. Glass equipment utilized for reactions under inert atmosphere was heated and dried under reduced pressure and flushed with argon prior to use.

Lyophilization

The peptides were freeze-drying using a *Christ Alpha 2-4* lyophilizer connected to a high vacuum pump. For small amounts in *Eppendorf* tubes an evaluable *Christ RVC-18* centrifuge connected to the lyophilizing device was applied.

Chromatography

a. Thin layer chromatography (TLC)

Analytical thin-layer chromatography (TLC) was performed on *Merck* silica gel 60 F₂₅₄ aluminum plates. Detection was done under UV light at 254 nm or dipping into a solution of ninhydrin (2.0 g ninhydrin, 100 mL EtOH and 1 mL AcOH), KMnO₄ (1.0 g KMnO₄, 6.75 g K₂CO₃, 1.5 mL 5% aq. NaOH and 100 mL H₂O) followed by heating using a heat-gun.

b. Flash column chromatography :

Flash column chromatography was performed using a *Merck* silica gel 60 (40 – 60 µm) under 0.1-1 bar of pressure. All solid compounds were dissolved and absorbed to the fritted glass column filled with silica gel (50-100 times weight excess relative to the amount of the loaded substance).

c. High performance liquid chromatography (HPLC):

The peptides were purified using *Amersham Pharmacia Biotech* (Freiburg, Germany) (*Äkta Basic* 900, pump type P-900, UV/VIS Detector UV-900). The UV-absorption was detected at 215 nm, 254 nm and 280 nm for non-labeled peptides. For NBD- or TAMRA-labeled peptides the UV-absorption was recorded at 460 nm or 550 nm respectively.^[197] All crude samples were dissolved in MeOH/H₂O and filtered prior to use. The columns used to purify the peptides were as follow:

- Analytical HPLC: *MN Nucleodur*[®] (250 × 4.65 mm, C18, 100 Å, 5.0 µM).
- Semi-preparative HPLC: *MN Nucleodur*[®] (250 × 10 mm, C18, 100 Å, 5.0 µM).
- Preparative HPLC: *MN Nucleodur*[®] (250 × 20 mm, C18, 100 Å, 5.0 µM).

Analytical HPLC was performed at flow rate of 1 ml/min, semi preparative HPLC at flow rate of 3 ml/min and preparative HPLC at flow rate of 10 ml/min. The solvents used for all the runs were: eluent A (water + 0.1%TFA) and eluent B (methanol + 0.1% TFA). The gradient of the solvents was chosen appropriate to each compound.

6.2 Characterization

Nuclear magnetic resonance spectroscopy (NMR)

The ^1H -NMR spectra were recorded at *Varian Unity 300*, *Bruker AMX 300* or *Varian INOVA 500* NMR spectrometer. Chemical shifts δ were denoted in ppm with TMS as an internal standard ($\delta_{\text{TMS}} = 0$ ppm) and referenced to the residual solvent peak of $[\text{D}_6]$ DMSO (^1H : $\delta = 2.49$ ppm). The multiplicities were classified by the following symbols: s (singlet), d (doublet), t (triplet), q (quadruplet), m (multiplet), br (broad signal). Coupling constants $^nJ_{\text{X,Y}}$ are in Hertz (Hz), where n is the order of coupling between atoms X and Y.

Mass spectrometry (MS)

Electrospray ionization mass spectra (ESI-MS) and high-resolution mass spectrometry (HRMS-ESI) spectra were obtained with MicroTOF and maXis from *Bruker* devices (Karlsruhe, Germany). Other mass-spectrometric measurements (ESI) were carried out on LCQ mass spectrometer from *Thermo Finnigan MAT* (Waltham, USA).

6.2.1 Analytical and Spectroscopic Methods

UV/VIS spectroscopy

Concentrations of stock solutions were measured using a *Thermo Scientific NanoDrop 2000c* spectrophotometer at 25 °C. Peptides concentration was calculated using *Lambert–Beer's law*, given by:

$$C = \frac{A}{\epsilon \cdot l}$$

Where C is the concentration of the compound in solution (mol L^{-1})

A is the absorbance (no units)

ϵ is the molar absorptivity ($\text{L mol}^{-1} \text{cm}^{-1}$)

l is the path length of the cuvette in which the sample is contained (cm)

For unlabeled peptides, the molar absorptivity of a single tryptophan at 280 nm was used ($\epsilon_{280} = 5690 \text{ M}^{-1} \text{cm}^{-1}$), while for labeled-peptides with TAMRA or NBD, the absorptions at 550 nm ($\epsilon_{550} = 92000 \text{ M}^{-1} \text{cm}^{-1}$) or at 460 nm ($\epsilon_{460} = 23000 \text{ M}^{-1} \text{cm}^{-1}$) were used, respectively.^[197]

Estimation of the loading density

To determine the loading capacity of the loaded resin, UV/VIS-Spectrometer V-550 from *Jasco* (Gross-Umstadt, Germany) was used. Thus, 40 μM of DBU [1,8-diazabicyclo [5.4.0] undec-7-en] and 2 ml of DMF were added to 5 mg of the dry loaded resin and gently shaken for 1-2 h. Thereafter, acetonitrile was added until 10 ml and the mixture was further diluted with acetonitrile (2/25) and transferred to an UV precision cuvette (1 cm x 1 cm). To estimate the loading capacity of the resin, the absorption of the dibenzofulven species was detected at 304 nm ($\epsilon_{304} = 7624 \text{ L mol}^{-1}\text{cm}^{-1}$)^[210] and calculated based on *Lambert-Beer's* law given by:

$$\rho(\text{resin}) \left[\frac{\text{mmol}}{\text{g}} \right] = \frac{1}{m(\text{resin})[\text{g}]} \cdot \left(\frac{A[\text{AU}] \cdot V[\text{L}] \cdot f}{\epsilon [\text{M}^{-1}\text{cm}^{-1}] \cdot d [\text{cm}]} \right) \cdot 10^3$$

Herewith, $\rho(\text{resin})$ is the loading density of the resin

A the absorption

V the volume of the graduated flask (here $1 \cdot 10^{-3}$ L)

f the thinning factor (here = 12.5)

ϵ the absorption coefficient of dibenzofulven

d the path length of cuvette

$m(\text{resin})$ the mass of the analyzed resin

Kaiser test^[212]

Kaiser test was also used to verify the successful coupling of the amino acids to the resin by determining the free amino groups. Thus, a few grains of the resin were placed into a small test tube and two drops of each of the following Kaiser test solutions were added to the resin:

Solution 1: phenol in ethanol (80 g/20 mL).

Solution 2: ninhydrin in ethanol (5 g/100 mL).

Solution 3: aq. KCN (1 mM, 2 mL) in pyridine (98 mL).

The resulting suspension was heated at 100 °C for 5 min. In the case of a positive test, a blue color appeared which means that there are free amino groups still on the resin. Otherwise, if a yellow color appeared confirming a negative test, which means an absence of free amino groups.

Circular dichroism spectroscopy (CD)

CD spectra were recorded on a *Jasco-1500* spectropolarimeter equipped with a *Julabo F250* temperature controlling unit. Measurements were carried out in a 1 mm QS quartz cuvette (*Suprasil® Hellma*) at different temperatures and in a wavelength range of 190-300 nm with 1.0 nm bandwidth using the 'continuous mode', 1.0 s response and 50 nm min⁻¹ as a scan speed. A nitrogen flux was used to flush the sample cell at a flow rate of 3-5 L min⁻¹. The measurements were carried out in organic solvent (MeOH, TFE) or vesicle suspensions containing 1:20 as P:L ratio in phosphate buffer (10 mM NaH₂PO₄ / Na₂HPO₄ buffer, pH = 7). The concentration of the peptides was adjusted to 30 μM and the temperature was recorded at 0 °C, 20 °C, 40 °C and 60 °C. Spectra were background-corrected against pure vesicle suspensions without incorporated peptides and the measurements were converted into molar ellipticity θ (deg cm²dmol⁻¹).^[211]

6.2.2 Fluorescence Spectroscopy

Förster resonance energy transfer (FRET)

To measure FRET, different samples were prepared separately by keeping the concentration of the donor NBD-labeled peptides constant at 2.75 μM while varying the concentration of the acceptor TAMRA-labeled peptides from 0 to 2.75 μM (range of 0-0.5 μM). The total peptide concentration was maintained at 5.5 μM by using unlabeled peptides. The FRET measurements were performed at different peptide-to-lipid ratios by changing the lipid concentration: 1:300 (1.65 mM POPC), 1:600 (3.30 mM POPC), 1:900 (4.95 mM POPC) and 1:1200 (6.60 mM POPC). All samples were prepared in phosphate buffer solution (10 mM, pH 7) and the resulted FRET data were calculated as described previously in the literature.^[192,194,199] For measuring FRET, fluorescence spectra were carried out on a *JascoFP 6200* fluorescence spectrometer (Gross-Umstadt, Germany) under temperature control using a *Jasco-thermostat* (Model ETC-272T, Groß-Umstadt, Germany). Fluorescence spectra were obtained by excitation at 465 nm with emission recorded in the wavelength range of 500-650 nm at two different temperatures (20 °C and 60 °C). The excitation and the emission bandwidth were set to 3 nm, the data pitch was 1 nm and the response time was adjusted to 0.2 s. Corrections for scattering were used by subtracting a spectrum of vesicles lacking peptides. For plotting the fluorescence of NBD-labeled peptides as a function of the mole

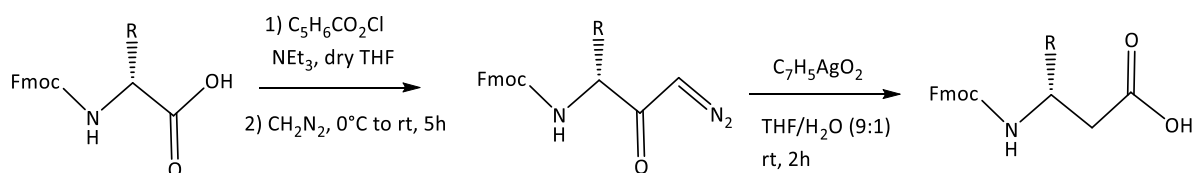
fraction (χ_A) of the labeled-TAMRA peptides, the fluorescence intensity at 530 nm was displayed.

Tryptophan fluorescence

The tryptophan fluorescence of the β -peptides either in TFE or within large unilamellar vesicles composed of POPC (ratio of 1:600) was measured. Thus, the tryptophan fluorescence of β -peptides was excited at 280 nm and the fluorescence emission was detected in the range of 300-400 nm using a *Jasco* FP 6200 (Gros-Umstadt, Germany) under temperature control using a *Jasco* thermostat (model ETC-272T, Gros-Umstadt, Germany).

6.3 Synthesis of β^3 -D-Amino Acids

The β^3 -D-amino acids (β^3 -AA) used in this work were obtained from their corresponding α -amino acids using *Arndt-Eistert* homologation intermediated by Wolff rearrangement.^[78,150]



Scheme 6.1. Schematic presentation for the synthesis of β^3 -D-amino acids.

Under argon atmosphere, the protected α -amino acid (1.0 eq.) was dissolved in dry THF and cooled to $-21^\circ C$, then triethylamine (1.10 eq.) and isobutyl chloroformate (1.10 eq.) were added and the mixture was stirred for 45 min. Under exclusion of light, the diazomethane (0.6-0.7 M in diethyl ether, 2.00 eq.) was added to the solution and the mixture was warmed to room temperature (rt) and stirred for 5h. After stopping the reaction, 6% $NaHCO_3$ (aq, 8.0 mL/mmol) and acetic acid (0.03 eq.) were added to the mixture and extracted with EtOAc (3 \times). The combined organic phases were further washed with saturated NH_4Cl (aq, 3 \times) and saturated $NaCl$ (aq., 3 \times) and then dried over $MgSO_4$. After removing the solvents under

reduced pressure, the obtained diazoketone was used for the next step without further purification.

As next step, the resulting product was dissolved in THF/H₂O (9:1) and silver benzoate (0.10 eq.) was added under exclusion of light. After 2 h of reaction in ultrasonic bath, the mixture was diluted with H₂O and acidified with HCl (1 M) to pH ~ 2-3. After extracting with EtOAc (3 x), the combined organic phases were dried over MgSO₄ and the solvents were removed under reduced pressure. Finally, the obtained product was purified either using Flash column chromatography or by precipitation in cold pentane (Table 1).

Table 6.3. Methods of purification of β^3 -D-amino acids.

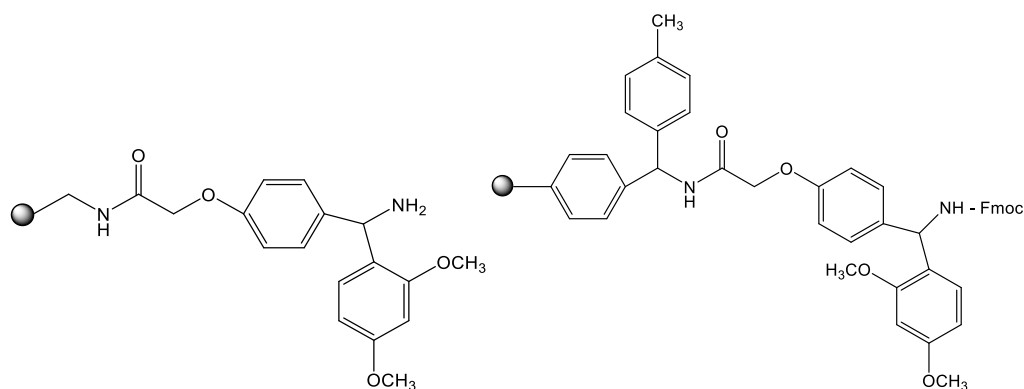
β^3 -D-Amino acids	Yield in %	Purification method
Fmoc- β^3 -D-Lys(Boc)-OH (1)	80	Flash chromatography DCM:MeOH (12:1)
Fmoc- β^3 -D-Trp(Boc)-OH (2)	76	Flash chromatography DCM:MeOH (24:1)
Fmoc- β^3 -D-Val-OH (3)	90	Precipitation in Pentane:DCM (10:1)
Fmoc- β^3 -D-Gln(Trt)-OH (4)	72	Flash chromatography DCM:MeOH (24:1)
Fmoc- β^3 -D-Lys(Alloc)-OH (5)	80	Flash chromatography DCM:MeOH (12:1)
Boc- β^3 -D-Lys(Fmoc)-OH (6)	79	Flash chromatography DCM:MeOH (12:1)

6.4 General Procedure for Solid Phase Peptide Synthesis (SPPS)

Loading the resin with the first Fmoc-D- β^3 -AA

The β -peptides were synthesized manually using a microwave-assisted Fmoc-solid phase peptide synthesis (SPPS), thus *Discover* microwave (MW) with reaction cavity (CEM) (Kamp-Lintfort, Germany) was applied. The resins used in this study were as follow: rink amide MBHA resin with a loading capacity of 0.57 mmol/g (for the β -peptides containing β^3 -Val) or NovaPEG

rink amide resin LL with a loading capacity of 0.18 mmol/g (for the β^3 -peptides containing β^3 -Leu). To load the first β^3 -AA, the resin (1 eq., 0.1 mmol) was transferred into an acid/base resistant syringe equipped with a polyethylene filter from *Becton-Dickinson* BD-Discardit II (Heidelberg, Germany) and swollen in a mixture of DCM:NMP (1:1, 6 ml) for 1-2 h. After removing the solvents, deprotection of the Fmoc-protecting group was performed for the rink amide MBHA resin twice by adding 4 ml of 20% piperidine in NMP for 30 s and then for 3 min, 50 °C and 25 W (NovaPEG rink amide resin does not have Fmoc-protecting group, see scheme 1). After filtration of the resin and washing with DMF (5 x), DCM (5 x) and NMP (5 x), the first coupling reaction was accomplished twice, using the same procedure for the two types of the resins, by adding a mixture containing the desired Fmoc-D- β^3 -AA (5 eq.), HOBT (5 eq.) and DIC (5 eq.) dissolved in 2 ml of NMP to the resin (20 min, 50 °C, 25 W). After washing the resin with DMF (3 x), DCM (3 x) and NMP (3 x), the second coupling was performed using a mixture containing the desired Fmoc-D- β^3 -AA (3 eq.), HOBT (3 eq.) and DIC (3 eq.) dissolved in 2 ml of NMP to the resin (20 min, 50 °C, 25 W). Finally, the resin was filtrated and washed with DMF (5 x), NMP (5 x), MeOH (10 x) and DCM (10 x) and dried overnight under vacuum. For each resin, the loading capacity was calculate as described previously.



Scheme 6.2. chemical structure of NovaPEG rink amide resin (left) and MBHA rink amide resin (right).

Synthesis cycle of the β -peptides using solid phase peptide synthesis (SPPS)

- For rink amide MBHA resin:

The synthesis cycle of β -peptides was continued by series of Fmoc-deprotection and β^3 -AA coupling procedures. Thus, the Fmoc-deprotection was achieved as described above and then the peptides were allowed to couple twice by adding a mixture of the required β^3 -AA (5 eq., 3

eq.), HATU (4.5 eq., 2.7 eq.), HOAt (5 eq., 3 eq.) and DIPEA (10 eq., 2 x) dissolved in 2 ml of NMP (20 min, 50 °C, 25 W). The resin was washed between each step with DMF (3 x), DCM (3 x) and NMP (3 x). After coupling the last β^3 -AA, Fmoc-deprotection was performed as described previously and the resin was washed with DMF (5x), NMP (5x), MeOH (10x) and DCM (10x) and dried under vacuum for the cleavage.

- For NovaPEG rink amide LL resin:

Due to the wide hydrophobicity of β -peptides containing β^3 -Leuamino acids, a third coupling was required, an addition of a stronger base (DBU) to remove the Fmoc-protecting group as well as an increase of the temperature to 75 °C during the coupling reaction. Thereby, after coupling the sixth amino acid as described above, the Fmoc-protecting group was removed using a mixture of 10% DBU, 10% piperidine in NMP twice for 3 min, 50 °C and 25 W. After washing the resin with DMF (3 x), DCM (3 x) and NMP (3 x), the next coupling was performed three times by adding the desired β^3 -AA (5 eq., 3 eq., 3 eq.), HATU (4.5 eq., 2.7 eq., 2.7 eq.), HOAt (5 eq., 3 eq., 3 eq.) and DIPEA (10 eq., 3 x) dissolved in 2 ml of NMP (20 min, 75 °C, 25 W). Finally, after coupling the last β^3 -AA, Fmoc-deprotection was performed and the resin was washed with DMF (5 x), NMP (5 x), MeOH (10 x) and DCM (10 x) and dried under vacuum for the cleavage.

Attaching the fluorophores to β -peptides

FRET studies require an acceptor-donor pair, thus, the fluorophores carboxytetramethylrhodamine (TAMRA) as an acceptor and 4-chloro-7-nitrobenzo-2-oxa-1,3-diazol (NBD-Cl) as a donor were selected in this work. The amino acids β^3 -Lys, β^3 -Trp and β^3 -Gln were orthogonally protected to avoid side chain reactions.

To attach the fluorophores to the β -peptides, the resins (5 μ mol scale) were swollen in a mixture of DCM:NMP (1:1 6 ml) for 1-2h. After removing the solvents, (NBD-Cl) (50.0 μ mol, 10 eq., 200 mM) and DIPEA (100 μ mol, 20 eq., 400 mM) dissolved in 750 μ L of NMP or respectively TAMRA (42.5 μ mol, 8.5 eq., 170 mM), PyBop (40 μ mol, 8 eq., 160 mM) and DIPEA (100 μ mol, 20 eq., 400 mM) dissolved in 750 μ L of NMP were added. The mixtures were shaken overnight under exclusion from light. Subsequently, the resins were filtrated and washed with NMP (5 x), DMF (5 x), MeOH (10 x) and DCM (5 x) and dried under vacuum prior to cleavage.

Cleavage of β -peptides from the resin:

β -Peptides were cleaved from the resin by adding 10 ml of a cocktail containing 95% TFA, 2.5% H₂O and 2.5% TIS. After 2 h of stirring at room temperature, the cleaved peptides were filtrated into a small plastic tube and concentrated under a nitrogen-stream. Finally, the crude peptide was isolated by precipitation from cold diethyl ether at -20 °C and dried under vacuum for further purification.

6.5 Preparation of Peptide/Lipid Vesicles

6.5.1 Multilamellar Vesicles (MLVs)

The lipids 1-palmitoyl-2-oleoyl-*sn*-glycero-3-phosphocholine (POPC) or 1,2-dilauroyl-*sn*-glycero-3-phosphocholine (DLPC) were dissolved in CHCl₃ and β -peptides were dissolved in TFE and mixed together with different peptide-to-lipid (P:L) ratios. At temperature (T) above the gel-to-fluid transition temperature of the lipids (T_m) which is -2 °C for POPC and \sim -1 °C for DLPC,^[164] the solvents were evaporated under a stream of nitrogen followed by several hours in vacuum to obtain clear peptide–lipid films. The latter were rehydrated with an appropriate amount of phosphate buffer solution (10 mM, pH 7) and let incubate for 1 h. Keeping always $T > T_m$, the suspension was vortexed several times for 30 seconds with subsequent incubation for 5 min (5 cycles).

6.5.2 Large Unilamellar Vesicles (LUVs)

To obtain large unillamellar vesicles (LUVs), the milky suspensions of MLVs were extruded 31 times through a 100 nm nominal pore size polycarbonate membrane using a mini extruder from *Liposofast* (Avestin, Ottawa, Canada) to produce a clear vesicle suspension containing LUVs of 100 nm size.

Fluorescence quenching analysis

To quench the fluorescence of NBD molecules, the reducing dithionite ions (S₂O₄²⁻) dissolved in phosphate buffer solution (10 mM, pH 7) were externally added to LUVs containing NBD-labeled peptides. Thus, after stabilization of NBD-fluorescence period (\sim 2 min), the vesicles

containing 5.5 μM NBD-labeled peptides (1:600 as P:L ratio) were treated with freshly prepared dithionite ions (100 μM) and the time course of NBD fluorescence was monitored for 20 min using an excitation and an emission wavelengths of 450 nm and 533 nm, respectively.^[178]

6.6 Analytical Data

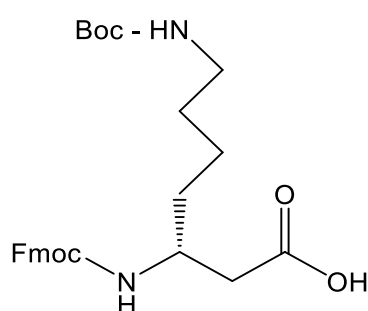
6.6.1 β^3 -D-Amino Acids

All the following β^3 -D-amino acids have been synthesized through *Arndt–Eistert* homologation from their α -D-amino acids counterparts (see section 6.3). The purification was performed for each β^3 -D-amino acid either using Flash column chromatography or by precipitation in cold pentane as described in Table 6.1.

6.6.1.1 β^3 -D-Fmoc-Lys(Boc)-OH

(R)-3-((9-fluoren-9-yl)-methoxy-carbonyl-amino)-7-(tert-butoxycarbonyl-amino) heptanoic acid (1)

$\text{C}_{27}\text{H}_{34}\text{N}_2\text{O}_6$ [482.58 g/mol]



$^1\text{H-NMR}$ (300 MHz, $[\text{D}_6]\text{DMSO}$): δ (ppm) = 1.13-1.47 (m, 15 H, $3 \times \text{CH}_3$, $3 \times \text{CH}_2$), 2.27-2.41 (m, 2 H, $2 \alpha\text{-CH}_2$), 2.81-2.91 (m, 2 H, CH_2), 3.69-3.82 (m, 1 H, $\beta\text{-CH}$), 4.14-4.32 (m, 3 H, Fmoc- CH_2 , Fmoc-CH), 6.69 (s, 1 H, NH), 7.17 (d, 1 H, $^3J_{\text{H,H}} = 8.7$ Hz, NH), 7.28-7.36 (m, 2 H, $2 \times$ Fmoc-CH), 7.42 (t, $^3J_{\text{H,H}} = 7.4$ Hz, 2 H, $2 \times$ Fmoc-CH), 7.69 (d, 2 H, $^3J_{\text{H,H}} = 7.5$ Hz, $2 \times$ Fmoc-CH), 7.88 (d, $^3J_{\text{H,H}} = 7.4$ Hz, 2 H, $2 \times$ Fmoc-CH), 12.08 (S_{br} , 1 H, COOH).

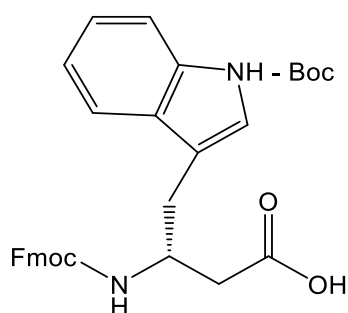
ESI-MS m/z (%) = 987.5 [2M+Na]⁺, 505.3 [M+Na]⁺, 483.3 [M+H]⁺.

HR-MS (ESI): calculated for 483.2490 [M+H]⁺, 505.2309 [M+Na]⁺, 481.2344 [M-H]⁻; found 483.2488 [M+H]⁺, 505.2312 [M+Na]⁺, 481.2341 [M-H]⁻.

6.6.1.2 β³-D-Fmoc-Trp(Boc)-OH

(R)-3-((9H-fluoren-9-yl)-methoxy-carbonyl-amino)-4-(1-(tert-butoxycarbonyl)-indol-3-yl)butanoic acid (2)

C₃₂H₃₂N₂O₆ [540.61 g/mol]



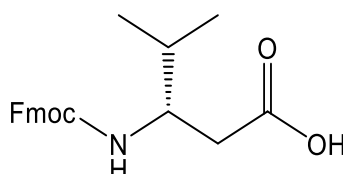
¹H-NMR (300 MHz, [D₆]DMSO): δ (ppm) = 1.58 - 1.66 (m, 9 H, 3 × CH₃), 2.42-2.52 (m, 2 H, CH₂), 2.86 (d, 2 H, ³J_{H,H} = 6.7 Hz, α-CH₂), 4.09-4.24 (m, 4 H, Fmoc-CH₂, Fmoc-CH, β-CH), 7.19-7.43 (m, 8 H, 4 × Fmoc-CH, NH, 3 × Trp-H), 7.54-7.64 (m, 2 H, 2 × Fmoc-CH), 7.69 (d, ³J_{H,H} = 7.2 Hz, 1 H, Trp-H), 7.86 (d, ³J_{H,H} = 7.2 Hz, 2 H, 2 × Fmoc-CH), 8.04 (d, ³J_{H,H} = 7.6 Hz, 1 H, Trp-H), 12.1 (s_{br}, 1 H, COOH).

ESI-MS m/z (%) = 541.3 [M+H]⁺, 558.3 [M+NH₄]⁺, 563.2 [M+Na]⁺.

HR-MS (ESI): calculated for 541.2333 [M+H]⁺, 563.2153 [M+Na]⁺, 558.2599 [M+NH₄]⁺; found 541.2318 [M+H]⁺, 563.2138 [M+Na]⁺, 558.2583[M+NH₄]⁺.

6.6.1.3 β^3 -D-Fmoc-Val-OH

(R)-3-((9H-fluoren-9-yl)-methoxy-carbonyl-amino)-4-methyl-pentanoic acid (3)

 $C_{21}H_{23}NO_4$ [353.42 g/mol]

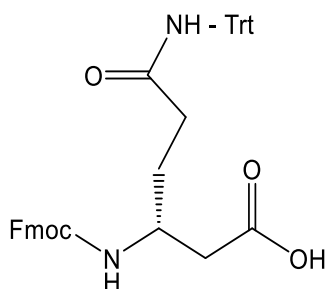
1H -NMR (300 MHz, $[D_6]DMSO$): δ (ppm) = 0.70-0.88 (m, 6 H, $2 \times CH_3$), 1.68-1.80 (m, 1 H, CH), 2.26-2.46 (m, 2 H, α - CH_2), 3.68-3.82 (m, 1 H, β -CH), 4.18-4.37 (m, 3 H, Fmoc-CH, Fmoc- CH_2), 7.20 (d, 1 H, $^3J_{H,H} = 8.1$ Hz, NH), 7.28-7.46 (m, 4 H, $4 \times$ Fmoc-CH), 7.68-7.78 (m, 2 H, $2 \times$ Fmoc-CH), 7.88 (d, 2 H, $^3J_{H,H} = 6.6$ Hz, $2 \times$ Fmoc-CH), 12.2 (s_{br} , 1 H, COOH).

ESI-MS m/z (%) = 354.2 $[M+H]^+$, 376.2 $[M+Na]^+$, 392.1 $[M+K]^+$, 729.3 $[2M+Na]^+$, 745.3 $[2M+K]^+$.

HR-MS (ESI): calculated for 354.1700 $[M+H]^+$, 376.1519 $[M+Na]^+$, 392.1259 $[M+K]^+$, 352.1554 $[M-H]^-$; found 354.1691 $[M+H]^+$, 376.1518 $[M+Na]^+$, 392.1261 $[M+K]^+$, 352.1556 $[M-H]^-$.

6.6.1.4 β^3 -D-Fmoc-Gln(Trt)-OH

(R)-3-((9H-fluoren-9-yl)-methoxy-carbonyl-amino)-6-oxo-6-(tritylamino) hexanoic acid (4)

 $C_{40}H_{36}N_2O_5$ [624.74 g/mol]

¹H-NMR (300 MHz, [D₆]DMSO): δ (ppm) = 1.50-1.74 (m, 2 H, α-CH₂), 2.22-2.39 (m, 4 H, 2 CH₂), 3.78-3.90 (m, 1 H, β-CH), 4.20-4.34 (m, 3 H, Fmoc-CH, Fmoc-CH₂), 7.17-7.46 (m, 20 H, 3 × C₅H₅, NH, 4 × Fmoc-CH), 7.70 (d, 2 H, ${}_3J_{H,H} = 7.3$ Hz, 2 × Fmoc-CH), 7.90 (d, 2 H, ${}_3J_{H,H} = 7.8$ Hz, 2 × Fmoc-CH), 8.50 (s, 1 H, NH), 12.2 (s_{br}, 1 H, COOH).

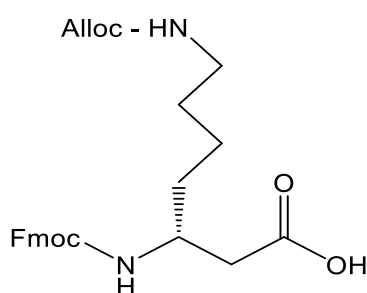
ESI-MS *m/z* (%) = 623.3.2 [M-H]⁻, 625.3 [M+H]⁺, 647.3 [M+Na]⁺, 1271.5 [2M+Na]⁺.

HR-MS (ESI): calculated for 625.2697 [M+H]⁺, 674.2516 [M+Na]⁺, 623.2551 [M-H]⁻; found 625.2687 [M+H]⁺, 647.2515 [M+Na]⁺, 623.2554 [M-H]⁻.

6.6.1.5 β³-D-Fmoc-Lys(Alloc)-OH

(R)-3-((9-fluorenyl-methoxy-carbonyl-amino)-7-(Allyloxy-carbonyl-amino) heptanoic acid
(5)

C₂₆H₃₀N₂O₆ [466.53 g/mol]



¹H-NMR (300 MHz, [D₆]DMSO): δ (ppm) = 1.14-1.50 (m, 6 H, 3 CH₂), 2.23-2.44 (m, 1 H, CH₂), 2.91-3.02 (m, 2 H, α-CH₂), 3.70-3.84 (m, 1 H, β-CH), 4.16-4.37 (m, 3 H, Fmoc-CH, Fmoc-CH₂), 4.40-4.50 (m, 2 H, Alloc-CH₂), 5.11-5.32 (m, 2 H, 2 Alloc-CH), 5.90 (ddt, 1 H, ${}_3J_{H,H} = 15.2, 9.6, 5.1$ Hz, Alloc-CH), 7.06-7.20 (m, 2 H, 2 × NH), 7.28-7.43 (m, 4 H, 4 × Fmoc-CH), 7.70 (d, 2 H, ${}_3J_{H,H} = 6.7$ Hz, 2 × Fmoc-CH), 7.90 (d, 2 H, ${}_3J_{H,H} = 6.7$ Hz, 2 × Fmoc-CH), 12.2 (s_{br}, 1 H, COOH).

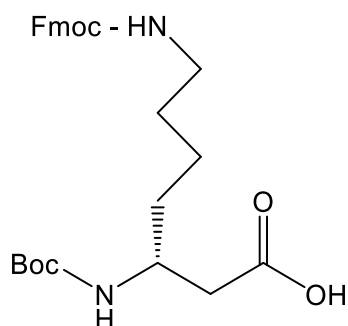
ESI-MS *m/z* (%) = 467.2 [M+H]⁺, 489.2 [M+Na]⁺, 955.4 [2M+Na]⁺.

HR-MS (ESI): calculated for 467.2177 [M+H]⁺, 489.1996 [M+Na]⁺, 465.2031 [M-H]⁻; found 467.2171 [M+H]⁺, 489.1995 [M+Na]⁺, 465.2027 [M-H]⁻.

6.6.1.6 β³-D-Boc-Lys(Fmoc)-OH

(R)-7-((9H-fluoren-9-yl)-methoxy-carbonyl-amino)-3-(tert-butoxycarbonyl-amino) heptanoic acid (6)

C₂₇H₃₄N₂O₆ [482.58 g/mol]



¹H-NMR (300 MHz, [D₆]DMSO): δ (ppm) = 1.17-1.42 (m, 15 H, 3 × CH₃, 2 CH₂), 2.22- 2.39 (m, 2 H, CH₂), 2.91-3.01 (m, 2 H, α-CH₂), 3.65-3.76 (m, 1 H, β-CH), 4.17-4.33 (m, 3 H, Fmoc-CH, Fmoc- CH₂), 6.60 (d, 1 H, ³J_{H,H} = 8.6 Hz, NH), 7.21 (t, 1 H, ³J_{H,H} = 5.8 Hz, NH), 7.28-7.43 (m, 4 H, 4 × Fmoc-CH), 7.68 (d, 2 H, ³J_{H,H} = 7.4 Hz, 2 × Fmoc-CH), 7.89 (d, 2 H, ³J_{H,H} = 7.1 Hz, 2 × Fmoc-CH), 12.2 (s_{br}, 1 H, COOH).

ESI-MS *m/z* (%): 483.3 [M+H]⁺, 505.3 [M+Na]⁺, 521.2 [M+K]⁺, 987.5 [2M+Na]⁺.

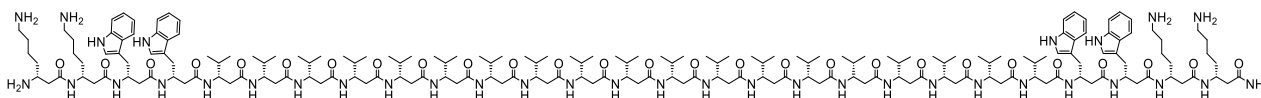
HR-MS (ESI): calculated for 505.2309 [M+Na]⁺, 521.2048 [M+K]⁺; found 505.2306 [M+Na]⁺, 521.2049 [M+K]⁺.

6.6.2 Synthesized β -Peptides

All the following β -peptides have been synthesized by manual microwave-assisted Fmoc-SPPS (see section 6.4), purified by HPLC using a C18 reversed-phase column, and characterized by mass spectrometry. Attaching the fluorophores to the β -peptides has been performed on the resin as described in section 6.4.

6.6.2.1 P0:H-hLys₂-hTrp₂-hVal₁₉-hTrp₂-hLys₂-NH₂

C₁₉₀H₃₁₆N₃₆O₂₇ [3534,45 g/mol]



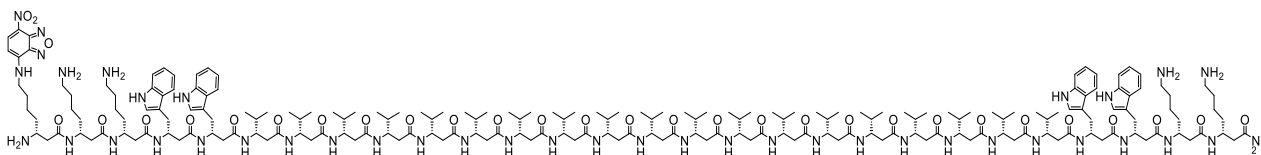
HPLC: (Gradient: 80-100% B in 60 min, λ : 215, 254, 280 nm) $t_R = 41.7$ min.

ESI-MS m/z (%): 708.3 [M+5H]⁵⁺, 885.1 [M+4H]⁴⁺, 1179.8 [M+3H]³⁺.

HR-MS (ESI): calculated for [M+3H]³⁺: 1179.8246, [M+4H]⁴⁺: 885.1203, [M+5H]⁵⁺: 708.2977; found [M+3H]³⁺: 1179.8249, [M+4H]⁴⁺: 885.1206, [M+5H]⁵⁺: 708.2984.

6.6.2.2 P0_D:H-hLys(NBD)-hLys₂-hTrp₂-hVal₁₉-hTrp₂-hLys₂-NH₂

C₂₀₃H₃₃₁N₄₁O₃₁ [3839,56 g/mol]



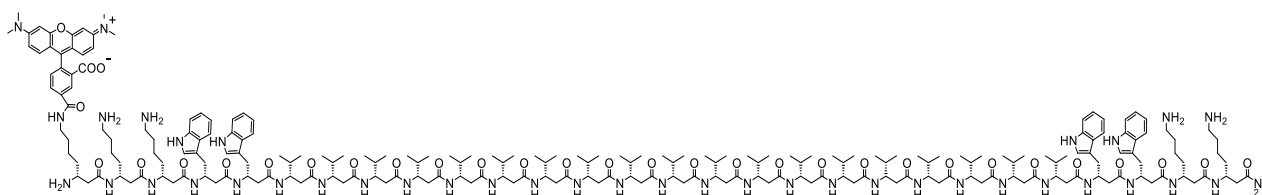
HPLC: (Gradient: 80-100% B in 50 min, λ : 215, 460, 280 nm) $t_R = 39.7$ min.

ESI-MS m/z (%): 769.3 [M+5H]⁵⁺, 961.41 [M+4H]⁴⁺, 1281.5 [M+3H]³⁺, 1921.8 [M+2H]²⁺.

HR-MS (ESI): calculated for $[M+2H]^{2+}$: 1921.7895, $[M+3H]^{3+}$: 1281.5288, $[M+4H]^{4+}$: 961.3984, $[M+5H]^{5+}$: 769.3202; found $[M+2H]^{2+}$: 1921.7890, $[M+3H]^{3+}$: 1281.5296, $[M+4H]^{4+}$: 961.3975, $[M+5H]^{5+}$: 769.3204.

6.6.2.3 P0_A:H-hLys(TAMRA)-hLys₂-hTrp₂-hVal₁₉-hTrp₂-hLys₂-NH₂

C₂₂₂H₃₅₀N₄₀O₃₂ [4088.70 g/mol]



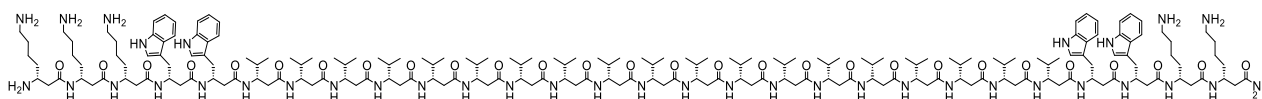
HPLC:(Gradient: 80-100% B in 50 min, λ : 215, 550, 280) t_R = 35 min.

ESI-MS m/z (%): 682.8 $[M+6H]^{6+}$, 819.1 $[M+5H]^{5+}$, 1023.7 $[M+4H]^{4+}$, 1364.6 $[M+3H]^{3+}$.

HR-MS (ESI): calculated for $[M+3H]^{3+}$: 1364.5756, $[M+4H]^{4+}$: 1023.6835, $[M+5H]^{5+}$: 819.1483, $[M+6H]^{6+}$: 682.7915; found $[M+3H]^{3+}$: 1364.5762, $[M+4H]^{4+}$: 1023.6849, $[M+5H]^{5+}$: 819.1483, $[M+6H]^{6+}$: 682.7917.

6.6.2.4 P0_U: H-hLys₃-hTrp₂-hVal₁₉-hTrp₂-hLys₂-NH₂

C₁₉₇H₃₃₀N₃₈O₂₈ [3676.56 g/mol]



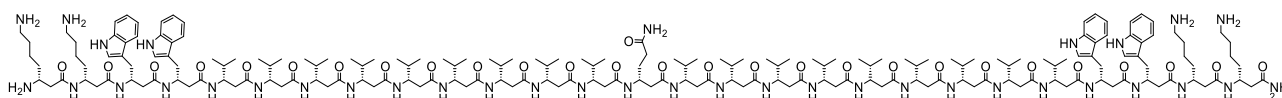
HPLC:(Gradient: 80-100% B in 60 min, λ : 215, 254, 280 nm) t_R = 37.3 min.

ESI-MS m/z (%): 614.1 $[M+6H]^{6+}$, 736.7 $[M+5H]^{5+}$, 920.6 $[M+4H]^{4+}$, 1227.2 $[M+3H]^{3+}$, 1840.3 $[M+2H]^{2+}$.

HR-MS (ESI): calculated for $[M+2H]^{2+}$: 1840.2886, $[M+3H]^{3+}$: 1227.1948, $[M+4H]^{4+}$: 920.6479, $[M+5H]^{5+}$: 736.7198, $[M+6H]^{6+}$: 614.1011; found $[M+2H]^{2+}$: 1840.2871, $[M+3H]^{3+}$: 1227.1959, $[M+4H]^{4+}$: 920.6487, $[M+5H]^{5+}$: 736.7204, $[M+6H]^{6+}$: 614.1011.

6.6.2.5 P1: H-hLys₂-hTrp₂-hVal₉-hGln-hVal₉-hTrp₂-hLys₂-NH₂

$C_{190}H_{315}N_{37}O_{28}$ [3563.44 g/mol]



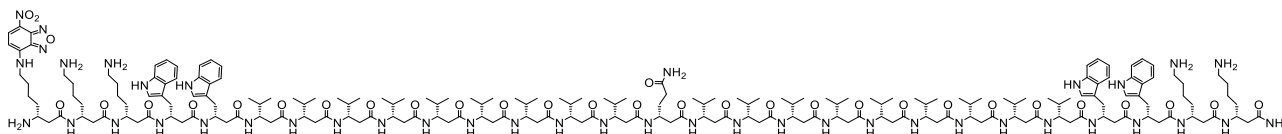
HPLC:(Gradient: 80-100% B in 60 min, λ : 215, 254, 280 nm) t_R = 45.3 min.

ESI-MS m/z (%): 714.1 $[M+5H]^{5+}$, 892.4 $[M+4H]^{4+}$, 1189.5 $[M+3H]^{3+}$.

HR-MS (ESI): calculated for $[M+3H]^{3+}$: 1189.4880, $[M+4H]^{4+}$: 892.3678, $[M+5H]^{5+}$: 714.0957; found $[M+3H]^{3+}$: 1189.4888, $[M+4H]^{4+}$: 892.3682, $[M+5H]^{5+}$: 714.0959.

6.6.2.6 P1_D: H-hLys(NBD)-hLys₂-hTrp₂-hVal₉-hGln-hVal₉-hTrp₂-hLys₂-NH₂

$C_{203}H_{330}N_{42}O_{32}$ [3871.14 g/mol]



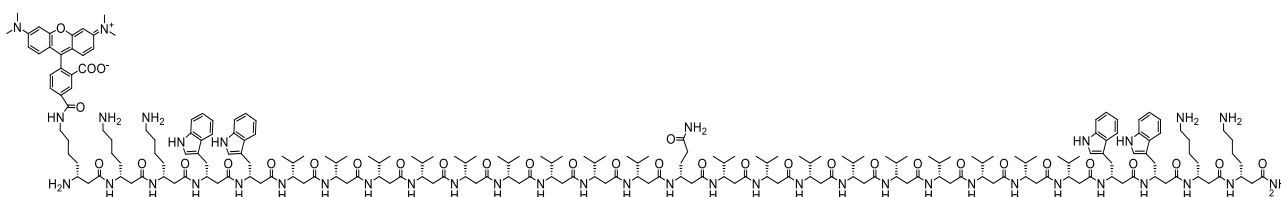
HPLC:(Gradient: 70-100% B in 60 min, λ : 215, 460, 280 nm) t_R = 38.2 min.

ESI-MS m/z (%): 775.1 $[M+5H]^{5+}$, 968.6 $[M+4H]^{4+}$, 1291.2 $[M+3H]^{3+}$, 1936.3 $[M+2H]^{2+}$.

HR-MS (ESI): calculated for $[M+3H]^{3+}$: 1291.1963, $[M+4H]^{4+}$: 968.6431, $[M+5H]^{5+}$: 775.1160; found $[M+3H]^{3+}$: 1291.1861, $[M+4H]^{4+}$: 968.6454, $[M+5H]^{5+}$: 775.1159.

6.6.2.7 P1_A: H-hLys(TAMRA)-hLys₂-hTrp₂-hVal₉-hGln-hVal₉-hTrp₂-hLys₂-NH₂

$C_{222}H_{349}N_{41}O_{33}$ [4117.69 g/mol]



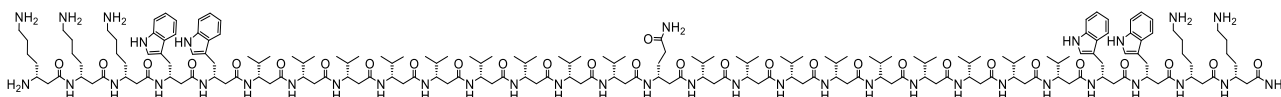
HPLC:(Gradient: 70-100% B in 60 min, λ : 215, 550, 280 nm) t_R = 34.5 min.

ESI-MS m/z (%): 687.6 $[M+6H]^{6+}$, 825.0 $[M+5H]^{5+}$, 1374.3 $[M+3H]^{3+}$.

HR-MS (ESI): calculated for $[M+5H]^{5+}$: 824.9488, $[M+6H]^{6+}$: 687.6252; found $[M+5H]^{5+}$: 824.9472, $[M+6H]^{6+}$: 687.6232.

6.6.2.8 P1_U: H-hLys₃-hTrp₂-hVal₉-hGln-hVal₉-hTrp₂-hLys₂-NH₂

$C_{197}H_{329}N_{39}O_{29}$ [3705.55 g/mol]



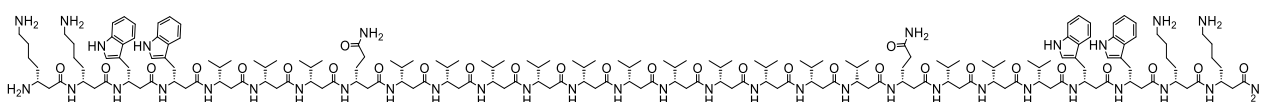
HPLC:(Gradient: 70-100% B in 60 min, λ : 215, 254, 280 nm) t_R = 43.8 min.

ESI-MS m/z (%): 618.9 $[M+6H]^{6+}$, 742.5 $[M+5H]^{5+}$, 927.9 $[M+4H]^{4+}$, 1236.9 $[M+3H]^{3+}$.

HR-MS (ESI): calculated for $[M+3H]^{3+}$: 1236.8582, $[M+4H]^{4+}$: 927.8955, $[M+5H]^{5+}$: 742.5178, $[M+6H]^{6+}$: 618.9321; found $[M+3H]^{3+}$: 1236.8598, $[M+4H]^{4+}$: 927.8954, $[M+5H]^{5+}$: 742.5187, $[M+6H]^{6+}$: 618.9320.

6.6.2.9 P2: H-hLys₂-hTrp₂-hVal₃-hGln-hVal₁₁-hGln-hVal₃-hTrp₂-hLys₂-NH₂

$C_{190}H_{314}N_{38}O_{29}$ [3592.43 g/mol]



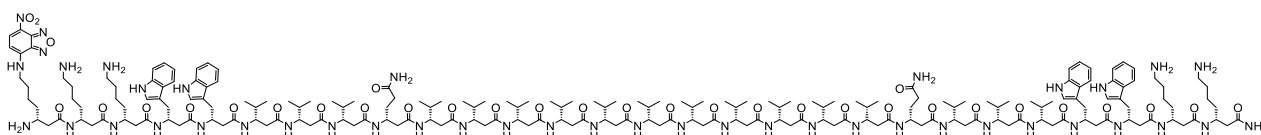
HPLC:(Gradient: 70-100% B in 60 min, λ : 215, 254, 280 nm) t_R = 48.1 min.

ESI-MS m/z (%): 719.5 $[M+5H]^{5+}$, 899.1 $[M+4H]^{4+}$, 1198.4 $[M+3H]^{3+}$.

HR-MS (ESI): calculated for $[M+3H]^{3+}$: 1198.4755, $[M+4H]^{4+}$: 899.1066, $[M+5H]^{5+}$: 719.4853; found $[M+3H]^{3+}$: 1198.4827, $[M+4H]^{4+}$: 899.1139, $[M+5H]^{5+}$: 719.4926.

6.6.2.10 P2_D: H-hLys(NBD)-hLys₂-hTrp₂-hVal₃-hGln-hVal₁₁-hGln-hVal₃-hTrp₂-hLys₂-NH₂

$C_{203}H_{329}N_{43}O_{33}$ [3868.55 g/mol]



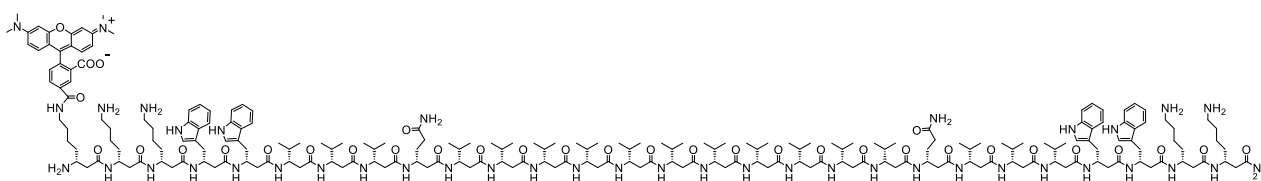
HPLC:(Gradient: 70-100% B in 60 min, λ : 215, 460, 280 nm) t_R = 36.1 min.

ESI-MS m/z (%): 650.9 $[M+6H]^{6+}$, 780.9 $[M+5H]^{5+}$, 975.9 $[M+4H]^{4+}$, 1300.9 $[M+3H]^{3+}$.

HR-MS (ESI): calculated for $[M+3H]^{3+}$: 1300.8555, $[M+4H]^{4+}$: 975.8935, $[M+5H]^{5+}$: 780.9162, $[M+6H]^{6+}$: 650.9314; found $[M+3H]^{3+}$: 1300.8571, $[M+4H]^{4+}$: 975.8943, $[M+5H]^{5+}$: 780.9168, $[M+6H]^{6+}$: 650.9314.

6.6.2.11 P2_A: H-hLys(TAMRA)-hLys₂-hTrp₂-hVal₃-hGln-hVal₁₁-hGln-hVal₃-hTrp₂-hLys₂-NH₂

$C_{222}H_{348}N_{42}O_{34}$ [4146.68 g/mol]



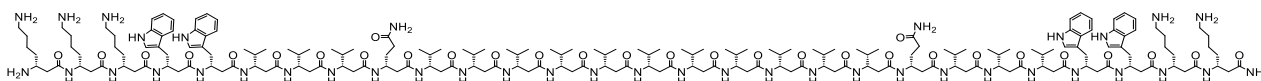
HPLC:(Gradient: 70-100% B in 60 min, λ : 215, 550, 280 nm) t_R = 31.6 min.

ESI-MS m/z (%): 692.5 $[M+6H]^{6+}$, 830.7 $[M+5H]^{5+}$, 1038.2 $[M+4H]^{4+}$, 1383.9 $[M+3H]^{3+}$.

HR-MS (ESI): calculated for $[M+3H]^{3+}$: 1383.9024, $[M+4H]^{4+}$: 1038.1786, $[M+5H]^{5+}$: 830.7443, $[M+6H]^{6+}$: 692.4548; found $[M+3H]^{3+}$: 1383.9037, $[M+4H]^{4+}$: 1038.1795, $[M+5H]^{5+}$: 830.7448, $[M+6H]^{6+}$: 692.4546.

6.6.2.12 P2_U: H-hLys₃-hTrp₂-hVal₃-hGln-hVal₁₁-hGln-hVal₃-hTrp₂-hLys₂-NH₂

$C_{197}H_{328}N_{40}O_{30}$ [3734.54 g/mol]



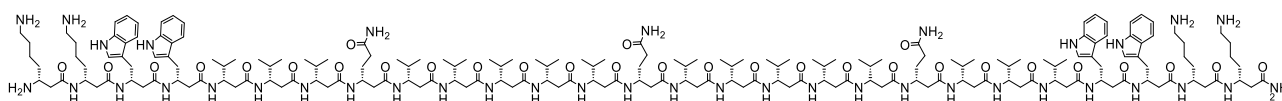
HPLC:(Gradient: 70-100% B in 60 min, λ : 215, 254, 280 nm) t_R = 44 min.

ESI-MS m/z (%): 623.8 $[M+6H]^{6+}$, 748.3 $[M+5H]^{5+}$, 935.1 $[M+4H]^{4+}$, 1246.5 $[M+3H]^{3+}$.

HR-MS (ESI): calculated for $[M+3H]^{3+}$: 1246.5216, $[M+4H]^{4+}$: 935.1430, $[M+5H]^{5+}$: 748.3159, $[M+6H]^{6+}$: 623.7644; found $[M+3H]^{3+}$: 1246.5235, $[M+4H]^{4+}$: 935.1443, $[M+5H]^{5+}$: 748.3166, $[M+6H]^{6+}$: 623.7647.

6.6.2.13 P3: H-hLys₂-hTrp₂-hVal₃-hGln-hVal₅-hGln-hVal₅-hGln-hVal₃-hTrp₂-hLys₂-NH₂

$C_{190}H_{313}N_{39}O_{30}$ [3621.42]



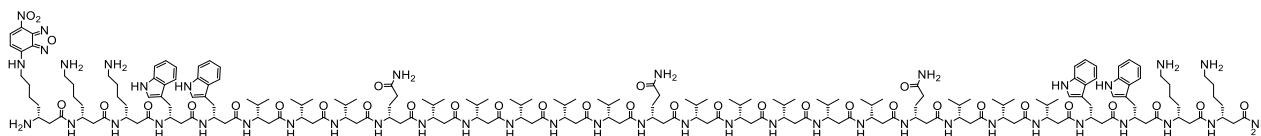
HPLC: (Gradient: 70-100% B in 60 min, λ : 215, 254, 280 nm) t_R = 48.7 min.

ESI-MS m/z (%): 725.3 $[M+5H]^{5+}$, 906.3 $[M+4H]^{4+}$, 1203.1 $[M+3H]^{3+}$.

HR-MS (ESI): calculated for $[M+3H]^{3+}$: 1203.1389, $[M+4H]^{4+}$: 906.3542, $[M+5H]^{5+}$: 725.2833; found $[M+3H]^{3+}$: 1208.1461, $[M+4H]^{4+}$: 906.3614, $[M+5H]^{5+}$: 725.2906.

6.6.2.14 P3_D: H-hLys(NBD)-hLys₂-hTrp₂-hVal₃-hGln-hVal₅-hGln-hVal₅-hGln-hVal₃-hTrp₂-hLys₂-NH₂

$C_{203}H_{328}N_{38}O_{29}$ [3926.53]



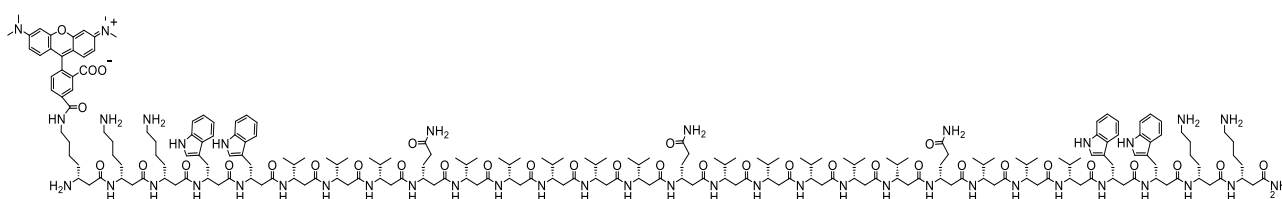
HPLC: (Gradient: 70-100% B in 60 min, λ : 215, 460, 280 nm) t_R = 35.5 min.

ESI-MS m/z (%): 655.7 $[M+6H]^{6+}$, 786.7 $[M+5H]^{5+}$, 983.1 $[M+4H]^{4+}$, 1310.5 $[M+3H]^{3+}$.

HR-MS (ESI): calculated for $[M+3H]^{3+}$: 1310.5189, $[M+4H]^{4+}$: 983.1410, $[M+5H]^{5+}$: 786.7143, $[M+6H]^{6+}$: 655.7631; found $[M+3H]^{3+}$: 1310.5196, $[M+4H]^{4+}$: 983.1414, $[M+5H]^{5+}$: 786.7145, $[M+6H]^{6+}$: 655.7624.

6.6.2.15 P3_A: H-hLys(TAMRA)-hLys₂-hTrp₂-hVal₃-hGln-hVal₅-hGln-hVal₅-hGln-hVal₃-hTrp₂-hLys₂-NH₂

$C_{222}H_{347}N_{43}O_{35}$ [4175.67]



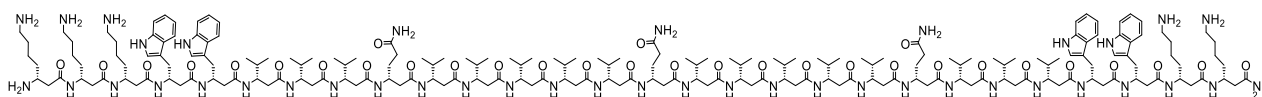
HPLC:(Gradient: 70-100% B in 60 min, λ : 215, 460, 280 nm) t_R = 33.8 min.

ESI-MS m/z (%): 597.8 $[M+7H]^{7+}$, 697.3 $[M+6H]^{6+}$, 7836.5 $[M+5H]^{5+}$, 1045.4 $[M+4H]^{4+}$, 1393.6 $[M+3H]^{3+}$.

HR-MS (ESI): calculated for $[M+3H]^{3+}$: 1393.5658, $[M+4H]^{4+}$: 1045.4261, $[M+5H]^{5+}$: 836.5424, $[M+6H]^{6+}$: 697.2865, $[M+7H]^{7+}$: 597.8181; found $[M+3H]^{3+}$: 1393.5669, $[M+4H]^{4+}$: 1045.4270, $[M+5H]^{5+}$: 836.5432, $[M+6H]^{6+}$: 697.2868, $[M+7H]^{7+}$: 597.8176.

6.6.2.16 P3_U: H-hLys₃-hTrp₂-hVal₃-hGln-hVal₅-hGln-hVal₅-hGln-hVal₃-hTrp₂-hLys₂-NH₂

$C_{197}H_{327}N_{41}O_{31}$ [3763.53 g/mol]



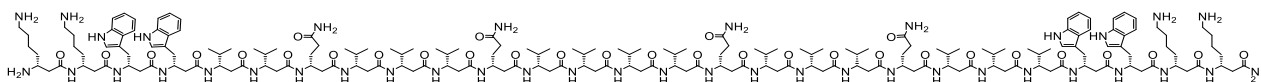
HPLC:(Gradient: 70-100% B in 60 min, λ : 215, 254, 280 nm) t_R = 42.6 min.

ESI-MS m/z (%): 628.6 [M+6H]⁶⁺, 754.1 [M+5H]⁵⁺, 942.4 [M+4H]⁴⁺, 1256.2 [M+3H]³⁺.

HR-MS (ESI): calculated for [M+3H]³⁺: 1256.1850, [M+4H]⁴⁺: 942.3906, [M+5H]⁵⁺: 754.1139, [M+6H]⁶⁺: 628.5961; found [M+3H]³⁺: 1256.1853, [M+4H]⁴⁺: 942.3910, [M+5H]⁵⁺: 754.1146, [M+6H]⁶⁺: 628.5958.

6.6.2.17 P4: H-hLys₂-hTrp₂-hVal₂-hGln-hVal₃-hGln-hVal₄-hGln-hVal₃-hGln-hVal₃-hTrp₂-hLys₂-NH₂

C₁₉₀H₃₁₂N₄₀O₃₁ [3650.41 g/mol]



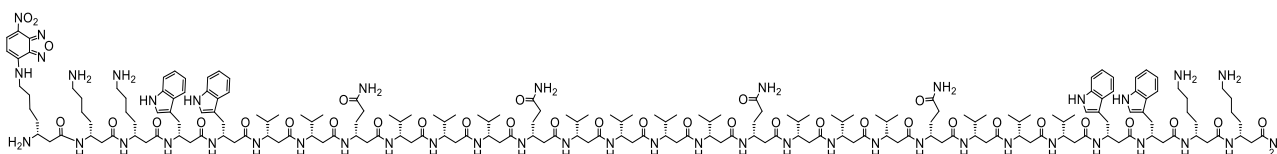
HPLC:(Gradient: 70-100% B in 70 min, λ : 215, 254, 280 nm) t_R = 34.5 min.

ESI-MS m/z (%): 628.6 [M+5H]⁵⁺, 754.1 [M+4H]⁴⁺, 942.4 [M+3H]³⁺, 1872.2[M+2H]²⁺.

HR-MS (ESI): calculated for [M+2H]²⁺: 1827.2136, [M+3H]³⁺: 1218.4782, [M+4H]⁴⁺: 914.1104, [M+5H]⁵⁺: 731.4898; found [M+2H]²⁺: 1827.2132, [M+3H]³⁺: 1218.4768, [M+4H]⁴⁺: 914.1101, [M+5H]⁵⁺: 731.4875.

6.6.2.18 P4_D: H-hLys₂(NBD)-hTrp₂-hVal₂-hGln-hVal₃-hGln-hVal₄-hGln-hVal₃-hGln-hVal₃-hTrp₂-hLys₂-hLys-NH₂

C₂₀₃H₃₂₇N₄₅O₃₅ [3955.52 g/mol]



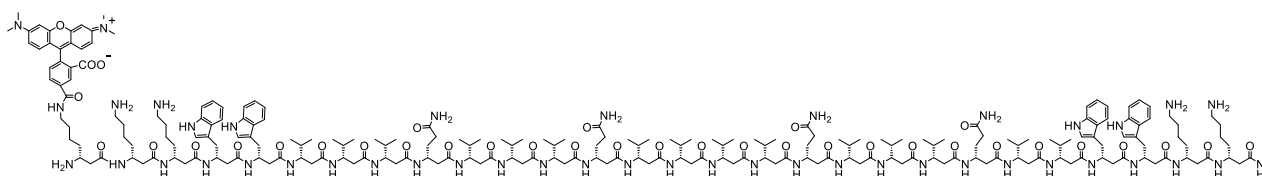
HPLC:(Gradient: 80-100% B in 70 min, λ : 215, 460, 280 nm) t_R = 28.3 min.

ESI-MS m/z (%): 792.5 [M+5H]⁵⁺, 990.4 [M+4H]⁴⁺, 1320.2 [M+3H]³⁺.

HR-MS (ESI): calculated for [M+3H]³⁺: 1320.1823, [M+4H]⁴⁺: 990.3885, [M+5H]⁵⁺: 792.5123; found [M+3H]³⁺: 1320.1817, [M+4H]⁴⁺: 990.3877, [M+5H]⁵⁺: 792.5117.

6.6.2.19 P4_A: H-hLys(TAMRA)-hLys₂-hTrp₂-hVal₃-hGln-hVal₃-hGln-hVal₄-hGln-hVal₃-hGln-hVal₂-hTrp₂-hLys₂-NH₂

C₂₂₂H₃₄₆N₄₄O₃₆ [4204.66 g/mol]



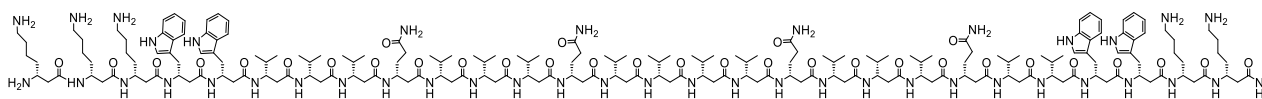
HPLC:(Gradient: 80-100% B in 70 min, λ : 215, 550, 280 nm) t_R = 25.1 min.

ESI-MS m/z (%): 702.1 [M+6H]⁶⁺, 842.3 [M+5H]⁵⁺, 1052.6 [M+4H]⁴⁺, 1403.2 [M+3H]³⁺.

HR-MS (ESI): calculated for [M+3H]³⁺: 1403.2292, [M+4H]⁴⁺: 1052.6737, [M+5H]⁵⁺: 842.3404, [M+6H]⁶⁺: 702.1182; found [M+3H]³⁺: 1403.2219, [M+4H]⁴⁺: 1052.7620, [M+5H]⁵⁺: 842.3379, [M+6H]⁶⁺: 702.1186.

6.6.2.20 P4_U: H-hLys₃-hTrp₂-hVal₂-hGln-hVal₃-hGln-hVal₄-hGln-hVal₃-hGln-hVal₃-hTrp₂-hLys₂-NH₂

C₁₉₇H₃₂₆N₄₂O₃₂ [3792.52 g/mol]



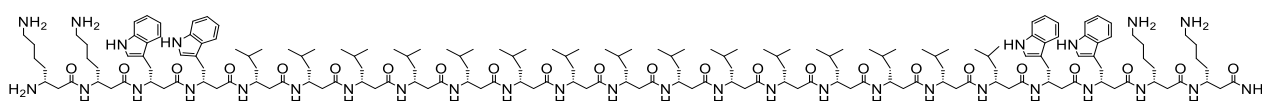
HPLC:(Gradient: 80-100% B in 70 min, λ : 215, 254, 280 nm) t_R = 36.1 min.

ESI-MS m/z (%): 759.9 [M+5H]⁵⁺, 949.6 [M+4H]⁴⁺, 1265.8 [M+3H]³⁺.

HR-MS (ESI): calculated for [M+3H]³⁺: 1265.8484, [M+4H]⁴⁺: 949.6381, [M+5H]⁵⁺: 759.9119;
found [M+3H]³⁺: 1265.8438, [M+4H]⁴⁺: 949.6394, [M+5H]⁵⁺: 759.9113.

6.6.2.21 P5: H-hLys₂-hTrp₂-hLeu₁₅-hTrp₂-hLys₂-NH₂

C₁₈₁H₃₀₂N₃₂O₂₃ [3292.34 g/mol]



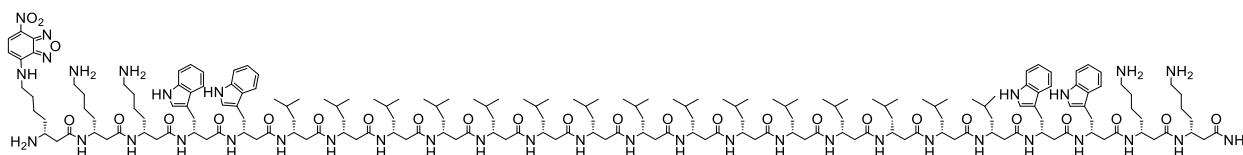
HPLC:(Gradient: 80-100% B in 70 min, λ : 215, 254, 280 nm) t_R = 41.6 min.

ESI-MS m/z (%): 759.9 [M+5H]⁵⁺, 949.6 [M+4H]⁴⁺, 1265.8 [M+3H]³⁺, 1655.6 [M+2H]²⁺.

HR-MS (ESI): calculated for [M+2H]²⁺: 1648.1828, [M+3H]³⁺: 1099.1243, [M+4H]⁴⁺: 824.5951,
[M+5H]⁵⁺: 659.8775; found [M+2H]²⁺: 1648.1827, [M+3H]³⁺: 1099.1246, [M+4H]⁴⁺: 824.5950,
[M+5H]⁵⁺: 659.8770.

6.6.2.22 P5_D: H-hLys(NBD)-hLys₂-hTrp₂-hLeu₁₅-hTrp₂-hLys₂-NH₂

C₁₉₄H₃₁₇N₃₇O₂₇ [3597.46 g/mol]



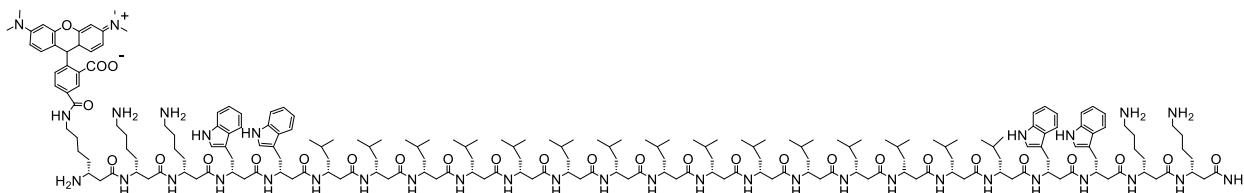
HPLC:(Gradient: 80-100% B in 60 min, λ : 215, 460, 280 nm) t_R = 27.5 min.

ESI-MS m/z (%): 720.9 [M+5H]⁵⁺, 900.8 [M+4H]⁴⁺.

HR-MS (ESI): calculated for $[M+4H]^{4+}$: 900.8730, $[M+5H]^{5+}$: 720.8999; found $[M+4H]^{4+}$: 900.8729, $[M+5H]^{5+}$: 720.8998.

6.6.2.23 P5_A: H-hLys(TAMRA)-hLys₂-hTrp₂-hLeu₁₅-hTrp₂-hLys₂-NH₂

$C_{213}H_{336}N_{36}O_{28}$ [3846.61 g/mol]



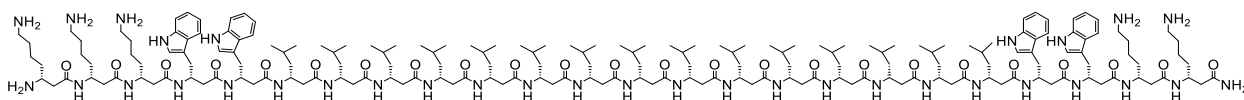
HPLC:(Gradient: 80-100% B in 60 min, λ : 215, 550, 280 nm) t_R = 25 min.

ESI-MS m/z (%): 642.4 $[M+6H]^{6+}$, 770.7 $[M+5H]^{5+}$, 963.1 $[M+4H]^{4+}$, 1283.8 $[M+3H]^{3+}$.

HR-MS (ESI): calculated for $[M+3H]^{3+}$: 1283.8751, $[M+4H]^{4+}$: 963.1582, $[M+5H]^{5+}$: 770.7280, $[M+6H]^{6+}$: 642.4412; found $[M+3H]^{3+}$: 1283.8765, $[M+4H]^{4+}$: 963.1577, $[M+5H]^{5+}$: 770.7286, $[M+6H]^{6+}$: 642.4416.

6.6.2.24 P5_U: H-hLys₃-hTrp₂-hLeu₁₅-hTrp₂-hLys₂-NH₂

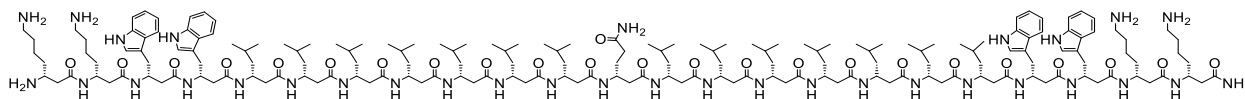
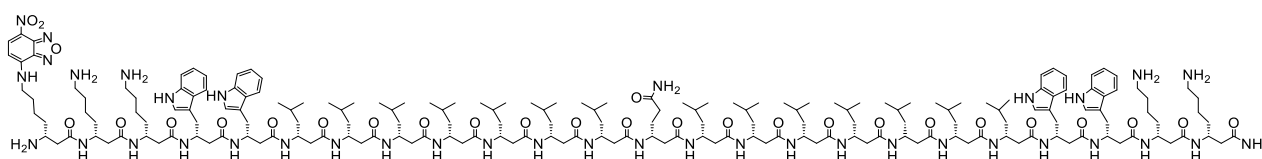
$C_{188}H_{316}N_{34}O_{24}$ [3434.46 g/mol]

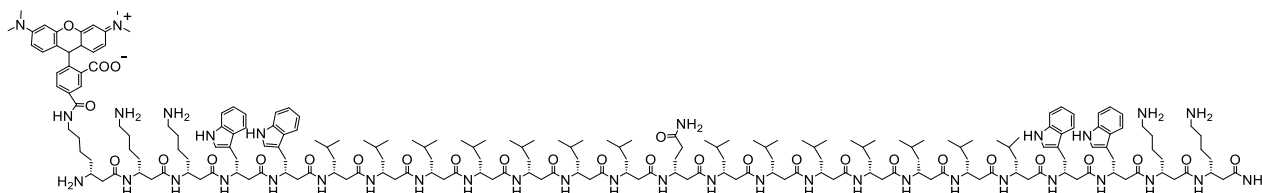
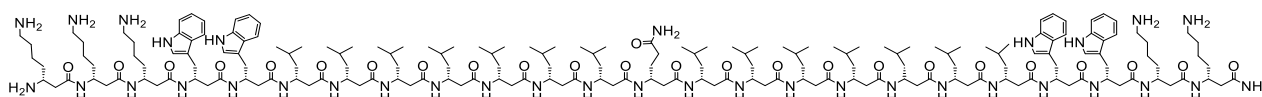


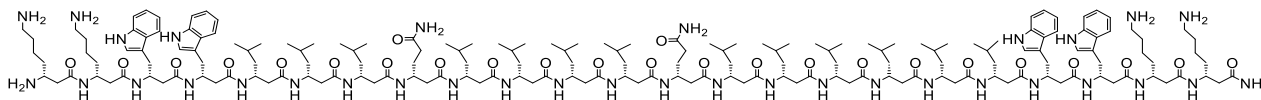
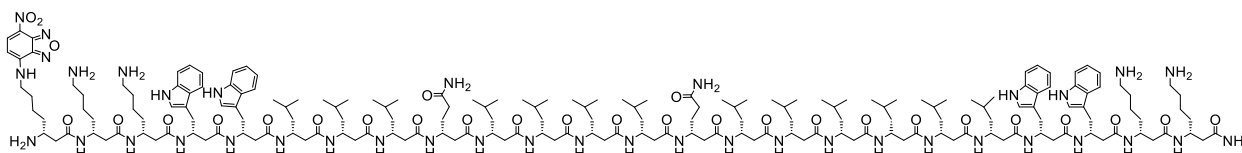
HPLC:(Gradient: 80-100% B in 70 min, λ : 215, 254, 280 nm) t_R = 30.7 min.

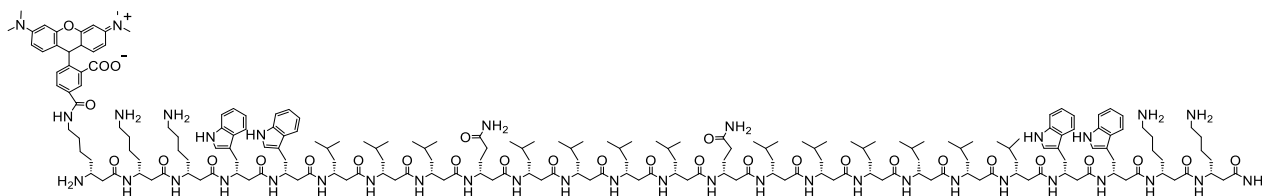
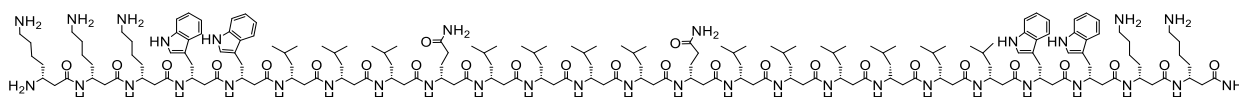
ESI-MS m/z (%): 759.9 $[M+5H]^{5+}$, 949.6 $[M+4H]^{4+}$, 1265.8 $[M+3H]^{3+}$.

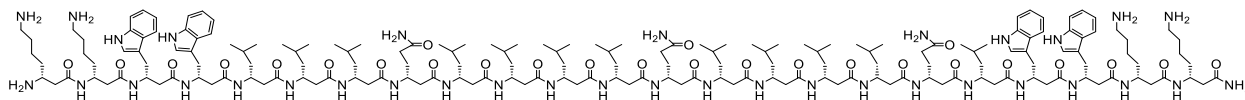
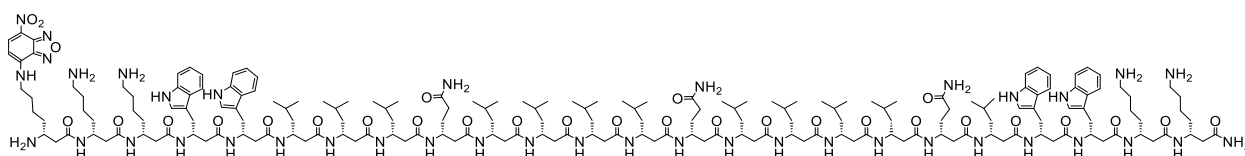
HR-MS (ESI): calculated for $[M+3H]^{3+}$: 1146.4944, $[M+4H]^{4+}$: 860.1226, $[M+5H]^{5+}$: 688.2995; found $[M+3H]^{3+}$: 1146.4938, $[M+4H]^{4+}$: 860.1209, $[M+5H]^{5+}$: 688.2996.

6.6.2.25 P6: H-hLys₂-hTrp₂-hLeu₇-hGln-hLeu₇-hTrp₂-hLys₂-NH₂C₁₈₀H₂₉₉N₃₃O₂₄ [3307.32 g/mol]**HPLC:**(Gradient: 80-100% B in 60 min, λ : 215, 254, 280 nm) t_R = 29.1 min.**ESI-MS** m/z (%): 759.9 [M+5H]⁵⁺, 949.6 [M+4H]⁴⁺, 1265.8 [M+3H]³⁺, 1655.6 [M+2H]²⁺.**HR-MS** (ESI): calculated for [M+2H]²⁺: 1655.6701, [M+3H]³⁺: 1104.1158, [M+4H]⁴⁺: 828.3387, [M+5H]⁵⁺: 662.8724; found [M+2H]²⁺: 1655.6692, [M+3H]³⁺: 1104.1166, [M+4H]⁴⁺: 828.3388, [M+5H]⁵⁺: 662.8718.**6.6.2.26 P6_D: H-hLys(NBD)-hLys₂-hTrp₂-hLeu₇-hGln-hLeu₇-hTrp₂-hLys₂-NH₂**C₁₉₃H₃₁₄N₃₈O₂₈ [3612.43 g/mol]**HPLC:**(Gradient: 80-100% B in 40 min, λ : 215, 460, 280 nm) t_R = 18 min.**ESI-MS** m/z (%): 723.9 [M+5H]⁵⁺, 904.6 [M+4H]⁴⁺, 1205.8 [M+3H]³⁺, 1808.2 [M+2H]²⁺.**HR-MS** (ESI): calculated for [M+2H]²⁺: 1808.2260, [M+3H]³⁺: 1205.8198, [M+4H]⁴⁺: 904.6166, [M+5H]⁵⁺: 723.8948; found [M+2H]²⁺: 1808.2260, [M+3H]³⁺: 1205.8212, [M+4H]⁴⁺: 904.6173, [M+5H]⁵⁺: 723.8951.

6.6.2.27 P6_A: H-hLys(TAMRA)-hLys₂-hTrp₂-hLeu₇-hGln-hLeu₇-hTrp₂-hLys₂-NH₂C₁₁₂H₃₃₃N₃₇O₂₉ [3861.57 g/mol]**HPLC:**(Gradient: 80-100% B in 40 min, λ : 215, 550, 280 nm) t_R = 13.3 min.**ESI-MS** m/z (%): 773.7 [M+5H]⁵⁺, 966.9 [M+4H]⁴⁺, 1288.8 [M+3H]³⁺.**HR-MS** (ESI): calculated for [M+3H]³⁺: 1288.8666, [M+4H]⁴⁺: 966.9018, [M+5H]⁵⁺: 773.7229;
found [M+3H]³⁺: 1288.8698, [M+4H]⁴⁺: 966.9023, [M+5H]⁵⁺: 773.7233.**6.6.2.28 P6_U: H-hLys₃-hTrp₂-hLeu₇-hGln-hLeu₇-hTrp₂-hLys₂-NH₂**C₁₈₇H₃₁₃N₃₅O₂₅ [3449.43 g/mol]**HPLC:**(Gradient: 80-100% B in 60 min, λ : 215, 254, 280 nm) t_R = 21.7 min.**ESI-MS** m/z (%): 773.7 [M+5H]⁵⁺, 966.9 [M+4H]⁴⁺, 1288.8 [M+3H]³⁺.**HR-MS** (ESI): calculated for [M+3H]³⁺: 1151.4859, [M+4H]⁴⁺: 863.8662, [M+5H]⁵⁺: 691.2944;
found [M+3H]³⁺: 1151.4858, [M+4H]⁴⁺: 863.8657, [M+5H]⁵⁺: 691.2936.

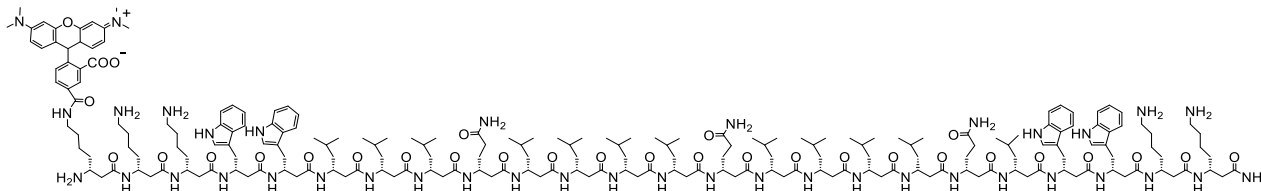
6.6.2.29 P7: H-hLys₂-hTrp₂-hLeu₃-hGln-hLeu₄-hGln-hLeu₆-hTrp₂-hLys₂-NH₂C₁₇₉H₂₉₆N₃₄O₂₅ [3322.29 g/mol]**HPLC:**(Gradient: 80-100% B in 50 min, λ : 215, 254, 280 nm) t_R = 26.1 min.**ESI-MS** m/z (%): 665.8 [M+5H]⁵⁺, 832.1 [M+4H]⁴⁺, 1109.1 [M+3H]³⁺.**HR-MS** (ESI): calculated for [M+3H]³⁺: 1109.1073, [M+4H]⁴⁺: 832.0823, [M+5H]⁵⁺: 665.8673;
found [M+3H]³⁺: 1109.1078, [M+4H]⁴⁺: 832.0816, [M+5H]⁵⁺: 665.8666.**6.6.2.30 P7_D: H-hLys(NBD)-hLys₂-hTrp₂-hLeu₃-hGln-hLeu₄-hGln-hLeu₆-hTrp₂-hLys₂-NH₂**C₁₉₂H₃₁₁N₃₉O₂₉ [3627.41 g/mol]**HPLC:**(Gradient: 80-100% B in 50 min, λ : 215, 460, 280 nm) t_R = 22.5 min.**ESI-MS** m/z (%): 726.9 [M+5H]⁵⁺, 908.3 [M+4H]⁴⁺, 1210.8 [M+3H]³⁺.**HR-MS** (ESI): calculated for [M+3H]³⁺: 1210.8113, [M+4H]⁴⁺: 908.3603, [M+5H]⁵⁺: 726.8897;
found [M+3H]³⁺: 1210.8119, [M+4H]⁴⁺: 908.3605, [M+5H]⁵⁺: 726.8953.

6.6.2.31 P7_A: H-hLys(TAMRA)-hLys₂-hTrp₂-hLeu₃-hGln-hLeu₄-hGln-hLeu₆-hTrp₂-hLys₂-NH₂C₂₁₁H₃₃₀N₃₈O₃₀ [3876.54 g/mol]**HPLC:**(Gradient: 80-100% B in 50 min, λ : 215, 550, 280 nm) t_R = 20.7 min.**ESI-MS** m/z (%): 776.7 [M+5H]⁵⁺, 970.6 [M+4H]⁴⁺, 1293.8 [M+3H]³⁺.**HR-MS** (ESI): calculated for [M+3H]³⁺: 1293.8581, [M+4H]⁴⁺: 970.6454, [M+5H]⁵⁺: 776.7178; found [M+3H]³⁺: 1293.8557, [M+4H]⁴⁺: 970.6447, [M+5H]⁵⁺: 776.7213.**6.6.2.32 P7_U: H-hLys₃-hTrp₂-hLeu₃-hGln-hLeu₄-hGln-hLeu₆-hTrp₂-hLys₂-NH₂**C₁₈₆H₃₁₀N₃₆O₂₆ [3464.40 g/mol]**HPLC:**(Gradient: 80-100% B in 60 min, λ : 215, 254, 280 nm) t_R = 41.7 min.**ESI-MS** m/z (%): 694.3 [M+5H]⁵⁺, 867.6 [M+4H]⁴⁺, 1156.4 [M+3H]³⁺.**HR-MS** (ESI): calculated for [M+3H]³⁺: 1156.4773, [M+4H]⁴⁺: 867.6098, [M+5H]⁵⁺: 694.3; found [M+3H]³⁺: 1156.4784, [M+4H]⁴⁺: 867.6117, [M+5H]⁵⁺: 694.3.

6.6.2.33 P8: H-hLys₂-hTrp₂-hLeu₃-hGln-hLeu₄-hGln-hLeu₄-hGln-hLeu₁-hTrp₂-hLys₂-NH₂C₁₇₈H₂₉₃N₃₅O₂₆ [3337.26 g/mol]**HPLC:**(Gradient: 80-100% B in 50 min, λ : 215, 254, 280 nm) t_R = 36.7 min.**ESI-MS** m/z (%): 835.8 [M+4H]⁴⁺, 1114.1 [M+3H]³⁺.**HR-MS** (ESI): calculated for [M+3H]³⁺: 1114.0988, [M+4H]⁴⁺: 835.8259; found [M+3H]³⁺: 1114.0981, [M+4H]⁴⁺: 835.8245.**6.6.2.34 P8_D: H-hLys(NBD)-hLys₂-hTrp₂-hLeu₃-hGln-hLeu₄-hGln-hLeu₄-hGln-hLeu₁-hTrp₂-hLys₂-NH₂**C₁₉₁H₃₀₈N₄₀O₃₀ [3642.38 g/mol]**HPLC:**(Gradient: 80-100% B in 50 min, λ : 215, 460, 280 nm) t_R = 30.5 min.**ESI-MS** m/z (%): 729.8 [M+5H]⁵⁺, 912.1 [M+4H]⁴⁺, 1215.8 [M+3H]³⁺, 1823.2 [M+2H]²⁺.**HR-MS** (ESI): calculated for [M+2H]²⁺: 1823.2005, [M+3H]³⁺: 1215.8028, [M+4H]⁴⁺: 912.1039, [M+5H]⁵⁺: 729.8846; found [M+2H]²⁺: 1823.1994, [M+3H]³⁺: 1215.8041, [M+4H]⁴⁺: 912.1051, [M+5H]⁵⁺: 729.8838.

6.6.2.35 P8_A: H-hLys(TAMRA)-hLys₂-hTrp₂-hLeu₃-hGln-hLeu₄-hGln-hLeu₄-hGln-hLeu₁-hTrp₂-hLys₂-NH₂

C₂₁₀H₃₂₇N₃₉O₃₁ [3891.52 g/mol]



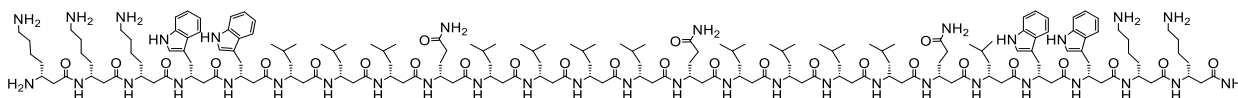
HPLC:(Gradient: 80-100% B in 40 min, λ : 215, 254, 280 nm) t_R = 28.3 min.

ESI-MS m/z (%): 779.7 [M+5H]⁵⁺, 974.4 [M+4H]⁴⁺, 1298.8 [M+3H]³⁺.

HR-MS (ESI): calculated for [M+3H]³⁺: 1298.8496, [M+4H]⁴⁺: 974.3890, [M+5H]⁵⁺: 779.7127;
found [M+3H]³⁺: 1298.8496, [M+4H]⁴⁺: 974.3890, [M+5H]⁵⁺: 779.7133.

6.6.2.36 P8_U: H-hLys₃-hTrp₂-hLeu₃-hGln-hLeu₄-hGln-hLeu₄-hGln-hLeu₁-hTrp₂-hLys₂-NH₂

C₁₈₅H₃₀₇N₃₇O₂₇ [3479.37 g/mol]



HPLC:(Gradient: 80-100% B in 50 min, λ : 215, 254, 280 nm) t_R = 32.5 min.

ESI-MS m/z (%): 697.3 [M+5H]⁵⁺, 871.3 [M+4H]⁴⁺, 1161.4 [M+3H]³⁺.

HR-MS (ESI): calculated for [M+3H]³⁺: 1161.4690, [M+4H]⁴⁺: 871.3536, [M+5H]⁵⁺: 697.2843;
found [M+3H]³⁺: 1161.4682, [M+4H]⁴⁺: 871.3530, [M+5H]⁵⁺: 697.2831.

7 Appendix

CD spectra of β -peptides **P1** - **P4** (containing β^3 -Val) and β -peptides **P6** - **P8** (containing β^3 -Leu) in TFE at 60 °C.

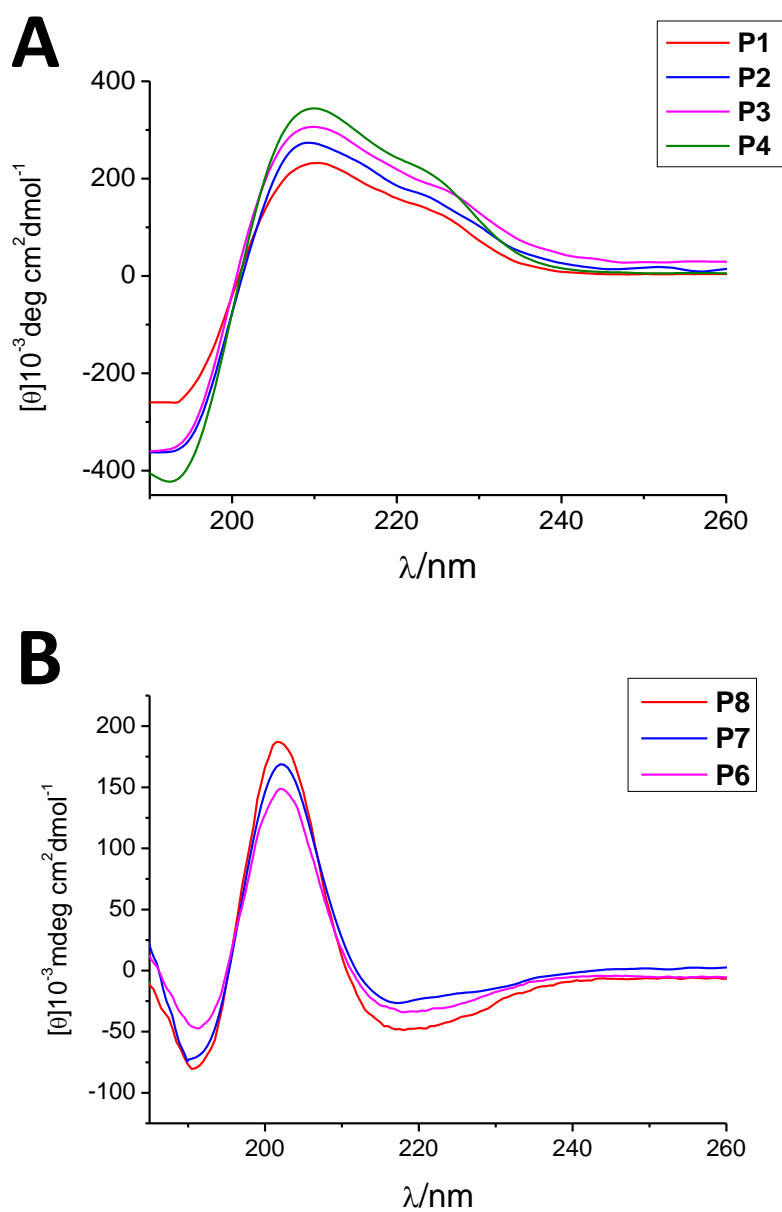


Figure 1.S. (A) CD spectra of β -peptides showing right-handed 14-helix (**P1**, **P2**, **P3** and **P4**) and (B) β -peptides showing left-handed 12-helix (**P6**, **P7** and **P8**) in TFE at 60 °C and concentration of 30 μM .

Helix Orientation of Transmembrane β -peptides **P3** and **P8** within POPC LUVs.

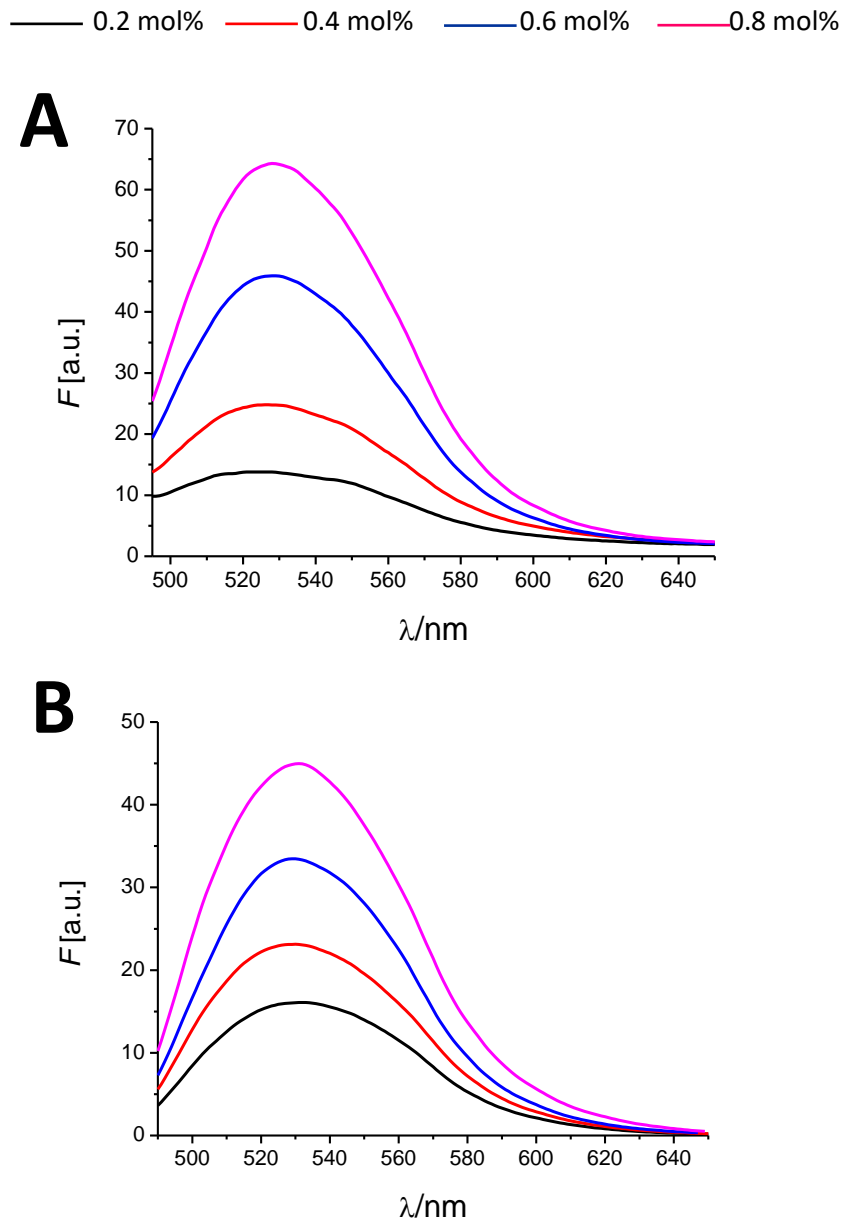
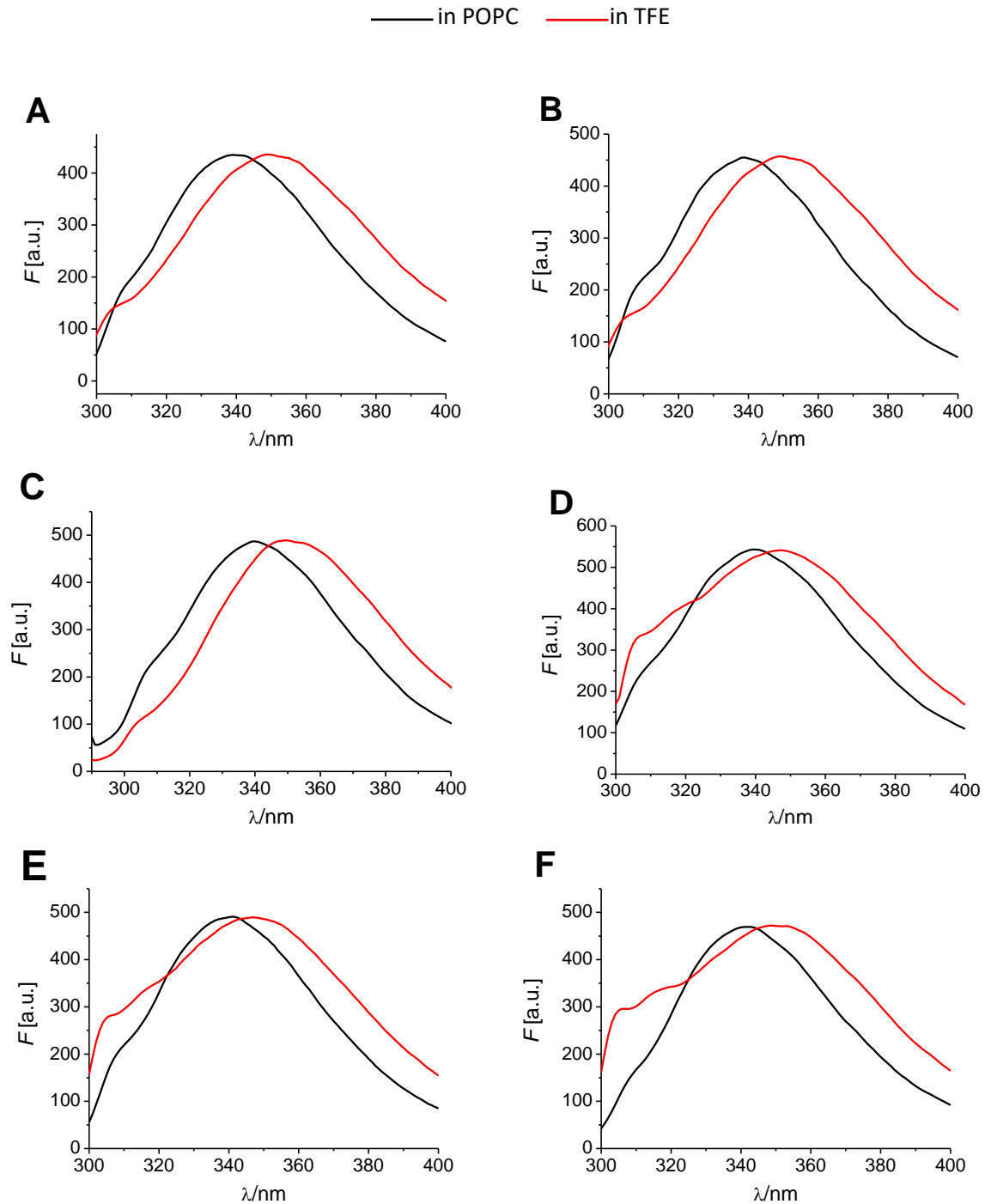


Figure 2.S. NBD-Fluorescence intensity defined as emission peak area in the range of 490-650 nm plotted as a function of β -peptide **P3_D** (A) and **P8_D** (B) mol% in POPC LUVs at 25 °C.

Insertion of transmembrane β -peptides **P1** - **P4** (containing β^3 -Val) and β -peptides **P6** - **P8** (containing β^3 -Leu) within the membrane.



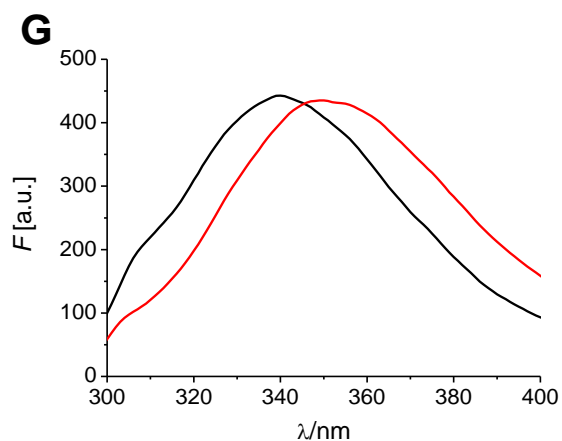


Figure 3.S. β^3 -Trp fluorescence spectra of **P1** (A), **P2** (B), **P3** (C), **P4** (D), **P6** (E), **P7** (F) and **P8** (G) within the lipid bilayer POPC LUVs using 1:600 as peptide-to-lipid ratio as well as in TFE at room temperature and concentration of 30 μ M.

Topological insertion of transmembrane β -peptides **P1** - **P4** (containing β^3 -Val) and β -peptides **P6**-**P8** (containing β^3 -Leu) into the lipid bilayer

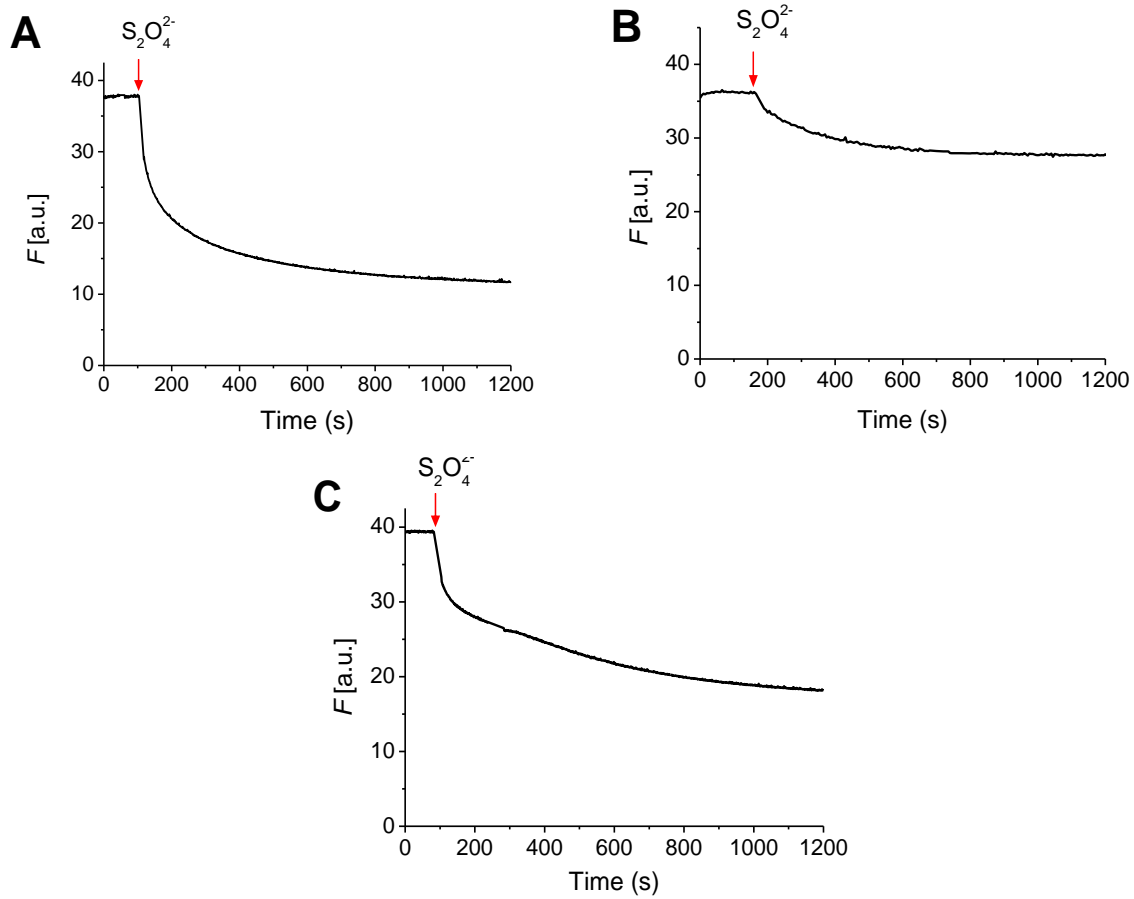
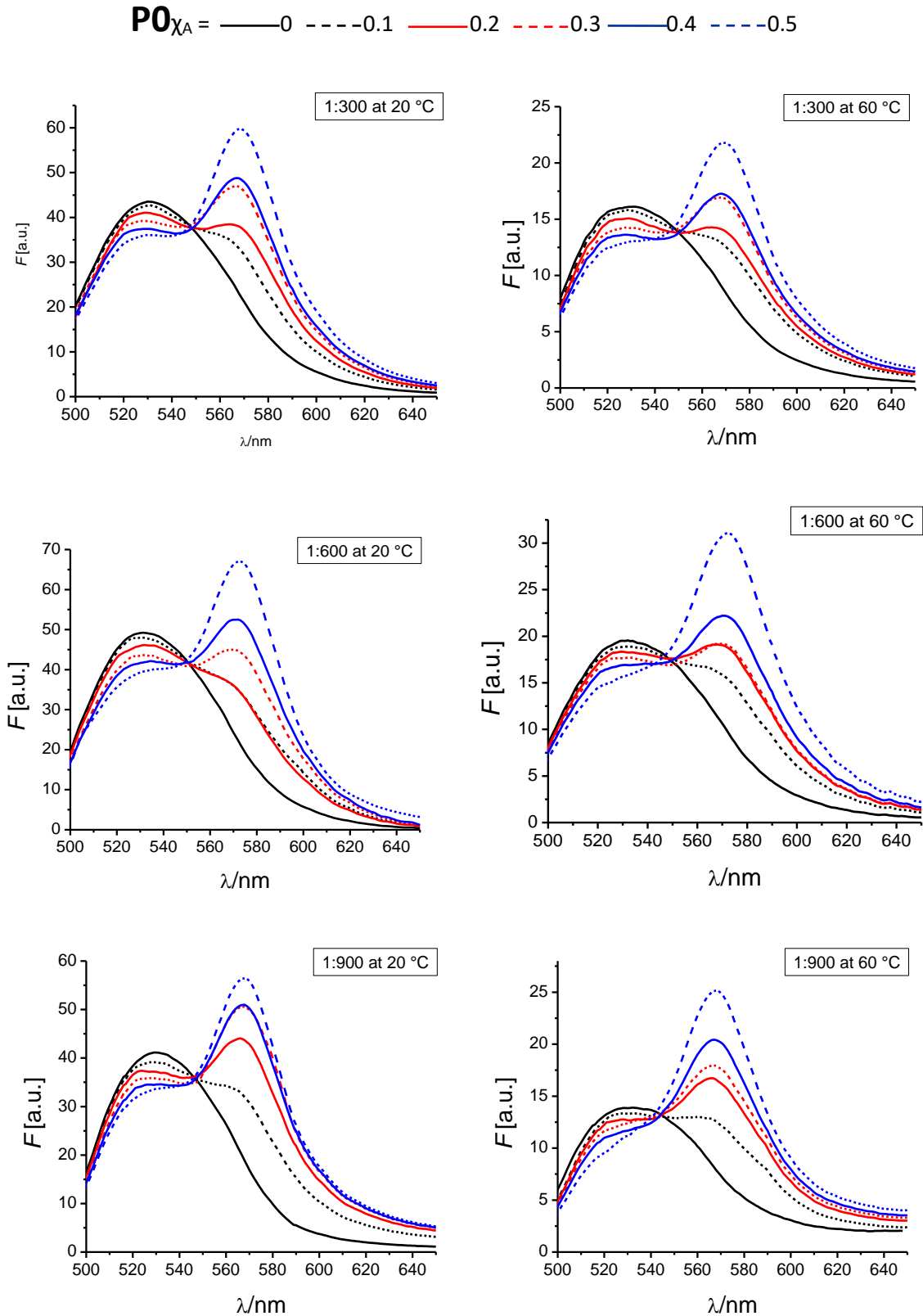
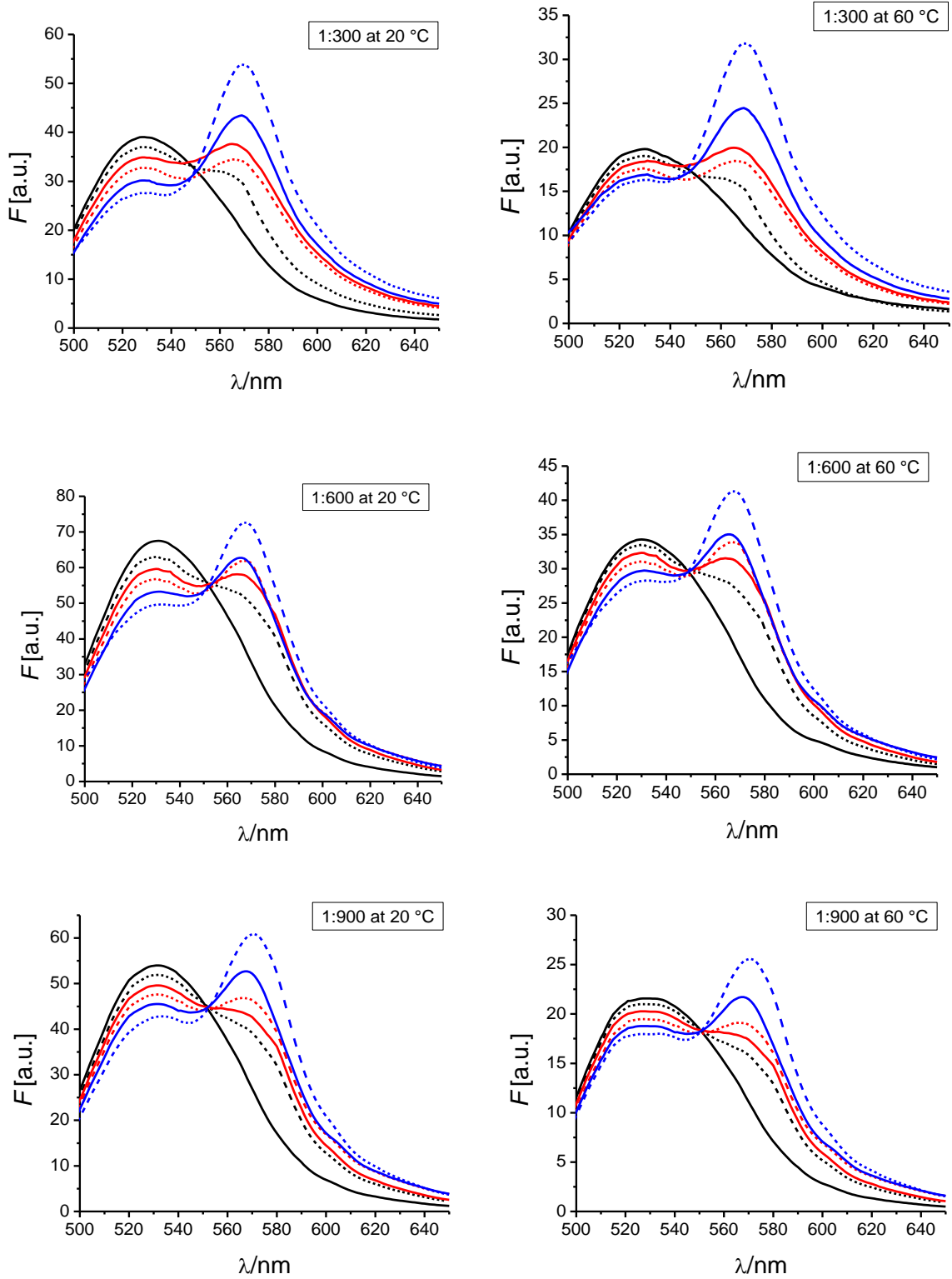
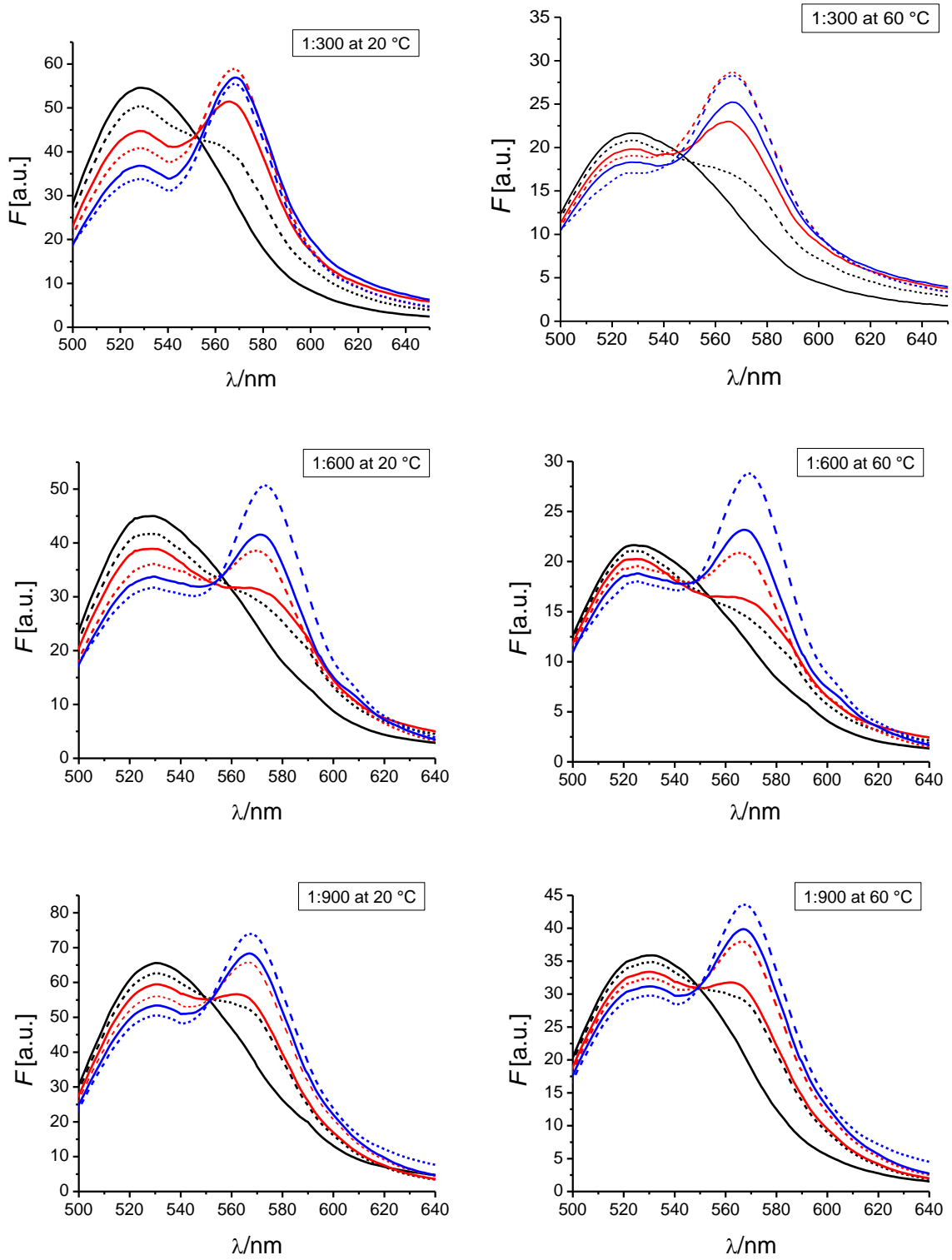


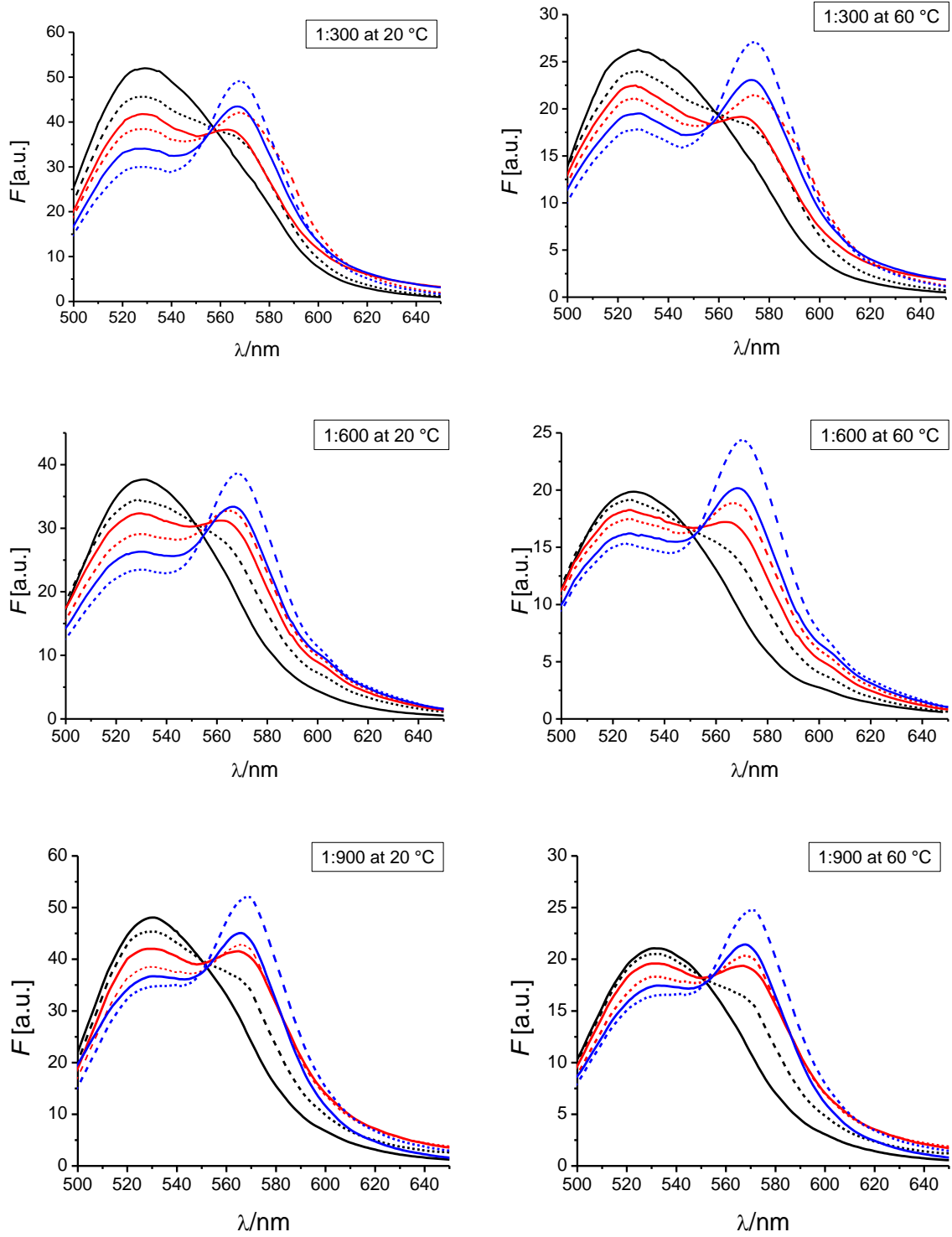
Figure 4.S. External addition of sodium dithionite solution to POPC LUVs containing 0.16 mol% fluorescent NBD-labeled **P3_D** (A), **P4_D** (B) and **P8_D** (C). Fluorescence signal and excitation wavelength of NBD fluorophores were monitored at 533 nm and at 450 nm, respectively.

Concentration dependent fluorescence spectra of transmembrane β -peptides **P0 - P4** (containing β^3 -Val) and β -peptides **P5-P8** (containing β^3 -Leu) at various peptide-to lipid ratios and at two different temperatures as indicated in the corresponding figure.

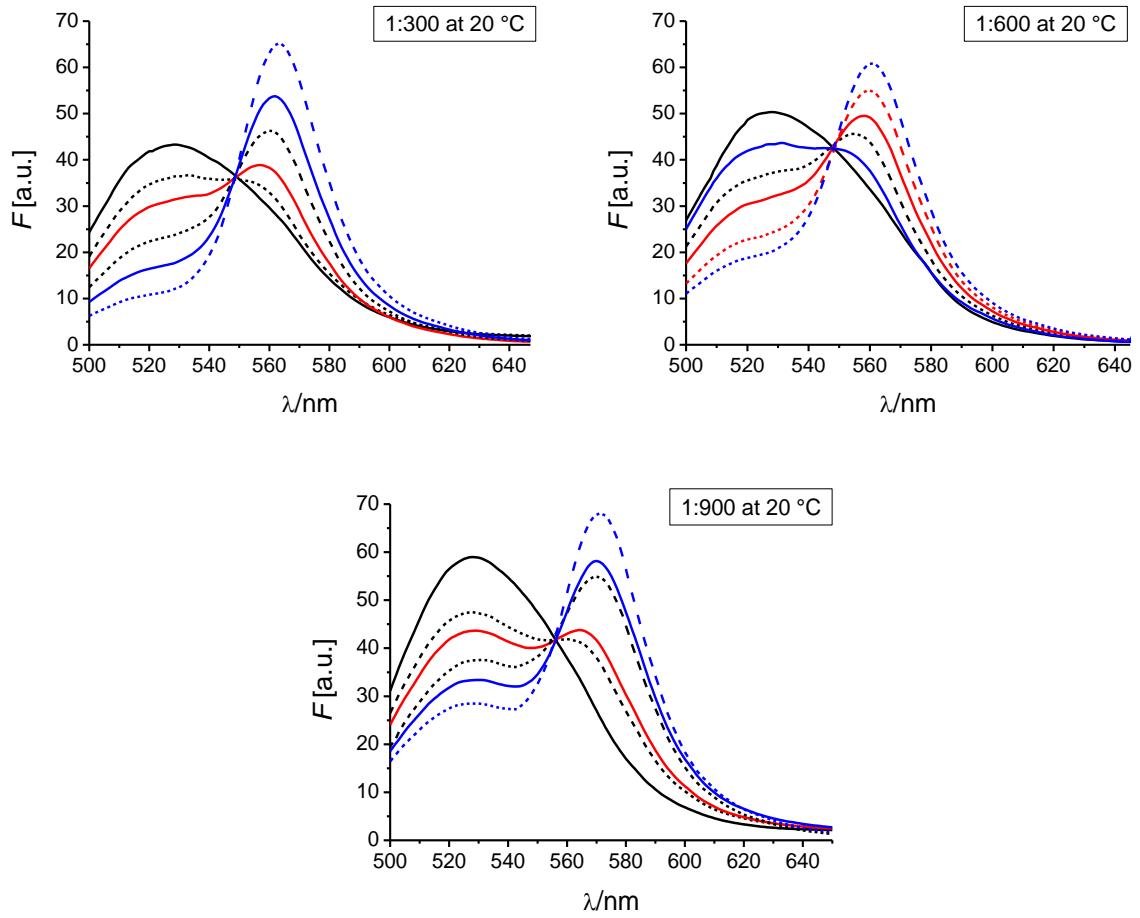


$P1_{\chi_A} =$ — 0 - - - 0.1 — 0.2 - - - 0.3 — 0.4 - - - 0.5

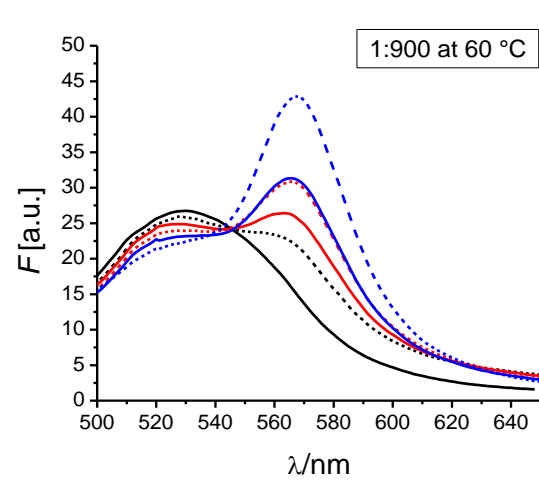
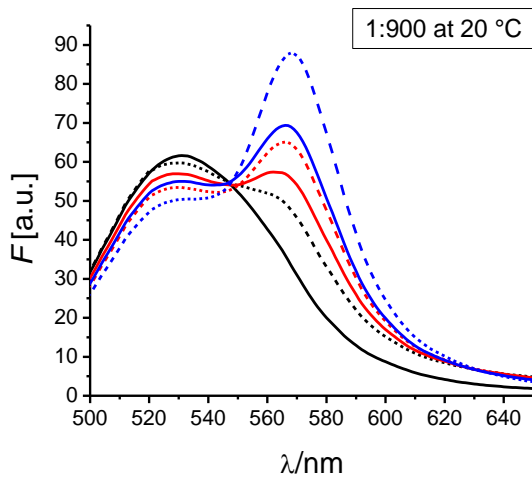
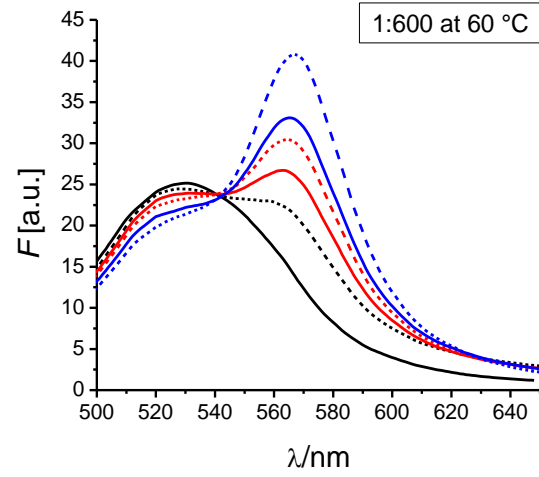
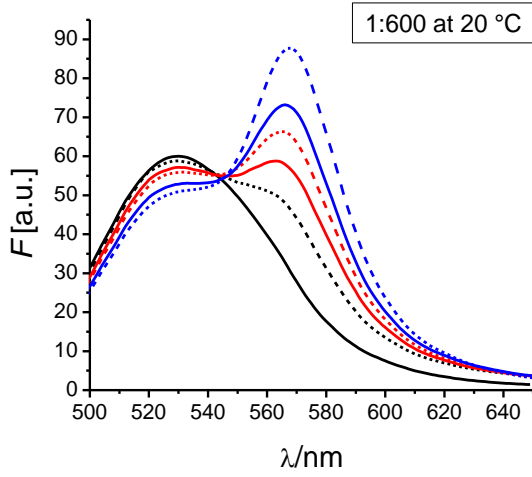
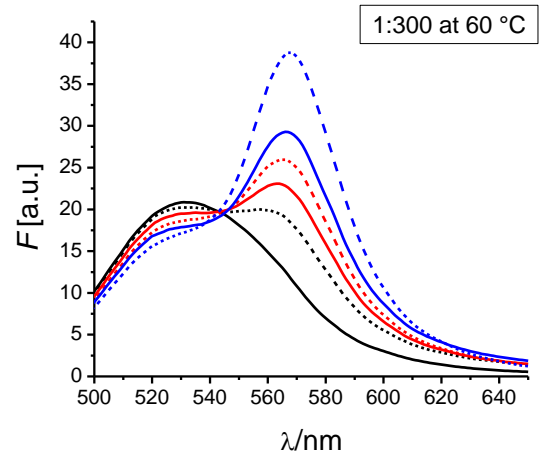
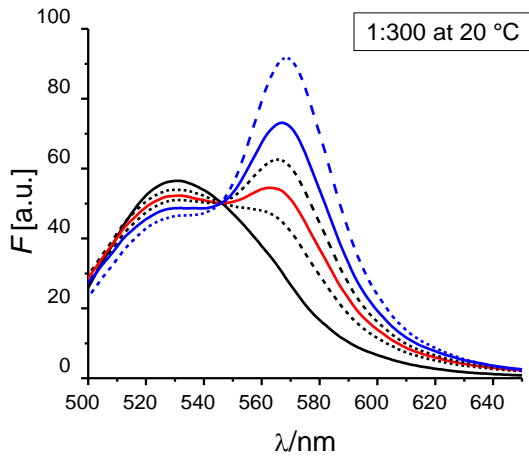
$P2_{\chi_A} =$ — 0 - - - 0.1 — 0.2 - - - 0.3 — 0.4 - - - 0.5

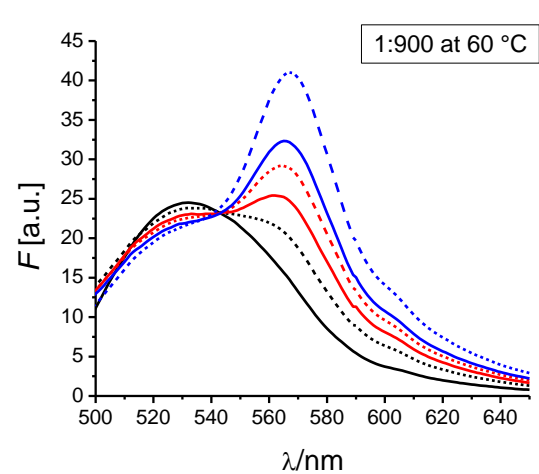
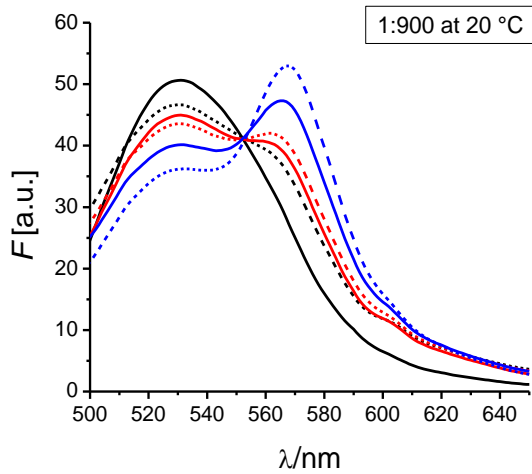
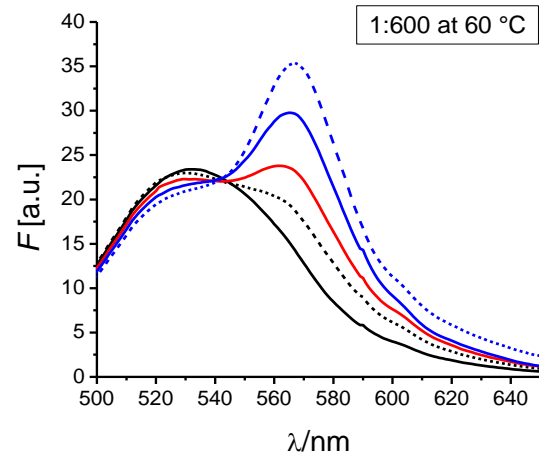
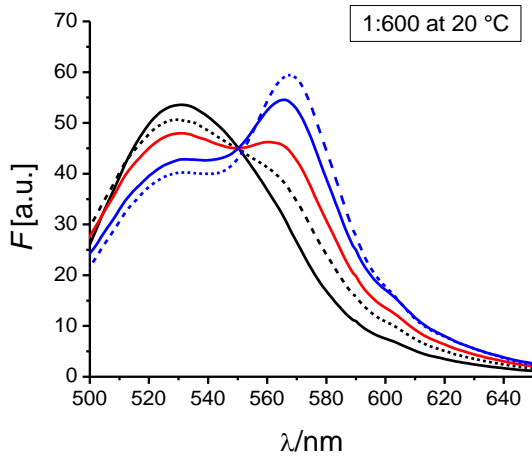
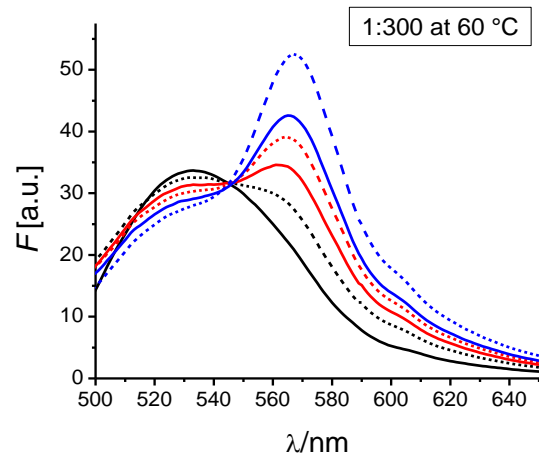
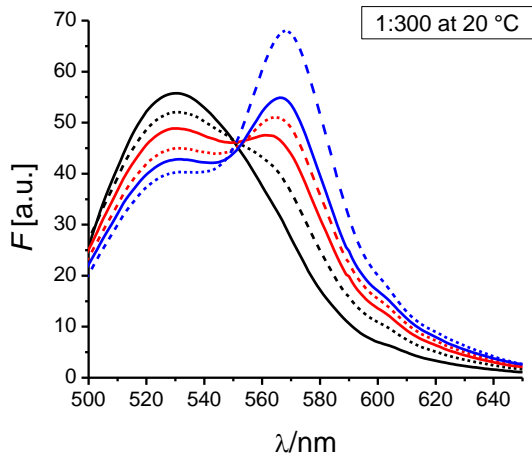
$P3_{\chi_A} =$ — 0 - - - 0.1 — 0.2 - - - 0.3 — 0.4 - - - 0.5

P4 $\chi_A =$ — 0 - - - 0.1 — 0.2 - - - 0.3 — 0.4 - - - 0.5

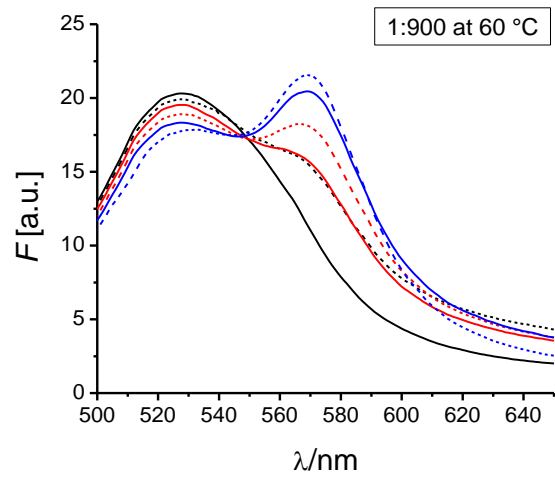
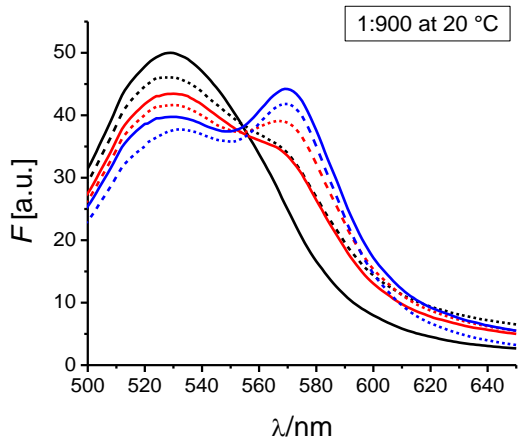
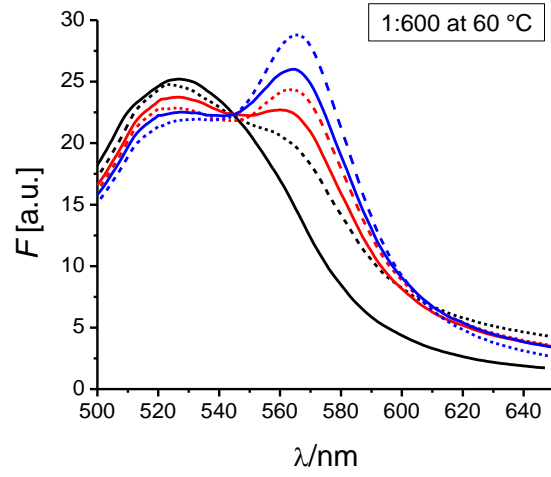
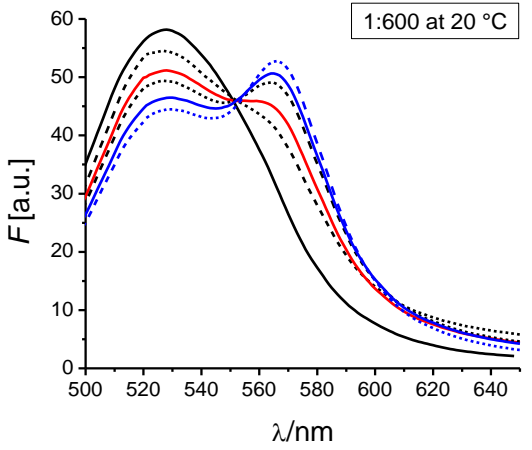
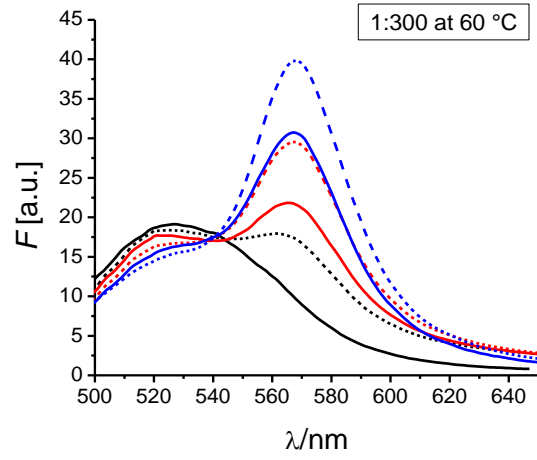
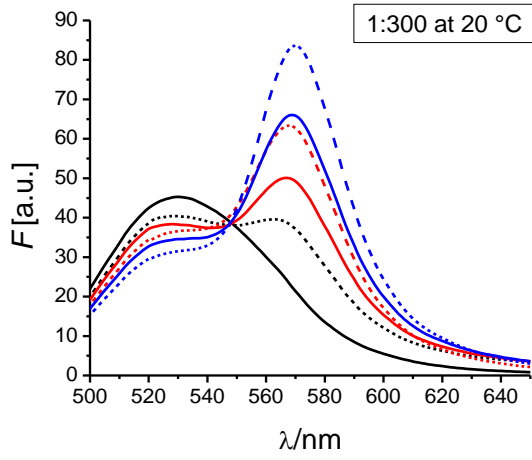


P5 $\chi_A =$ — 0 - - - 0.1 — 0.2 - - - 0.3 — 0.4 - - - 0.5



$P6_{\chi_A} =$ — 0 - - - 0.1 — 0.2 - - - 0.3 — 0.4 - - - 0.5

P7 $\chi_A =$ — 0 - - - 0.1 — 0.2 - - - 0.3 — 0.4 - - - 0.5



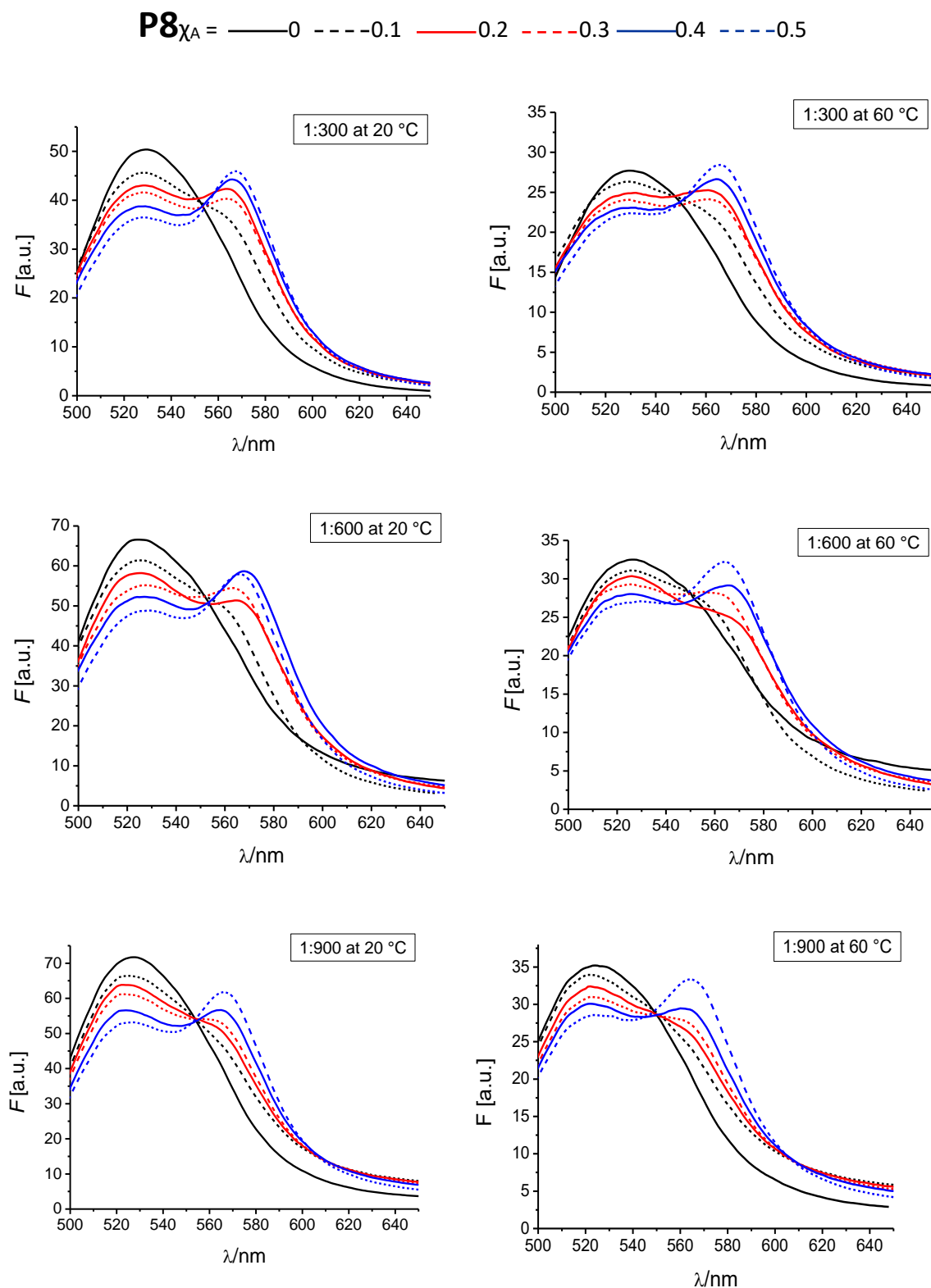


Figure 5.S. Fluorescence emission spectra of NBD-labeled species for different peptide-to-lipid ratio and at temperature as indicated in the respective figure. The concentration of NBD-labeled peptides (donor) was kept constant at $2.75 \mu\text{M}$ while varying the concentration of TAMRA-labeled peptides (acceptor) from $0.00 \chi_A$ to $0.50 \chi_A$ mole fraction. The overall β -peptides concentration was kept constant at $5.5 \mu\text{M}$ by adding non-labeled species.

8 Abbreviation

Å	angstrom (10^{-8}cm)
AcOH	acetic acid
Alloc	allyloxycarbonyl
aq	aqueous
Boc	<i>tert</i> -butoxycarbonyl
°C	degree Celsius
CD	circular dichroism
δ	chemical shift
d	doublet
DBU	1,8-diazabicyclo[5.4.0]undec-7-en
DCM	dichloromethane
DIC	<i>N,N'</i> -diisopropylcarbodiimide
DIPEA	<i>N,N</i> -diisopropylethylamine
DLPC	1,2-dilauroyl- <i>sn</i> -glycero-3-phosphocholine
DMF	<i>N,N</i> -dimethylformamide
DMSO	dimethyl sulfoxide
eq.	equivalent
ESI	electrospray-ionisation
EtOAc	ethyl acetate
Fmoc	fluorenylmethoxycarbonyl
FRET	förster resonance energy transfer
HATU	<i>O</i> -(7-azabenzotriazol-1-yl)- <i>N,N,N',N'</i> -tetramethyluronium hexafluorophosphate
HBTU	<i>O</i> -(1 <i>H</i> -benzotriazol-1-yl)- <i>N,N,N',N'</i> -tetramethyluronium hexafluorophosphate
HOAt	1-hydroxy-7-azabenzotriazole
HOBt	1-hydroxybenzotriazole
HPLC	high performance liquid chromatography
HR-MS	high resolution mass spectrometry
LUV	large unilamellar vesicle
λ	wavelength

M	molar
MBHA	4-methylbenzhydramine
MeOH	methanol
MF	mole fraction
MLV	Multilamellar Vesicles
<i>m/z</i>	ratio of mass to charge
NBD	7-nitrobenz-2-oxa-1,3-diazol-4-yl
NMP	<i>N</i> -methyl-pyrrolidone
NMR	nuclear magnetic resonance
P:L	peptide-to-lipid
POPC	1-palmitoyl-2-oleoyl- <i>sn</i> -glycero-3-phosphocholine
pH	the negative logarithm hydrogen-ion activity ($-\log_{10}[\text{H}_3\text{O}^+]$)
ppm	parts per million
PyBOP	benzotriazole-1-yl-oxy-tris-pyrrolodino-phosphonium hexafluorophosphate
rt	room temperature
SPPS	solid phase peptide synthesis
SUV	small unilamellar vesicle
TAMRA	5(6)-carboxytetramethylrhodamine
TFA	trifluoroacetic acid
TFE	trifluoroethanol
THF	tetrahydrofuran
TLC	thin-layer chromatography
TIS	triisopropylsilan
TMS	trimethylsilan
t_R	retention time
Trt	trityl
UV	ultraviolet
VIS	visual

9 References

- [1] S. Fiedler, J. Broecker, S. Keller, *Cell. Mol. Life Sci.* **2010**, *67*, 1779-1798.
- [2] J. A. Kritzer, J. Tirado-Rives, S. A. Hart, J. D. Lear, W. L. Jorgensen, A. Schepartz, *J. Am. Chem. Soc.* **2005**, *127*, 167-178.
- [3] H. S. Gellman, *Acc. Chem. Res.* **1998**, *31*, 173-180.
- [4] A. M. Brückner, P. Chakraborty, S. H. Gellman, U. Diederichsen, *Angew. Chem. Int. Ed.* **2003**, *42*, 4395-4399.
- [5] R. P. Cheng, W. F. DeGrado, *J. Am. Chem. Soc.* **2002**, *124*, 11564-11565.
- [6] T. L. Raguse, J. R. Lai, P. R. LePlae, S. H. Gellman, *Org. Lett.* **2001**, *3*, 3963-3966.
- [7] M. R. R. de Planque, J. A. Killian, *Mol. Membr. Biol.* **2003**, *20*, 271-284.
- [8] M. Eeman, M. Deleu, *Biotechnol. Agron. Soc. Environ.* **2010**, *14*, 719-736.
- [9] S.J. Singer, G.L. Nicholson, *Science* **1972**, *175*, 720-731.
- [10] H. Eibl, P. Kaufmann-Kolle, *J. Liposome Res.* **2008**, *5*, 131-148.
- [11] S. G. Antimisiaris, P. Kallinteri, D. G. Fatouros, *Liposomes and drug delivery. In Pharmaceutical manufacturing handbook.* (ed. S Cox Gad). Hoboken, N. J. John Wiley and Sons, Inc. **2007**.
- [12] M. C. Geoffrey, *The Cell, a molecular approach.* Boston University Press, Sunderland (MA), **2000**.
- [13] G. van Meer, D. R. Voelker, G. W. Feigenson, *Nat. Rev. Mol. Cell Biol.* **2008**, *9*, 112-124.
- [14] P. B. Messersmith, S. Vallabhaneni, V. Nguyen, *Chem. Mat.* **1998**, *10*, 109-116.
- [15] J. H. Collier, P. B. Messersmith. *Annu. Rev. Mater. Res.* **2001**, *31*, 237-263.
- [16] J. Israelachvili, *Intermolecular and Surface Forces.* London: Academic. **1992**.
- [17] Y. Agzenai Ben Salem, Dissertation, UNED, Madrid, Spain, **2013**.
- [18] F. Frézard, *Braz. J. Med. Biol. Res.* **1999**, *32*, 181-189.
- [19] R. Koynova, M. Caffrey. *BBA Rev. Biomembr.* **1998**, *1376*, 91-145.
- [20] N. Maurer, D. B. Fenske, P. R. Cullis. *Expert Opin. Biol. Ther.* **2001**, *1*, 923-947.

- [21] A. Akbarzadeh, R. Rezaei-Sadabady, S. Davaran, S. W. Joo, N. Zarghami, Y. Hanifehpour, M. Samiei, M. Kouhi, K. Nejati-Koshki. *Nanoscale Res. Lett.* **2013**, *8*, 102.
- [22] N. Monteiro, A. Martins, R. L. Reis, N. M. Neves, *J. R. Soc. Interface***2014**, *11*.
- [23] A. J. de Jesus, T. W. Allen, *Biochim. Biophys. Acta* **2013**,*1828*, 851-863.
- [24] S. H. White, A. S. Ladokhin, S. Jayasinghe, K. Hristova, *J. Biol. Chem.***2001**, *276*, 32395-32398.
- [25] A. L. Lomize, M. Y. Reibarkh, I. D. Pogozheva, *Protein Sci.***2002**,*11*, 1984-2000.
- [26] A. L. Lomize, I. D. Pogozheva, H. I. Mosberg, *Protein Sci.***2004**,*13*, 2600-2612.
- [27] T. J. Denich, L. A. Beaudette, H. Lee, J. T. Trevors, *J. Microbiol. Methods***2003**, *52*, 149-182.
- [28] H. Lodish, A. Berk, S. L. Zipursky, P. Matsudaira, D. Baltimore, J. Darnell; *Molecular cell biology*. Freeman & Co., New York, NY, **2000**.
- [29] I. D. Pogozheva, S. Tristram-Nagle, H. I. Mosberg, A. L. Lomize, *Biochim. Biophys. Acta***2013**, *1828*, 2592-2608.
- [30] M. S. Almén, K. J. V. Nordström, R. Fredriksson, H. B. Schiöth, *BMC Biology***2009**, *7*.
- [31] Y. F. Zhai, M. H. Saier. *Protein Sci.***2002**, *11*, 2196-2207.
- [32] W. C. Wimley. *Protein Sci.***2002**, *11*, 301-312.
- [33] B. A. Wallace, *Annu. Rev. Biophys. Biophys. Chem.* **1990**, *19*, 127-157.
- [34] J. A. Killian, G. von Heijne, *Trends Biochem. Sci.* **2000**, *25*, 429-434.
- [35] J. A. Killian, *Biochim. Biophys. Acta Rev. Biomembr.* **1998**, *1376*, 401-416.
- [36] A. Johannsson, G. A. Smith, J. C. Metcalfe, *Biochim. Biophys. Acta Biomembr.* **1981**, *641*, 416-421.
- [37] S. Morein, J. A. Killian, M. M. Sperotto, *Biophys. J.***2002**, *82*, 1405-1417.
- [38] M. M. Sperotto, O. G. Mouritsen, *Eur. Biophys. J.* **1993**, *22*, 323-328.
- [39] A. V. Botelho, T. Huber, T. P. Sakmar, M. F. Brown, *Biophys. J.* **2006**, *91*, 4464-4477.
- [40] a) I. Casuso, P. Sens, F. Rico, S. Scheuring, *Biophys. J.* **2010**, *99*, L47-L49; b) R. Phillips, T. Ursell, P. Wiggins, P. Sens, *Nature***2009**, *459*, 379-385.

- [41] T. K. M. Nyholm, S. Özdirekcan, J. A. Killian, *Biochemistry***2007**, *46*, 1457-1465.
- [42] J. Vonck, *Biochemistry***1996**, *35*, 5870-5878.
- [43] T. Berggård, S. Linse, P. James, *Proteomics* **2007**, *7*, 2833-2842.
- [44] F. X. Zhou, M. J. Cocco, W. P. Russ, A. T. Brunger, D. M. Engelman. *Nat. struct. Biol.* **2000**, *7*, 154-160.
- [45] J. L. Popot, D. M. Engelman, *Biochemistry* **1990**, *29*, 4031-4037.
- [46] S.H. White, W.C. Wimley, *Annu. Rev. Biophys. Biomol. Struct.***1999**, *28*, 319-365.
- [47] W. F. DeGrado, H. Gratkowski, J. D. Lear, *Protein Science***2003**, *12*, 647-665.
- [48] C. N. Pace, G. R. Grimsley, J. A. Thomson, B. J. Barnett, *J. Biol. Chem.* **1988**, *263*, 11820-11825.
- [49] C. Choma, H. Gratkowski, J. D. Lear, W. F. DeGrado, *Nature Struct. Biol.***2000**, *7*, 161-166.
- [50] H. Gratkowski, J. D. Lear, W. F. DeGrado, *Proc. Natl. Acad. Sci.* **2001**, *98*, 880-885.
- [51] D. Shigematsu, M. Matsutani, T. Furuya, T. Kiyota, S. Lee, G. Sugihara, S. Yamashita, *Biochim. Biophys. Acta***2002**, *1564*, 271-280.
- [52] C. Landhold-Marticorena, K. A. Williams, C. M. Deber, R. A. F. Reithmeier, *J. Mol. Biol.* **1993**, *229*, 602-608.
- [53] I. T. Arkin, A. T. Brunger, *Biochim. Biophys. Acta* **1998**, *1429*, 113-128.
- [54] W. P. Russ, D. M. Engelman, *J. Mol. Biol.* **2000**, *296*, 911-919.
- [55] A. Ridder, P. Skupjen, S. Unterreitmeier, D. Langosch, *J. Mol. Biol.* **2005**, *354*, 894-902.
- [56] S. Unterreitmeier, A. Fuchs, T. Schäffler, R. G. Heym, D. Frishman, D. Langosch, *J. Mol. Biol.***2007**, *374*, 705-718.
- [57] L. Adamian, J. Liang, *J. Mol. Biol.* **2001**, *311*, 891-907.
- [58] H. Zhu, S. A., Celinski, J. M. Scholtz, J. C. Hu, *J. Mol. Biol.***2000**, *300*, 1377-1387.
- [59] F. X. Zhou, H. J. Merianos, A. T. Brunger, D. M. Engelman, *Proc. Natl. Acad. Sci.* **2001**, *98*, 2250-2255.
- [60] M. L. Waters *Curr. Opin. Chem. Biol.* **2002**, *6*, 736-741.
- [61] D. A. Dougherty, *Science***1996**, *271*, 163-168.

- [62] R. M. Johnson, K. Hecht, C. M. Deber, *Biochemistry* **2007**, *46*, 9208-9214.
- [63] D. J. Hill, M. J. Mio, R. B. Prince, T. S. Hughes, J. S. Moore, *Chem. Rev.* **2001**, *101*, 3893-4011.
- [64] J. Rizo, L. M. Gierasch, *Annu. Rev. Biochem.* **1992**, *61*, 387-418.
- [65] J. P. Schneider, J. W. Kelly, *Chem. Rev.* **1995**, *95*, 2169-2187.
- [66] J. S. Nowick, E. M. Smith, M. Pairish, *Chem. Soc. Rev.* **1996**, *25*, 401-415.
- [67] D. Seebach, P. E. Ciceri, M. Overhand, B. Jaun, D. Rigo, L. Oberer, U. Hommel, R. Amstutz, H. Widmer, *Helv. Chim. Acta* **1996**, *79*, 2043-2066.
- [68] D. Seebach, S. Abele, K. Gademann, G. Guichard, T. Hintermann, B. Jaun, J. L. Matthews, J. V. Schreiber, L. Oberer, U. Hommel, H. Widmer, *Helv. Chim. Acta* **1998**, *81*, 932-982.
- [69] G. P. Dado, S. H. Gellman, *J. Am. Chem. Soc.* **1994**, *116*, 1054-1062.
- [70] D. H. Appella, L. A. Christianson, D. A. Klein, D. R. Powell, X. Huang, J. J. Barchi, S. H. Gellman, *Nature* **1997**, *387*, 381-384.
- [71] S. J. Edelstein, *Biophys. J.* **1980**, *32*, 347-360.
- [72] J. Kovacs, R. Ballina, R. L. Rodin, D. Balasubramanian, J. Applequist, *J. Am. Chem. Soc.* **1965**, *87*, 119-120.
- [73] A. Banerjee, P. Balaram, *Curr. Science* **1997**, *73*, 1067-1077.
- [74] J. Podlech, D. Seebach, *Angew. Chem. Int. Ed. Engl.* **1995**, *34*, 471-472.
- [75] E. Juaristi, *Enantioselective Synthesis of β -Amino Acids*; Wiley-VCH: New York, **1997**.
- [76] A. G. Gravis, N. N. Romanova, Y. G. Bundel, *Russ. Chem. Rev.* **1996**, *65*, 1083-1092.
- [77] G. Quinkert, E. Egert, C. Griesinger, In *Peptides: Synthesis, Structure, and Applications*; Gutte, Ed. Academic Press: San Diego, **1995**.
- [78] D. Seebach, J. L. Matthews, *Chem. Commun.* **1997**, 2015-2022.
- [79] X. Daura, K. Gademann, H. Schafer, B. Jaun, D. Seebach, W.F. van Gunsteren, *J. Am. Chem. Soc.* **2001**, *123*, 2393-2404.
- [80] K. A. Bode, J. Applequist, *Macromolecules* **1997**, *30*, 2144-2150.

- [81] J. Applequist, K. A. Bode, D. H. Appella, L. A. Christianson, S. A. Gellman, *J. Am. Chem. Soc.* **1998**, *120*, 4891-4892.
- [82] T. E. Creighton, *Proteins*, 2nd ed. W. H. Freeman and Co. New York, **1993**.
- [83] D. H. Appella, L. A. Christianson, I. L. Karle, D. R. Powell, S. H. Gellman, *J. Am. Chem. Soc.* **1996**, *118*, 13071-13072.
- [84] D. H. Appella, J. J. J. Barchi, S. R. Durrell, S. H. Gellman, *J. Am. Chem. Soc.* **1999**, *121*, 2309-2310.
- [85] D. H. Appella, L. A. Christianson, I. L. Karle, D. R. Powell, S. H. Gellman, *J. Am. Chem. Soc.* **1999**, *121*, 6206-6212.
- [86] J. J. J. Barchi, X. Huang, D. H. Appella, L. A. Christianson, S. R. Durell, S. H. Gellman, *J. Am. Chem. Soc.* **2000**, *122*, 2711-2718.
- [87] D. H. Appella, L. A. Christianson, D. A. Klein, M. R. Richards, D. R. Powell, S. H. Gellman, *J. Am. Chem. Soc.* **1999**, *121*, 7574-7581.
- [88] M. G. Woll, J. D. Fisk, P. R. LePlae, S. H. Gellman, *J. Am. Chem. Soc.* **2002**, *124*, 12447-12452.
- [89] J. S. Park, H. S. Lee, J. R. Lai, B. M. Kim, S. H. Gellman, *J. Am. Chem. Soc.* **2003**, *125*, 8539-8545.
- [90] Y. Wu, W. E. I. Han, D. Wang, Y. I. Gao, Y. Zhao, *Acc.* **2008**, *41*, 1418-1427.
- [91] J. M. Langenhan, I. A. Guzei, S. H. Gellman, *Angew. Chem. Int. Edit.* **2003**, *42*, 2402-2405.
- [92] D. H. Appella, P. R. LePlae, T. L. Raguse, S. H. Gellman, *J. Org. Chem.* **2000**, *65*, 4766-4769.
- [93] D. Seebach, M. Overhand, F. N. M. Kuhnle, B. Martinoni, L. Oberer, U. Hommel, H. Widmer, *Helv. Chim. Acta* **1996**, *79*, 913-941.
- [94] D. Seebach, J. V. Schreiber, S. Abele, X. Daura, W. F. van Gunsteren, *Helv. Chim. Acta* **2000**, *83*, 34-57.
- [95] R. P. Cheng, S. H. Gellman, W. F. DeGrado, *Chem. Rev.* **2001**, *101*, 3219-3232.
- [96] M. Rueping, B. Jaun, D. Seebach, *Chem. Commun.* **2000**, 2267-2268.
- [97] R. P. Cheng and W. F. DeGrado, *J. Am. Chem. Soc.* **2002**, *124*, 11564-11565.
- [98] P. I. Arvidsson, M. Rueping, D. Seebach, *Chem. Commun.* **2001**, *7*, 649-650.

- [99] R. P. Cheng, W. F. DeGrado, *J. Am. Chem. Soc.* **2001**, *123*, 5162-5163.
- [100] S. A. Hart, A. B. F. Bahadoor, E. E. Matthews, X. Y. J. Qiu, A. Schepartz, *J. Am. Chem. Soc.* **2003**, *125*, 4022-4023.
- [101] X. Wang, J. F. Espinosa, S. H. Gellman, *J. Am. Chem. Soc.* **2000**, *122*, 4821-4822.
- [102] T. D. W. Claridge, J. M. Goodman, A. Moreno, D. Angus, S. F. Barker, C. T. Aillefumer, M. P. Watterson, G. W. J. Fleet, *Tetrahedron Lett.* **2001**, *42*, 4251-4255.
- [103] S. Abele, P. Seiler, D. Seebach, *Helv. Chim. Acta* **1999**, *82*, 1559-1571.
- [104] J. Masamoto, K. Sasaguri, C. Ohizumi, H. Kobayashi, *J. Polym. Sci. A-2* **1970**, *8*, 1703-1711.
- [105] J. D. Glickson, J. Applequist, *J. Am. Chem. Soc.* **1971**, *93*, 3276-3281.
- [106] S. Krauthäuser, L. A. Christianson, D. R. Powell, S. H. Gellman, *J. Am. Chem. Soc.* **1997**, *119*, 11719-11720.
- [107] M. Werder, H. Hauser, S. Abele, D. Seebach, *Helv. Chim. Acta* **1999**, *82*, 1774-1783.
- [108] T. Hintermann, D. Seebach, *Chimia*. **1997**, *50*, 244-247.
- [109] J. Frackenpohl, P. I. Arvidsson, J. V. Schreiber, D. Seebach, *Chembiochem.* **2001**, *2*, 445-455.
- [110] M. Rueping, Y. Mahajan, M. Sauer, D. Seebach, *Chembiochem.* **2002**, *3*, 257-259.
- [111] N. Umezawa, M. A. Gelman, M. C. Haigis, R. T. Raines, S. H. Gellman, *J. Am. Chem. Soc.* **2002**, *124*, 368-369.
- [112] T. B. Potocky, A. K. Menon, S. H. Gellman, *J. Biol. Chem.* **2003**, *278*, 50188-50194.
- [113] T. B. Potocky, A. K. Menon, S. H. Gellman, *J. Am. Chem. Soc.* **2005**, *127*, 3686-3687.
- [114] W. L. Maloy, U. P. Kari, *Biopolymers* **1995**, *37*, 105-122.
- [115] Y. Hamuro, J. P. Schneider, W. F. DeGrado, *J. Am. Chem. Soc.* **1999**, *121*, 12200-12201.
- [116] D. Liu, W. F. DeGrado, *J. Am. Chem. Soc.* **2001**, *123*, 7553-7559.
- [117] E. A. Porter, X. Wang, H.S. Lee, B. Weisblum, S. H. Gellman, *Nature* **2000**, *404*, 565.
- [118] P. I. Arvidsson, N. S. Ryder, H. M. Weiss, G. Gross, O. Kretz, R. Woessner, D. Seebach, *Chembiochem.* **2003**, *4*, 1345-1347.

- [119] C. M. Goodman, S. Choi, S. Shandler, W. F. DeGrado, *Nature Chem. Biol.* **2007**, *3*, 252-262.
- [120] A. R. Curran, D.M.Engelman, *Curr. Opin. Struct. Biol.* **2003**, *13*, 412-417
- [121] D. Boyd, C. Schierle, J. Beckwith, *Protein Sci.* **1998**, *7*, 201-205.
- [122] E.Wallin, G.von Heijne, *Protein Sci.* **1998**, *7*, 1029-1038.
- [123] M. M.Javadpour, M.Eilers,M. Groesbeek, S. O.Smith, *Biophys. J.* **1999**, *77*, 1609-1618.
- [124] M.Eilers, S. C.Shekar, T.Shieh, S. O. Smith, P. J. Fleming, *Proc. Natl Acad. Sci.* **2000**, *97*, 5796-5801.
- [125] R. Srivastava, A. K. Ray, U. Diederichsen, *Eur. J. Org. Chem.* **2009**, 4793-4800.
- [126] A. M. Brückner, P. Chakraborty, S. H. Gellman, U. Diederichsen, *Angew. Chem. Int. Ed.* **2003**, *42*, 4395-4399.
- [127] P. Chakraborty, U. Diederichsen, *Chem. Eur. J.* **2005**, *11*, 3207-3216.
- [128] R. F. Epand, T. L. Raguse, S. H. Gellman, R. M. Epand, *Biochemistry* **2004**, *43*, 9527-9535.
- [129] H. S.Lee, F. A. Syud, X.Wang, S. H. Gellman, *J. Am. Chem. Soc.* **2001**, *123*, 7721-7722.
- [130] R. F. Epand, N.Umezawa, E. A. Porter, S. H. Gellman, R. M. Epand, *Eur. J. Biochem.* **2003**, *270*, 1240-1248.
- [131] B. W. Gung, D. Zou, A. M. Stalcup, C. E. Cottrell, *J. Org. Chem.* **1999**, *64*, 2176-2177.
- [132] T. L. Raguse, J. R. Lai, S. H. Gellman, *Helv. Chim. Acta* **2002**, *85*, 4154-4164.
- [133] H. Sun, D. V. Greathouse, R. E. Koeppe, *J. Biol. Chem.* **2008**, *283*, 22233-22243.
- [134] J. A. Killian, I. Salemink, M. R. R. de Planque, G. Lindblom, R. E. Koeppe, D. V. Greathouse, *Biochemistry* **1996**, *35*, 1037-1045.
- [135] K. M. Sanchez, G. Kang, B. Wu, J. E Kim, *Biophys. J.* **2011**, *100*, 2121-2130.
- [136] M. R. R De Planque, J. A. W. Kruijtzter, R. M. J. Liskamp, D. Marsh, D. V. Greathouse, R. E. Koeppe, B. de Kruijff, J. A. Killian, *J. Biol. Chem.* **1999**, *274*, 20839-20846.
- [137] B. M. Ulmschneider, M. S.P. Sansom, *Biochim. Biophys. Acta* **2001**, *1512*, 1-14.
- [138] D. Petersen, Dissertation, Universität Göttingen, **2015**.

- [139] P. R. LePlae, J. D. Fisk, E. A. Porter, B. Weisblum, S. H. Gellman, *J. Am. Chem. Soc.* **2002**, *124*, 6820-6821.
- [140] E. Oliveira, A. Miranda, F. Albericio, D. Andreu, A. C. M. Paiva, C. R. Nakaie, M. Tominaga, *J. Pept. Res.* **1997**, *49*, 300-307.
- [141] C. K. Taylor, P. W. Abel, M. Hulce, D. D. Smith, *J. Pept. Res.* **2005**, *65*, 84-89.
- [142] P. I. Arvidsson, J. Frackenhohl, D. Seebach, *Helv. Chim. Acta* **2003**, *86*, 1522-1553.
- [143] a) A. Thalerl, D. Seebach, F. Cardinaux, *Helv. Chim. Acta* **1991**, *74*, 617-627. b) A. Thalerl, D. Seebach, F. Cardinaux, *Helv. Chim. Acta* **1991**, *74*, 628-643.
- [144] J. D. Wade, J. Bedford, R. C. Sheppard, G. W. Tregear, *Pept. Res.* **1991**, *4*, 194-199.
- [145] M. Varanda, M. T. L. Miranda, *J. Pept. Res.* **1997**, *50*, 10210-10218.
- [146] B. E. Kaplan, L. J. Hefta, R. C. Blake, K. M. Swiderek, J. E. Shively, *J. Pept. Res.* **1998**, *52*, 249-260.
- [147] P. Sieber, *Tetrahedron Lett.* **1987**, *54*, 1637.
- [148] G. A. Lengyel, W. S. Horne, *J. Am. Chem. Soc.* **2012**, *134*, 15906-15913.
- [149] A. K. Tickler, C. J. Barrow, J. D. Wade, *J. Pept. Sci.* **2001**, *7*, 488-94.
- [150] B. S. Patil, G. B. Vasanthakumar, V. V. S. Babu, *Lett. Pept. Sci.* **2002**, *9*, 231-233.
- [151] U. Rost, C. Steinem, U. Diederichsen, *Chem. Sci.* **2016**, *7*, 5900-5907.
- [152] S. M. Kelly, N. C. Price, *Curr. Prot. Pept. Sci.* **2000**, *1*, 349-384.
- [153] S. M. Kelly, T. J. Jess, N. C. Price, *Biochim. Biophys. Acta* **2005**, *1751*, 119-139.
- [154] R. W. Woody, *Biopolymers* **1978**, *17*, 1451-1467.
- [155] G. D. Fasman (Ed.), *Circular Dichroism and the Conformational Analysis of Biomolecules*, Plenum Press, New York, **1996**.
- [156] N. Berova, K. Nakanishi, R. W. Woody (Eds.), *Circular Dichroism: Principles and Applications*, 2nd ed, Wiley-VCH, New York, **2000**.
- [157] A. Rodger, B. Nordén, *Circular Dichroism and Linear Dichroism*, Oxford Univ. Press, Oxford, **1997**.
- [158] P. Luo, R. L. Baldwin, *Biochemistry* **1997**, *3*, 8413-8421.

- [159] F. D. Sönnichsen, J. E. Van Eyk, R. S. Hodges, B. D. Sykes. *Biochemistry***1992**, *31*, 8790-8798.
- [160] J. W. Nelson, N. R. Kallenbach, *Proteins* **1986**, *1*, 211-217.
- [161] R. W. Woody, *Biopolymers***1978**, *17*, 1451-1467.
- [162] A. Chakrabartty, T. Kortemme, S. Padmanabhan and R. L. Baldwin, *Biochemistry (Mosc.)***1993**, *32*, 5560-5565.
- [163] H. E. Auer, *J. Am. Chem. Soc.***1973**, *95*, 3003-3011.
- [164] N. Kučerka, M. P. Nieh, J. Katsaras *Biochim. Biophys. Acta***2011**, *1808*, 2761-2771.
- [165] S. Morein, R. E. Koeppe, G. Lindblom, B. de Kruijff, J. A. Killian. *Biophys. J.***2000**, *78*, 2475-2485.
- [166] N. Rathore, S. H. Gellman, J. J. de Pablo, *Biophys. J.* **2006**, *91*, 3425-3435.
- [167] J. T. Vivian, P. R. Callis. *Biophys. J.***2001**, *80*, 2093-2109.
- [168] S. Lew, J. Ren, E. London, *Biochemistry (Mosc.)***2000**, *39*, 9632-9640.
- [169] J. Ren, S. Lew S, Z. Wang, E. London, *Biochemistry (Mosc.)***1997**, *36*, 10213-10220.
- [170] J. Ren, S. Lew, J. Wang, E. London. *Biochemistry (Mosc.)***1999**, *38*, 5905-5912.
- [171] Y. K. Reshetnyak, E. A. Burstein, *Biophys. J.* **2001**, *81*, 1710-1734.
- [172] Y. K. Reshetnyak, Y. Koshevnik, E. A. Burstein. *Biophys. J.* **2001**, *81*, 1735-1758.
- [173] J. R. Lakowicz, *Principles of Fluorescence Spectroscopy*, 3rd ed. **2006**.
- [174] J. C. McIntyre, R. G. Sleight, *Biochemistry***1991**, *30*, 11819-11827.
- [175] R. E. Feeney, R. B. Yamasaki, K. F. Geoghegan, *Adv. Chem.***1982**, *198*, 3-55.
- [176] C. D. Spicer, B. G. Davis, *Nat. Communications* **2014**, *5*, 1-14.
- [177] Y. K. Reshetnyak, M. Segala, O. A. Andreev, D. M. Engelman. *Biophys. J.***2007**, *93*, 2363-2372.
- [178] Y. Yano, K Matsuzaki, *Biochemistry* **2002**, *41*, 12407-12413.
- [179] Y. K. Reshetnyak, O. A. Andreev, U. Lehnert, D. M. Engelman, *PNAS***2006**, *103*, 6460-6465.
- [180] C. R. Wasmuth, C. Edwards, R. Hutcherson, *J. Phys. Chem.* **1964**, *68*, 423-425.

- [181] C. J. W. Gutch, W. A. Waters, *Chem. Commun.* **1966**, 2, 39-41.
- [182] M. Sokolovsky, J. F. Riordan, B. L. Vallee, *Biochem. Biophys. Res. Commun.* **1967**, 27, 20-25.
- [183] A. S. Lygina, K. Meyenberg, R. Jahn, U. Diederichsen. *Angew. Chem. Int. Ed.* **2011**, 50, 8597-8601.
- [184] J. W. Lichtman, J. A. Conchello, *Nat. Methods* **2005**, 2, 910-919.
- [185] J. Szöllosi, S. Damjanovich, L. Mátyus, *Cytometry* **1998**, 34, 159-179.
- [186] Z. Fazekas, M. Petrás, Á. Fábrián, Z. Pályi-Krekk, P. Nagy, S. Damjanovich, G. Vereb, J. Szöllösi, *Cytometry* **2008**, 73A, 209-219.
- [187] L. Stryer, *Science* **1968**, 162, 526-533.
- [188] D. Frackowiak, *J. Photochem. Photobiol. B.* **1988**, 2, 399.
- [189] T. Förster, *Ann. Phys.* **1948**, 437, 55-75.
- [190] R. Winter, F. Noll, *Methoden der Biophysikalischen Chemie*, Stuttgart, **1998**.
- [191] R. Parthasarathy, J. T. Groves, *Cell Biochem. Biophys.* **2004**, 41, 391-414.
- [192] P. K. Wolber, B. S. Hudson, *Biophys. J.* **1979**, 28, 197-210.
- [193] M. Li, L. G. Reddy, R. Bennett, N. D. Silva, L. R. Jones, D. D. Thomas, *Biophys. J.* **1999**, 76, 2587-2599.
- [194] B. D. Adair, D. M. Engelman, *Biochemistry (Mosc.)* **1994**, 33, 5539-5544.
- [195] R. M. Clegg, *Curr. Opin. Biotechnol.* **1995**, 6, 103-110.
- [196] N. Naarmann, B. Bilgiçer, K. Kumar, C. Steinem, *Biochemistry* **2005**, 44, 5188-5195.
- [197] N. Naarmann, B. Bilgiçer, H. Meng, K. Kumar, C. Steinem, *Angew. Chem. Int. Ed.* **2006**, 45, 2588-2591.
- [198] B. Bilgiçer, K. Kumar, *PNAS* **2004**, 101, 15324-15329.
- [199] P. E. Schneggenburger, S. Müller, B. Worbs, C. Steinem, U. Diederichsen, *J. Am. Chem. Soc.* **2010**, 132, 8020-8028.
- [200] A. Chattopadhyay, *Chem. Phys. Lipid* **1990**, 53, 1-15.

- [201] Y. Yano, T. Takemoto, S. Kobayashi, H. Yasui, H. Sakurai, W. Ohashi, M. Niwa, S. Futaki, Y. Sugiura, K. Matsuzaki, *Biochemistry* **2002**, *41*, 3073-3080.
- [202] M. Gimpelev, L. R. Forrest, D. Murray, B. Honig, *Biophys. J.* **2004**, *87*, 4075-4086.
- [203] J. U. Bowie, *J. Mol. Biol.* **1997**, *272*, 780-789.
- [204] W. G. J. Hol, *Adv. Biophys.* **1985**, *19*, 133-165.
- [205] M. K. Gilson, B. Honig, *Proc. Natl. Acad. Sci.* **1989**, *86*, 1524-1528.
- [206] E. Sparr, W. L. Ash, P. V. Nazarov, D. T. S. Rijkers, M. A. Hemminga, D. P. Tieleman, J. A. Killian, *J. Biol. Chem.* **2005**, *280*, 39324-39331.
- [207] J. -M. Lehn, *Supramolecular Chemistry: Concepts and Perspectives*, Wiley-VCH, Weinheim, **1995**.
- [208] E. Frieden, *J. Chem. Educ.* **1975**, *52*, 754-761.
- [209] M. Rueping, Y. R. Mahajan, B. Jaun, D. Seebach, *Chem. Eur. J.* **2004**, *10*, 1607-1615.
- [210] M. Gude, J. Ryf, P. D. White, *Lett. Pept. Sci.* **2002**, *9*, 203-206.
- [211] A. S. Ladokhin, M. F. Vidal, S. H. White, *J. Membr. Biol.* **2010**, *236*, 247-253.
- [212] E. Kaiser, R. L. Colescott, C. D. Bossinger, P. I. Cook, *Anal. Biochem.* **1970**, *34*, 595-598.

Acknowledgements

Firstly, I would like to express my sincere gratitude to my advisor Prof. Dr. Ulf Diederichsen for the interesting research topic, the continuous support, and his encouraging guidance during my PhD.

I am very grateful to Prof. Dr. Claudia Steinem for co-referring my thesis and for the helpful discussions during my PhD work. I would like to express my gratitude to Dr. Franziska Thomas for the interesting comments and the useful discussions in the field of my work.

I express my special thanks to my labmates Jan-Dirk Wehland, Barbara Hubrich, and Brigitte Worbs for the nice climate and for being supportive during this work. I would like also to thank Dr. Marta Anna Cal, Martin Börsken, Geralin Höger, Anastasiya Schirmacher, and Barbara Hubrich for proofreading of this thesis

I am very thankful to Angela Heinemann and Aoife Neville for their competent help in solving different organizational problems.

I would like to express my gratitude to the German Academic Exchange Service for the financial support during my PhD. I am thankful to Collaborative Research Center 803 for the interesting lectures that have been held in SFB 803 Colloquium.

Last but not the least, I would like to express my very special thanks to my parents, my husband, my sisters and brother for supporting me spiritually throughout my thesis and for their encouragement during my live.

Curriculum Vitae

Personal Data

Name, Surname	Zanbot, Dina
Date/Place of Birth	January 4 th , 1988/Tetouan
Nationality	Moroccan

Scientific Education

10/2013 – 08/2017	<i>PhD thesis</i> in the group of Prof. Dr. U. Diederichsen, Institute of Organic and Biomolecular Chemistry, Georg-August University, Göttingen, Germany <i>Title:</i> Dynamics, intermolecular interactions, and organization of transmembrane β -peptides.
10/2010 – 07/2012	<i>Master in chemistry</i> , specialty in physical chemistry. Abdelmalek Essaâdi University, Tetouan, Morocco.
10/2006 – 07/2010	<i>Bachelor in chemistry</i> , specialty in organic chemistry. Abdelmalek Essaâdi University, Tetouan, Morocco.
04/2013 – 09/2013	German language course at the Goethe-Institute, Dresden, Germany.
06/2006	Final secondary school examination, Tetouan, Morocco.

Research and Teaching Experience

04/2017 – 09/2017	Research assistant at the institute of Organic and Biomolecular Chemistry, Georg-August University, Göttingen, Germany.
-------------------	---

- 04/2016 – 06/2016 Teaching and supervising students in the practical lab course for biochemistry students.
- 02/2016 – 08/2016 Supervising a Bachelor student in biochemistry during the finale project.
- 04/2015 – 06/2015 Teaching and supervising students in the practical lab course for biochemistry students.
- 02/2015 – 08/2015 Supervising a Bachelor student in biochemistry during the finale project.
- 04/2014 – 06/2014 Teaching and supervising students in the practical lab course for biochemistry students.